Natural England Commissioned Report NECR279

Recent evidence from the Lizard Peninsula for the existence of microrefugia

First published : January 2020

www.gov.uk/natural-england

Foreword

Natural England commission a range of reports from external contractors to provide evidence and advice to assist us in delivering our duties. The views in this report are those of the authors and do not necessarily represent those of Natural England.

Background

.

This report should be cited as: Maclean IMD, Suggitt AJ, Greenwood O, Wilson RJ, Duffy JP, Hopkins JJ, Lawson CCR and Bennie JJ. (2020) Recent evidence from the Lizard Peninsula for the existence of microrefugia. Natural England Commissioned Report NECR279, Natural England, York.

An important part of responding to climate change in nature conservation is to try to increase the resilience of species populations and help them to survive in at least some parts of their current ranges.

One way that this might be achieved is to identify and protect ‘refugia’; places that might enable species populations to persist despite climate change making the surrounding areas unsuitable. Refugia are a well-established feature of the last glaciation, harbouring many of the species occupying England today that are adapted to relatively warmer climates. But is the refugia concept also valid under current and future climate change?

Through an earlier Natural England project with the University of Exeter and other partners, we investigated evidence for refugia under current climate change by modelling the survival and extinction of over 1,000 species that retracted their range over the past 40 years against environmental characteristics (such as geology, elevation, water availability, exposure to solar radiation) thought likely (from a literature review) to influence refugium potential. The models also included agricultural intensity and level of recent climatic change.

The results indicated that local extinctions have been higher in areas of England that have experienced greater climatic change. This provided further evidence that recent climate change is already affecting species. Importantly, the results also suggested that areas with more varied topography and a wider range of, or more stable, microclimates appear to give many species a better chance of persisting. Thus, refugia appear to exist under current climate change, just as they did in past glacial/interglacial cycles.

The analysis in the earlier study was done at a fairly course spatial resolution. The research outlined in this new report extends our investigation of the refugium concept by looking at whether species persistence is associated with variability in microclimate at finer spatial scales. Focusing on the Lizard Peninsula in Cornwall, our colleagues at the University of Exeter have produced exciting evidence not just that fine-scale landscape variation can create significant variation in microclimates but that this variation in microclimate can provide microrefugia for plant species associated with cooler climates.

Together, the two studies have greatly advanced our knowledge in this important area of applied ecology. Knowledge about potential refugia could be useful when making decisions both about where to create new protected areas and how to manage the landscape within existing conservation areas. The findings have already been used to inform the development of the new Countryside Stewardship agri-environment scheme and will be used by Natural England, alongside other evidence, in developing and implementing its new conservation strategy.

Natural England Project Manager – Nicholas Macgregor

Contractor - Environment and Sustainability Institute, University of Exeter Cornwall Campus, TR10 9FE, United Kingdom

Keywords – climate change, climatic refugia, microrefugia, adaptation, The Lizard

Further information
This report can be downloaded from the Natural England Access to Evidence Catalogue: **http://publications.naturalengland.org.uk/** . For information on Natural England publications contact the Natural England Enquiry Service on 0300 060 3900 or e-mail **enquiries@naturalengland.org.uk**.

ISBN 978-1-78354-548-3

Recent evidence from the Lizard Peninsula for the existence of microrefugia

Ilya M.D. Maclean[1], Andrew J. Suggitt[1], Owen Greenwood[1], Robert J. Wilson[2], James P. Duffy[1], John J Hopkins[1], Callum C.R. Lawson[3] and Jonathan J. Bennie[1]

[1]Environment and Sustainability Institute, University of Exeter Cornwall Campus, TR10 9FE, United Kingdom.

[2]College of Life and Environmental Sciences, University of Exeter, Exeter, EX4 4PS, United Kingdom.

[3]Department of Animal Ecology, Netherlands Institute of Ecology (NIOO-KNAW), Wageningen 6708 PB, Netherlands.

Contents

Executive summary

1. Microrefugia are small pockets of suitable microclimate that enable populations of species to persist in areas of unsuitable regional climate during periods of climatic change. However, empirical evidence for their existence is scarce and hindered by a lack of fine-scale climate and biological data. Here we provide empirical evidence for their existence.

2. In chapter one, we present a model that is applied to provide fine-grained, multi-decadal estimates of temperature change across a region of England, based on the underlying physical processes that influence microclimate. Weather station and remotely-derived environmental data are used to construct physical variables that capture the effects of terrain, sea-surface temperatures, altitude and surface albedo on the solar radiation budget and other processes that influence local temperatures. These are then calibrated statistically to derive gridded estimates of temperature. We apply the model to the Lizard Peninsula, United Kingdom to provide hourly estimates of temperature at a resolution of 100 m for the period 1977 to 2014.

3. We show that rates of warming vary across a landscape primarily due to long-term trends in synoptic weather conditions. Within our study area, the total warming (at one metre above the ground) that occurred between 1977 and 2014 varies from 0.87 to 1.16ºC, with the slowest rates of warming evident on north-east facing slopes. Total warming varied from 0.87 to 1.16ºC, with the slowest rates of warming evident on north-east-facing slopes. This variation contributed to substantial spatial heterogeneity in trends in bioclimatic variables: for example, the change in the length of the frost-free season varied from +11 to -54 days and the increase annual growing degree-days from 51 to 267 ºC days.

4. Spatial variation in warming was caused primarily by a decrease in daytime cloud cover with a resulting increase in received solar radiation, and secondarily by a decrease in the strength of westerly winds, which has amplified the effects on temperature of solar radiation on west-facing slopes.

5. In chapter two, we examine fine-scale changes in plant communities of a coastal grassland on the Lizard Peninsula, UK, over a 30 year period in which spring temperatures increased by 1.4ºC. We determine whether changes in community composition and local patterns of colonisation and extinction are related to microclimatic conditions.

6. We show that, while community reassembly was consistent with warming, changes were smaller on cooler, north-facing slopes. Closer inspection of patterns of species turnover revealed that species with low temperature requirements were able to persist on cooler slopes, while those with high moisture requirements suffered similar decreases in occupancy across all microclimates. Overall, our results suggest that cooler slopes, also those that have experienced the least warming, may act as microrefugia, buffering the effects of increases in temperature on plant communities by delaying extinctions of species with low temperature requirements.

7. In chapter three, we test whether fine-scale variation in rates of warming affects local patterns of extinction and persistence for a suite of plant species vulnerable to climate change. We show that, across all species, persistence is, on average, high at locations experiencing the slowest rates of warming. However, the effects are weak and there are a number of limitations associated with the method. Nonetheless, in common with chapter two, our results suggest that north- and east-facing slopes, which have

experienced less warming may act as microrefugia, by increasing the likelihood that climate-vulnerable species are able to persist.

8. Overall we highlight the importance of multi-decadal trends in weather conditions in determining spatial variation in rates of warming. We suggest that locations identified as potential microrefugia using recent climatic data, may not serve as such indefinitely. More refined knowledge of the circumstances in which coarse-scale models fail to predict how species respond to climate change, and greater empirical validation using fine-scale data, is required before the nature of microrefugia can be fully understood. Nonetheless, we provide compelling evidence that, at least over the last 30 years, north and east facing slopes may have served as microrefugia for plant species associated with cooler climates.

General background

The success of conservation in the 21st century will depend much on our ability to predict the consequence of climate change on species, communities and ecosystems. Over the last 20 years, bioclimate envelope models have emerged as the most widely used tool for making such predictions (see e.g. Pearson & Dawson 2003; Hijmans & Graham 2006; Elith & Leathwick 2009). Results from these models suggest catastrophic consequences for life on earth, predicting, for example, that by 2050, between 15 and 37% of species will be committed to extinction (Thomas *et al.* 2004). Thus far, however, climate change has been implicated as a major cause of the extinction of just nine species (IUCN 2015). A growing body of evidence highlights a possible reason for this discrepancy: most bioclimate models rely on coarse-resolution spatial associations between species distributions and climate variables measured over tens to hundreds of kilometres, whereas the conditions experienced by many organisms vary over scales far smaller than this. It has been proposed that the existence of fine-scale variation in microclimate may buffer species against climate change, by providing safe-havens for biodiversity, termed 'microrefugia'.

While microrefugia may only constitute a fraction of a species original area of occupancy, the concept has gained prominence in the literature only in recent years (e.g. Rull 2009; Keppel *et al*. 2012; Worth *et al*. 2014), it owes its origin to the observation in the 19th century that the speed of post-glacial recolonization of northern hemisphere forest vegetation was incompatible with known dispersal mechanisms of the species involved in the absence of closer surviving populations (Reid 1899). While implicitly accepted as an explanation of post-glacial colonization, the refugium concept is often criticised as being a convenient 'theoretical necessity' and its validity as a concept and biogeographic characterisation are still much debated (Rull 2009; Tzedakis *et al*. 2013; Hylender *et al*. 2015). While recent understanding of the topographic controls of local variation in climate has helped to quantify and locate potential microrefugia (Dobrowski 2010; Ashcroft *et al*. 2012; Suggitt *et al*. 2015) empirical evidence for their existence, particularly in the context of recent climate change, is remarkably scarce. De Frenne *et al*. (2014) show that plant community responses to macroclimatic warming are attenuated in forests whose canopies have become denser, but micro-climatically-determined spatial variation in responses to climate warming remains largely unknown.

In this study we set out to test some of the concepts associated with microrefugia using fine-scale data from the Lizard Peninsula in Cornwall, UK. In chapter one, we present a model that is applied to provide fine-grained, multi-decadal estimates of temperature change across an entire region, based on the underlying physical processes that influence microclimate. Weather station and remotely-derived environmental data are used to construct physical variables that capture the effects of terrain, sea-surface temperatures, altitude and surface albedo on the solar radiation budget and other processes that influence local temperatures. These are then calibrated statistically to derive gridded estimates of temperature at one metre above the ground. We apply the model to the Lizard Peninsula to provide hourly estimates of temperature at a resolution of 100 m for the period 1977 to 2014. We investigate whether rates of warming vary across a landscape and the underlying landscape features and weather processes that influence this variation. In chapter two we investigate whether the existence of cool and damp microclimates buffers plant community responses to climate change, by examining fine-scale changes in the community composition of a coastal grassland on the Lizard Peninsula over a 30 year period in which spring temperatures increased by 1.4ºC.

Specifically, we determine whether changes in community composition and local colonisations and extinctions are related to microclimatic conditions. Finally, in chapter 3, we examine how patterns in the extinction and persistence of plant species are related to rates of warming. Specifically, we test whether the localised persistence of a suite of plant species vulnerable to climate change is higher at localities experiencing the slowest rates of warming.

Chapter 1: Fine-scale climate change: modelling spatial variation in biologically meaningful rates of warming

Published version: Maclean IMD, Suggitt AJ, Wilson RJ, Duffy JP, Bennie JJ (2016) Fine-scale climate change: modelling spatial variation in biologically meaningful rates of warming. *Global Change Biology*, in press. DOI: 10.1111/gcb.13343

Summary

The existence of fine-grain climate heterogeneity has prompted suggestions that species may be able to survive future climate change in pockets of suitable microclimate, termed 'microrefugia'. However, evidence for microrefugia is hindered by lack of understanding of how rates of warming vary across a landscape. Here we present a model that is applied to provide fine-grained, multi-decadal estimates of temperature change based on the underlying physical processes that influence microclimate. Weather station and remotely-derived environmental data were used to construct physical variables that capture the effects of terrain, sea-surface temperatures, altitude and surface albedo on local temperatures, which were then calibrated statistically to derive gridded estimates of temperature. We apply the model to the Lizard Peninsula, United Kingdom to provide accurate (mean error = 1.21ºC; RMS error = 1.63ºC) hourly estimates of temperature at a resolution of 100 m for the period 1977 to 2014. We show that rates of warming vary across a landscape primarily due to long-term trends in weather conditions. Total warming varied from 0.87 to 1.16ºC, with the slowest rates of warming evident on north-east-facing slopes. This variation contributed to substantial spatial heterogeneity in trends in bioclimatic variables: for example, the change in the length of the frost-free season varied from +11 to -54 days and the increase annual growing degree-days from 51 to 267 ºC days. Spatial variation in warming was caused primarily by a decrease in daytime cloud cover with a resulting increase in received solar radiation, and secondarily by a decrease in the strength of westerly winds, which has amplified the effects on temperature of solar radiation on west-facing slopes. We emphasise the importance of multi-decadal trends in weather conditions in determining spatial variation in rates of warming, suggesting that locations experiencing least warming may not remain consistent under future climate change.

Introduction

Biodiversity conservation and environmental management increasingly depend on our ability to understand and predict the responses of species and ecological communities to environmental drivers including climatic change. To date, however, most predictions for the effects of climatic change on biodiversity have been derived using grid cell resolutions that are three to four orders of magnitude coarser than the size of the focal species being studied (Potter *et al*., 2013). Wind patterns and landscape features such as local terrain, vegetation and soil properties interact with regional climate to create complex mosaics of temperature and water availability (Dobrowski, 2011, Hannah *et al*., 2014, Maclean *et al*., 2012, Suggitt *et al*., 2011). This fine-grained variation in climate strongly influences species' distributions (Lassueur *et al*., 2006, Randin *et al*., 2009, Scherrer & Körner, 2011, Sebastiá, 2004) and their projected responses to future climatic change (Franklin *et al*., 2013, Gillingham *et al*., 2012).

The existence of fine-grain heterogeneity has prompted suggestions that species may be able to survive future climatic change by exploiting pockets of suitable microclimate, often termed 'microrefugia' (Hannah *et al*., 2014, Rull, 2009). The term 'microrefugia' is borrowed from paleoecology and is usually used to describe locations with unusual microclimates in which isolated populations survive unsuitable regional climate (Rull, 2009). After the Last Glacial Maximum, many species recolonized parts of their historic range at rates much faster than predicted from dispersal models (Clark *et al*., 1998). While long-distance dispersal may be important in explaining this phenomenon (Phillips *et al*., 2008), an alternative explanation is that species recolonized from localities with suitable microclimate much closer to their former range (Stewart & Lister, 2001). Nonetheless, the possible existence of microrefugia is still widely debated (Hylander *et al*., 2015, Tzedakis *et al*., 2013) and empirical evidence for the existence of microrefugia, particularly in the context of recent and ongoing climatic change, is still remarkably scarce (Suggitt *et al*., 2014).

It is sometimes argued that the existence of fine-grained climatic heterogeneity in itself will buffer species against the effects of climatic change (e.g. Willis & Bagwhat 2009). However, many species are already restricted to specific microclimates, and if warming microclimates at the trailing edge of species' ranges are vacated at the same rate as sites become newly occupied at the leading edge, then the effects of microclimate variation will "average out" (Bennie *et al*., 2014). A further consideration of whether or not microclimates buffer the effects on species of regional climate warming is whether or not all parts of the landscape are undergoing climatic change at the same rate. To date, however, the extent to which rates of change in local climate are decoupled from regional climate has received little attention from biologists, in spite of its importance as a mechanism for explaining how species are able to persist in microrefugia (though see Pepin *et al*. 2011 and Pike *et al*. 2013 for examples in the climate literature). A possible reason for this is that it is difficult to quantify fine-grained variation in rates of climatic change, because this requires climate to be modelled or measured both: a) over a sufficiently long time period to encompass an appreciable level of global warming, and b) at a sufficiently fine resolution to quantify local variation in rates of change.

While next-generation fine-grained climate models are emerging, our understanding of local variation in rates of change remains limited. Kearney *et al.* (2014) present a mechanistic model of gridded hourly estimates based on local modifiers of the solar radiation budget for the period 1961 to 1990, but the grid cell resolution of this model is a relatively coarse 15 km and local variation in rates of change is not explored. Dobrowski (2011) identifies terrain features that are likely to be effectively decoupled from regional climatic patterns, but stops short of explicitly modelling the effects of these features over an extended time period. Gunton et al., (2015) model local ground temperatures across Europe, but do not provide long-term estimates of change. Likewise Bennie *et al*. (2008), using similar principles, modelled near-surface temperatures at resolutions of one metre, but again do not assess local variation in long-term change. Heterogeneity in long-term warming was assessed in a study by Ashcroft *et al*., (2009)

in which rates of warming between 1972 and 2007 were modelled within a 10 km x 10 km region approximately 80 km south of Sydney, Australia. However, long-term estimates of temperature change in this study and determinants of local variation in change are estimated using a phenomenological approach based on statistical relationships established over a relatively short period. Models based on phenomenological descriptions can be unreliable when used to predict beyond the realm of existing data (e.g. Rice, 2004). While models based on the physical processes can be difficult to parameterise and necessitate assumptions to be made about model structure, they are often more likely to provide reliable predictions under novel conditions (Evans, 2012).

Here we present a model that incorporates the important mechanistic processes that govern variation in climate to provide fine-grained (100 m) hourly estimates of temperature over decades at regional scales. The model is applied to assess spatial variation in rates of warming and changes in biologically meaningful derivatives of temperature between 1977 and 2014 across a 20 x 30 km region located on the southwest coast of Britain (The Lizard Peninsula in Cornwall). While all parts of the landscape warmed during this period, rates of warming differed by a factor of 1.3, with significantly slower rates of mean warming evident on north-east-facing slopes and valley bottoms. This spatial variation in temperature change has led to even greater spatial variation in the rate at which bioclimatic variables have altered, with the overall change in the length of the frost free growing season, for example, varying from a decrease of 11 days to an increase of 54 days. We provide insight into the mechanisms governing rates of warming, demonstrating how landscape features interact with changing weather patterns to decouple local changes in climate from regional averages.

Material and methods

Overview of approach

The study was conducted on the Lizard Peninsula (50º 2'N, 5º 10'W), a Special Area for Conservation (92/43/EEC) located on the most southerly point of Britain (Fig. 1.1). The climate has a strong maritime influence with mild winters and low annual temperature range. The site is surrounded on three sides by the sea, has an elevation range of 0 to 185 metres above sea level and comprises a mosaic of grassland, woodland and heath on a variety of slopes and aspects. We model hourly local temperature anomalies from a standard meteorological station as a function of landscape features that interact with physical determinants of local temperatures. Estimates are for one metre above the ground at a grid cell resolution of 100 m for the period 1st January 1977 to 31st December 2014.

To drive the model, hourly weather data for the period 1st January 1977 to 31st December 2014 were obtained for Culdrose weather station (Fig. 1.1). A small number (<0.01%) of observations were missing and were imputed by fitting a cubic spline using the Forsyth *et al*. (1977) method implemented by the spline function in R (R Development Core Team, 2013). Five groups of factors were considered to influence local temperatures, details of which are provided below: (i) coastal influences, as a function of sea surface temperatures, wind speed and direction and sea-exposure; (ii) the local radiation balance, as a function of weather conditions, surface albedo, slope and aspect; (iii) altitudinal effects, as function of elevation and humidity; (iv) latent heat exchange, as function of evapotranspiration and condensation; and (v) cold air drainage into valley bottoms, as a function of flow accumulation potential and weather conditions that lead to katabatic flow.

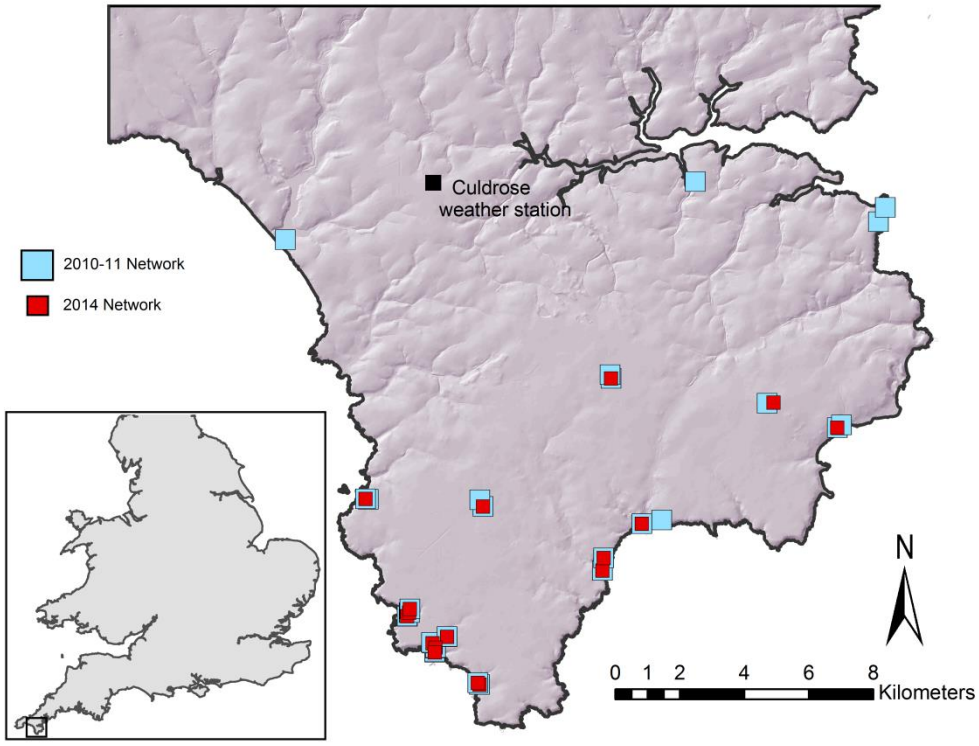

Fig. 1.1. *Study area showing locations of iButton temperature dataloggers deployed across the Lizard Peninsula between March 2010 and 14th December 2011 (blue squares) and between March and November 2014 (red squares). The location of Culdrose weather station is indicated by the larger black square. The shaded relief map was derived from a digital terrain model obtained from Bluesky (Bluesky International Ltd, Coalville, UK)*

To calibrate the model, 35 iButton temperature dataloggers were deployed in open, unwooded areas across the Lizard Peninsula between 1st March 2010 and 14th December 2011, and set to record temperatures at hourly intervals. Loggers were placed to capture spatial gradients in the main determinants of climate and provided 89,250 measurements of temperature for model calibration. Each logger recorded temperature with a specified accuracy of ± 0.5 ° C, and 0.0625 ° C resolution. Loggers were attached to a wooden pole one metre above the ground and orientated to face north and shielded from direct sunlight using a white plastic screen. To provide an independent validation of the model results, an additional 30 loggers were deployed between March and November 2014 at nearby, but not identical locations to those deployed in 2010-11 (mean distance between pairs of locations: 381 m; Fig. 1.1).

To improve readability, we omit mathematical details of our methods from the main text. Further details and functions for implementing individual components of the model, written using R statistical software (R Development Core Team, 2013), are provided on our website (http://www.microclim.org.uk) and in the supporting information accompanying the published paper (http://onlinelibrary.wiley.com/doi/10.1111/gcb.13343/abstract). However, an overview of the underlying rationale and a synopsis of our approach are provided below.

Coastal influences

We obtained a one degree gridded dataset of monthly sea surface temperatures from the Met Office Hadley Centre (Rayner *et al*., 2003) and extracted data for the four grid cells corresponding to the region 49-51ºN and 4-6ºW. We resampled these datasets at 100m grid cell resolution using bilinear interpolation and projecting them onto the Ordnance Survey equal area grid (OSGB36). We then calculated the mean sea surface temperature for the marine portion of our entire study area. We obtained hourly values by simple linear interpolation, assuming that the mean value for each month corresponded to the mid-point of that month. Due to the high specific heat capacity of water, sea surface temperatures undergo only minor high frequency fluctuations (Stacey & Davis, 1977), so simple interpolation was deemed a reasonable approximation.

To capture the influence of sea temperatures on local temperatures, which is itself affected by wind direction (Haugen & Brown, 1980), we calculated the proportion of 100 m x 100 m pixels that were land as opposed to sea upwind of each focal pixel in each of 36 different compass directions (0º, 10º…350º) using a 100 m resolution gridded dataset of land and sea. We then weighted these proportions by the inverse of the distance to the coast, to ensure that coastal grid cells were attributed a higher coastal exposure influence. Coastal effects on local temperatures are also influenced strongly by wind speed (Haugen & Brown, 1980). However, surface friction tends to reduce airflow, and wind speeds at one metre height differ from those measured at the height of the Culdrose anemometer (33 m above the ground). To adjust for height, and derive estimates for one metre above the ground, a logarithmic wind speed profile was assumed (Allen *et al*., 1998). The sheltering effect of local topography was accounted for by computing the shelter coefficient described by Ryan (1977).

Solar radiation

Local temperature anomalies due to variation in solar radiation approximate a linear function of the net radiation flux at a location, with the slope of this relationship determined by local wind speed (Bennie *et al*., 2008). Net radiation is determined by the balance of short- and long-wave radiation and surface albedo. We estimated surface albedo from 25 cm resolution visual and 50 cm colour-infrared aerial photographs obtained from Bluesky (Bluesky International Ltd, Coalville, UK). We weighted the reflectance value in each band by the expected proportion of total solar energy contributed by each band by assuming that the

relationship between energy and wave-length approximates the 5250ºC blackbody spectrum described by Planck's law. This ignores temporally variable, but relatively minor discrepancies caused by atmospheric absorption of specific wavelengths. The mean value in each 100 m grid cell was calculated.

Satellite-derived estimates of direct and diffuse shortwave radiation are available at hourly intervals at a horizontal grid cell resolution of 0.03º from the Satellite Application Facility on Climate Monitoring (Posselt *et al*., 2011). However, as they do not span the duration of our study, we developed a model for predicting solar radiation from meteorological station estimates of cloud cover (recorded in oktas). First we obtained satellite-derived estimates of radiation for the grid cell corresponding to the location of Culdrose weather station for every hour in 2005 (the year with fewest missing weather station observations). Then, because solar irradiance is affected by solar azimuth and zenith, we computed the proportion of potential direct irradiance intercepted by a flat surface located at Culdrose (hereafter referred to as the solar coefficient) for every hour using the methods outlined in Hofierka & Ŝúri (2002). Second, because solar energy is attenuated more by clouds when the sun is low above the horizon, we calculated the airmass coefficient for every hour in 2005. The airmass coefficient is the direct optical path length of a solar beam through the Earth's atmosphere, expressed as a ratio relative to the path length vertically upwards. To account for the earth's curvature, we used the method by Kaston and Young (1989) in which the air mass coefficient can be derived from the solar zenith. Next, to estimate the effects of cloud cover on full beam solar irradiance, we divided each satellite-derived estimate of direct and diffuse solar irradiance by the solar coefficient. As direct irradiance is affected both by cloud cover and the airmass coefficient, we fitted a linear model with the full beam estimates of direct irradiance as a dependent variable, and airmass coefficient, cloud cover and an interaction between cloud cover and the airmass coefficient as predictor variables. To reduce heteroscedasticity, we performed square-root transforms on cloud cover and full-beam irradiance and a logarithmic transform on the airmass coefficient. As diffuse irradiance is highest with intermediate levels of cloud cover, we fitted a linear model with diffuse radiation as the dependent variable and just cloud cover and the square of cloud cover as predictor variables. Again to reduce heteroscedascity, we square-root transformed scaled solar irradiance. Coefficient estimates of these models were used to derive hourly estimates of full beam solar irradiance and diffuse radiation for the entire duration of our study.

Slope, aspect and topographic shading influence strongly the amount of radiation intercepted by a surface and act as one of the dominant influences on local temperatures (Bennie *et al*. 2008). To account for the effects of local terrain on direct radiation, we calculated the solar coefficient for an inclined surface using the method detailed in Bennie *et al*. (2008) and multiplied our coarse-grained cloud-cover derived estimates of full beam radiation by this coefficient. Topographic shading is also accounted for when implementing this method by assuming that a surface receives no direct radiation when the sun is below the local horizon. Slope, aspect and horizon angles were derived from a 5 m resolution digital terrain model obtained from Bluesky (Bluesky International Ltd, Coalville, UK) coarsened to 100 m resolution by computing mean values across grid cells. Local topographic effects on diffuse radiation were calculated by scaling our cloud-cover derived estimates of diffuse radiation by the proportion of sky in view, using methods described in Hofierka & Ŝúri (2002).

Net long-wave radiation was calculated from temperature and relative humidity data using the method described in Allen *et al*. (1998). Using this approach, the effects of cloudiness are accounted for by estimating the ratio of net shortwave to clear sky shortwave radiation, which in our model was estimated directly from cloud cover. Longwave radiation was assumed to be uniform across the landscape and hence the meteorological station temperature was used.

Altitudinal effects

We assumed a simple dry adiabatic lapse rate such that temperature declines with altitude at a standard dry adiabatic lapse rate of 9.8ºC per 1000 m, but accounted for shallower temperature-altitude gradients under saturated conditions by explicitly calculating latent heat exchange (see below), resulting in typical adiabatic lapse rates of 4 to 6ºC per 1000 m. Differences in altitude between the standard meteorological station and each location were calculated from digital elevation data.

Latent heat exchange

Condensation releases latent heat energy warming local air temperatures by as much as 2ºC (Geiger, 1965). Conversely, evapotranspiration uses latent heat energy, cooling local temperatures. Localised variation in these can result in small, but important variations in temperature. As calculation of condensation and evapotranspiration relies on knowledge of local temperatures, but in this instance is also used to derive local temperatures, we used the local temperature anomaly (i.e. the difference between modelled local temperature and that at the meteorological station) in the previous time step, to derive estimates of local differences in latent heat exchange from our reference meteorological station. We assume condensation occurs when drops in temperature result in relative humidity exceeding 100%. First, from Allen *et al*. (1998) we calculate the local relative humidity as a function of the relative humidity measured at the met station, saturated vapour pressure and absolute humidity, which is assumed to remain constant, thus allowing local relative humidity to exceed 100%. Where local relative humidity is less than 100%, condensation is assumed not to occur, but where relative humidity would exceed 100% as a result of temperature decreases, the surplus water is assumed to condense. Following Allen *et al*. (1998) potential evapotranspiration was calculated as a function of net radiation, local temperatures (estimated from anomalies in the previous time step), relative humidity, atmospheric pressure and wind speed using the Penman-Monteith equation.

Cold-air drainage

Under clear sky conditions with low wind speed, katabatic flow occurs, such that cold air drains into valley bottoms (Dobrowski, 2011). Two components of cold air drainage were considered. First we modelled the potential for different parts of the land surface to receive cold air by calculating accumulated flow to each cell, as determined by accumulating the weight for all cells that flow into each downslope cell, using the hydrological tools in ArcGIS 10.2 (ESRI, Redlands). We then identified the synoptic weather conditions under which cold air drainage is likely. Following McGregor & Bamzelis (1995), we first collated and/or calculated the following meteorological variables from the meteorological station data, aggregating data into 24-hour averages: (i) cloud cover (oktas), (ii) mean temperature (ºC), (iii) diurnal temperature range (ºC), (iv) surface atmospheric pressure (hPA), (v) relative humidity (%), (vi) wet bulb temperature (ºC), (vii) the dew point temperature (ºC), (viii) visibility (km), (ix) net radiation (MJ m-2 hr-1), (x) the westerly wind component (m s-1) and (xi) the southerly wind component (m s-1). Visibility data were log-transformed to reduce heteroscedasticity and all variables were z-score standardised. Meteorological variables were also de-seasoned by applying a 15 day running mean filter. Second, as the resulting variables were highly correlated with one another, we performed principal components analysis (PCA). To determine how many components to retain, we produced a scree plot, retaining four components which together explained 85% of the variance in the original data. Finally we performed Bayesian model-based clustering on these data using the R package mclust (Fritsch & Ickstadt, 2009), to group our data into distinct synoptic weather types. Using this approach, prior cluster partitions are identified using hierarchical agglomeration, and then Bayesian expectation-maximization is performed to automatically identify the final cluster number and membership thereof. Seven was considered the most likely number of distinct synoptic weather types using this method (see results). The synoptic weather type characterised by clear sky, high pressure, a high diurnal temperature range, good visibility and low relative humidity was considered to be the conditions under which temperature inversions occur (see e.g. Barr & Orgill, 1989). Temperature inversions

were set to occur at night only as daytime cold air drainage into valleys is highly unusual in maritime climates (Gustavsson *et al*., 1998).

Model calibration

Temperature anomalies were modelled using standard linear regression as a function of the following sets of terms:

Radiation effects:	$R_{net} + u_1 + u_1 R_{net}$
Coastal influences:	$u_i L + u_1 L + L T_s$
Altitudinal effects:	ΔT_a
Latent heat exchange:	$E + C + W$
Cold air drainage:	$I_C F$

Where R_{net} is net radiation, u_1 is wind speed one metre above the ground, u_i is the inverse of wind speed given by $1/(u_1^{0.5}+1)$, L is the inverse distance-weighted measure upwind land-to-sea ratio at Culdrose minus that at the site, T_s is sea-surface temperature minus that at Culdrose, ΔT_a is the expected difference in temperature due to altitude, E is evapotranspiration at Culdrose minus that at the site, C is condensation at Culdrose minus that at the site, W is the change in lapse rate due to water condensation, F is accumulated flow and I_c is a categorical variable set at one when temperature inversions exist, and 0 when temperature inversion conditions do not exist. The terms are listed in anticipated descending order of importance.

To fit the model, we sequentially added each set of terms to linear models and assessed whether their inclusion improved model parsimony by computing the Akaike Information Criterion (AIC). To reduce the effects of temporal autocorrelation, we randomly selected 2000 of the 89,250 logger-derived local temperature data and repeated the analyses 9999 times, computing AICs and coefficient estimates for each model run. To test the effects of sample size on the retention of model terms, we repeated analyses varying the number of randomly selected data points. To assess the sensitivity of our model selection to the sequential adding of terms, we also fitted models with all possible combinations of terms, but due to computational constraints, did this for 999 model runs only.

Running and testing the model

To run the model, median model coefficient estimates were used. The model was run in hourly time steps for the period 1st January 1977 to 31st December 2014, deriving temperature estimates for each 100 m grid cell of our study area. To test the model, model predictions were compared with the observed data obtained through the deployment of temperature loggers in 2014. To assess the relative contribution of individual components of the model, we re-ran the model with only the set of coefficients with each effect included, holding other coefficients at their mean. The model was coded and deployed in R statistical software (R Development Core Team 2015) using a 2032 CPU Core Beowulf cluster.

Spatial variation in climate change

To examine spatial variation in rates of warming, we calculated the overall degree of temperature change in each grid cell using linear regression on hourly values over (a) the entire duration of our study and (b) for 2010 to 2014, a period in which land temperature rose much faster than sea temperatures. To examine how spatial variation in temperature change manifests itself in changes to bioclimatic variables, we calculated the overall 1977-2014 change in (i) exposure to high temperatures, (ii) the number of growing degree-days, (iii) the length of the frost-free season, (iv) diurnal temperature ranges, (v) isothermality, (vi)

temperature seasonality, (vii) maximum annual temperatures, (viii) minimum annual temperatures, (ix) annual variations in temperature and (x-xiii) mean temperatures in the warmest, coldest, driest and wettest quarter of each year. Exposure to high temperatures was expressed as the number of hours in which temperatures equalled or exceeded 20ºC, growing degree-days were calculated as the difference between mean daily temperatures and a base temperature of 10ºC, with temperatures capped at 30ºC and values summed for each year, and the frost free season is the number of days between the last day in spring in which air temperatures drop below zero and the first such day in autumn, with spring frost set at 1st of Jan and autumn frost at 31st Dec in instances when temperatures did not drop below zero. The diurnal temperature range was calculated as the difference between the maximum and minimum hourly temperature in any given 24-hour period, the annual temperature range as the difference between the maximum and minimum temperatures in any given year and isothermality as the mean diurnal range divided by the annual temperature range. The temperature seasonality was expressed as the standard deviation of temperatures expressed as a percentage of the mean of those temperatures, with temperatures expressed in Kelvin (Hijmans *et al*., 2005). A quarter is here defined as any 90 day period. Temperature data from the Culdrose weather station were used to calculate the warmest and coldest periods, and 5km grid daily rainfall data available from the UK Met Office used to calculate the wettest and driest periods. In each case, values were calculated separately for each year and linear-regression on yearly values used to calculate the overall change. To gain insight into the factors affecting warming, we reran the model calculating the separate contribution of each of the five groups of factors to produce hourly temperatures. This was achieved by fitting the model using only coefficients associated with to each group of terms, holding all other terms constant at their mean value. Long-term trend in selected weather variables (wind speed and direction, cloud cover and the prevalence of each synoptic weather type) were also calculated using linear-regression.

Results

Model performance

Our cloud-cover derived model provided good approximations of direct (Mean error = 34.9 Wm-2; RMS error = 71.8 Wm-2), diffuse (mean error = 21.1 Wm-2; RMS error = 39.5 Wm-2) and total solar irradiance (Mean error = 38.6 Wm-2; RMS error = 74.6 Wm-2). Full results are presented in Appendix 1.

Our cluster analysis of weather variables identified seven synoptic weather types, one of which represents conditions where no clear pattern could be discerned (Table S1 in Appendix 1). Box and whisker plots indicating the median and range in meteorological variables associated with each weather type and UK Met Office synoptic charts for dates conforming to each synoptic weather type are shown in Appendix 1.

The most parsimonious model was that which included all terms. This model explained on average 78% of the variation in local temperature anomalies (r^2 = 0.711 to 0.831), with a mean error of 1.21 ºC and RMS error of 1.63ºC. Parameter estimates, their standard deviation and partial r-squared values are shown in Table 1.1. Comparisons between modelled hourly predictions of temperature and recorded temperatures at two sites with divergent local climatic conditions are shown in Figure 1.2. Further details of model performance are shown in Appendix 1.

Table 1.1. *Model parameter estimates (median, mean and standard deviation) and their coefficient of partial determination (partial R^2) derived from the 9999 model runs. See text for a description of model parameters.*

Parameter	Median	Mean	Standard Deviation	Partial R^2
R_{net}	0.57	0.57	0.18	0.311
u_1	-0.071	-0.072	0.034	0.027
u_1R_{net}	-0.15	-0.15	0.023	0.014
u_i	-2.5	-2.4	0.59	0.004
L	-0.18	-0.17	0.46	0.052
T_S	-0.15	-0.15	0.015	0.056
u_iL	-0.45	-0.48	1.2	0.015
u_1T_S	0.011	0.011	0.0043	0.050
E	-5.8	-5.8	0.31	0.052
C	0.064	0.063	0.0047	0.023
W	0.28	0.28	0.0086	0.092
I_cF	-0.10	-0.10	0.0014	0.015

Changes in weather variables

Linear regression of hourly temperatures recorded at Culdrose weather station revealed an increase of 0.94 ºC between 1977 and 2014 (95% CI = 0.89 to 0.99, n = 333096; Fig. 1.3a). Over the same period, linear regression of monthly sea-surface temperatures showed an overall increase of 0.89 ºC (95% CI = 0.21 to 1.57, n = 649; Fig. 1.3b). Among other weather variables, there were two notable trends. First, linear regression on hourly estimates reveals that although cloud cover has changed little (<0.2%) over the duration of the study (95% CI = -0.49% to 0.15%, n = 333096), daytime cloud cover decreased by 4.0% (95% CI = -5.1% to -2.9%, n = 166602; Fig. 1.3c), whereas night-time cloud cover increased by 1.2% (95% CI = 0.7% to 1.7%, n = 166602; Fig. 1.3d). Changes in cloud cover appear to have manifested themselves in moderate increases in received solar radiation: direct radiation was estimated to have increased by 11.9 Wm-2 over the period of the study (95% CI = 5.2 to 18.7, n =333096; Fig. 1.3e). However, diffuse radiation has changed little (95% CI = -2.8 to 7.0 Wm-2, n =333096; Fig. 1.3f).

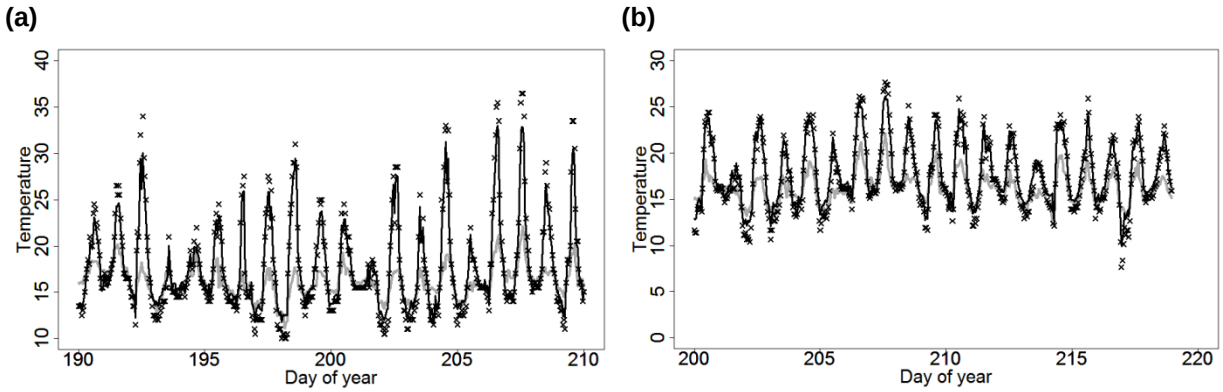

Fig. 1.2 *Hourly temperatures recorded during summer 2014 using iButton temperature loggers (black crosses) and modelled using a 100 m spatial resolution mesoclimate model (black lines) compared to temperatures observed at a regional weather station (grey lines) five km from the sample site (RNAS Culdrose). Data for two sites with divergent mesoclimatic conditions are shown, (a) Poltesco (49.9981ºN, 5.1727ºW), a steep south-facing slope, and (b) Kennack Sands (50.0070ºN, 5.1594ºW), a relatively flat and open coastal area. Observed temperature variation (1 m above ground level) on the south-facing slope can be 15°C greater than air temperatures measured at the nearby weather station, and is accurately predicted by our model.*

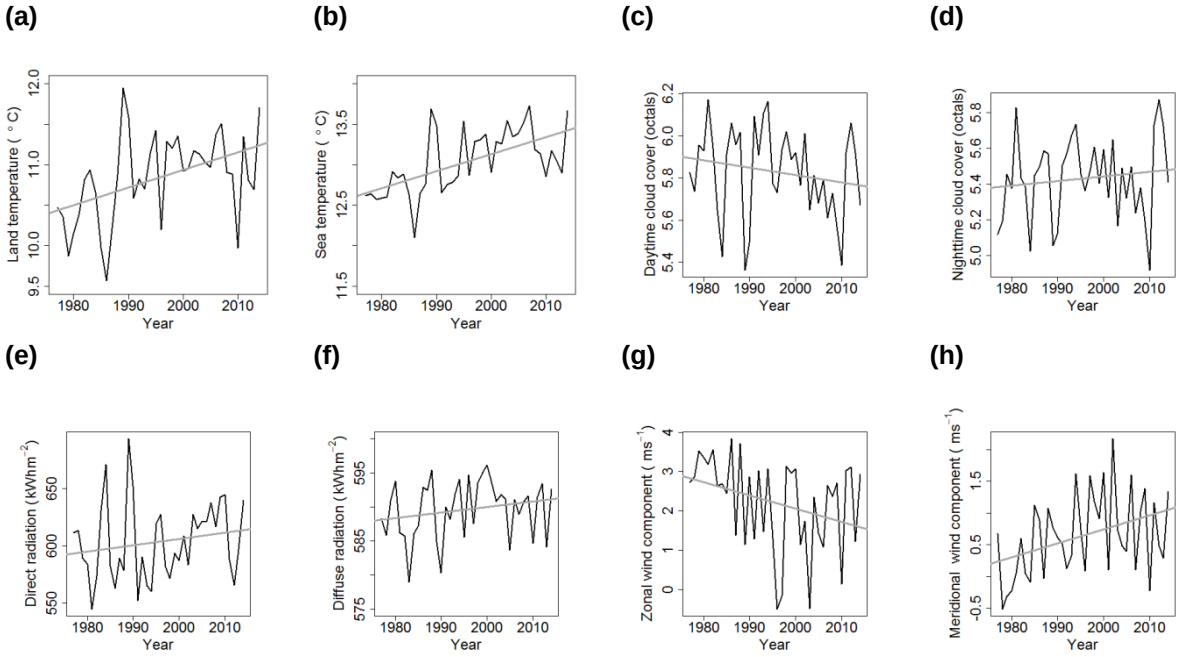

Fig. 1.3. *Mean yearly values (black lines) and linear trends (grey lines) in selected climate variables. Weather station (a) and sea-surface temperatures (b) both increased at similar rates between 1977 and 2014, but between 2010 and 2014, after an uncharacteristically cold year, land temperatures rose much more quickly. Daytime cloud cover (c) decreased during the period 1977 to 2014, whereas night-time cloud cover (d) underwent a moderate increase. As a result, both direct shortwave (e) and diffuse (f) radiation increased over the same period (though diffuse radiation, non-significantly). Zonal (west to east) wind velocities (g) generally decreased, whereas meridional (south to north) wind velocities in ms-1 (h) increased.*

Second, there appears to have been a shift in wind vectors. Linear regression of hourly values reveals a decrease in zonal (west to east) wind velocity of 0.66 ms-1 over the duration of the study (n =333096, 95% CI = -0.71 to -0.60; Fig. 1.3g) and a decrease in meridional wind velocity (the northerly wind component) of 0.44 ms-1 (n =333096, 95% CI = -0.49 to -0.39;

Fig. 1.3h). Somewhat paradoxically, however, the synoptic weather type associated with easterly winds, weather type 1, also indicative of weakly anticyclonic conditions, high pressure and high relative humidity, decreased by 2.2% from 10.1% to 8.0% (n=38, 95% CI = -4.3 to -1.3%) and was the only type for which a trend was evident (Fig. S1.6 in Appendix 1). The most likely explanation of this is that while the mean zonal component of the wind vector in any given year remained relatively constant over time during periods in which synoptic weather type 1 prevailed (95% CI = -0.93 to 1.01 ms-1, n=38), the zonal component in any given year during periods in which synoptic weather types other than type 1 prevailed, decreased substantially (-1.75 ms-1 over the duration of the study; 95% CI = -1.41 to -2.09 ms-1, n=38).

Spatial variation in climate change

Linear regression of hourly temperatures in each 100 m grid cell demonstrated that grid cells have warmed, but rates of warming between 1977 and 2014 varied from 0.87ºC to 1.16ºC, with two dominant patterns evident (Fig. 1.4a). First, grid cells receiving high solar radiation have, on average warmed by more than those receiving low radiation. Second, east-facing slopes, particularly those exposed to the sea have warmed the least. The period 2010 to 2014, in which temperatures recorded at Culdrose rose by 2.30 ºC in comparison to sea-surface temperatures rising by 1.34 ºC (Fig. 1.3a,b), reveals broadly similar patterns, although an east-west gradient is more evident, with the highest temperature increases occurring towards the west of our study area (Fig. 1.4b).

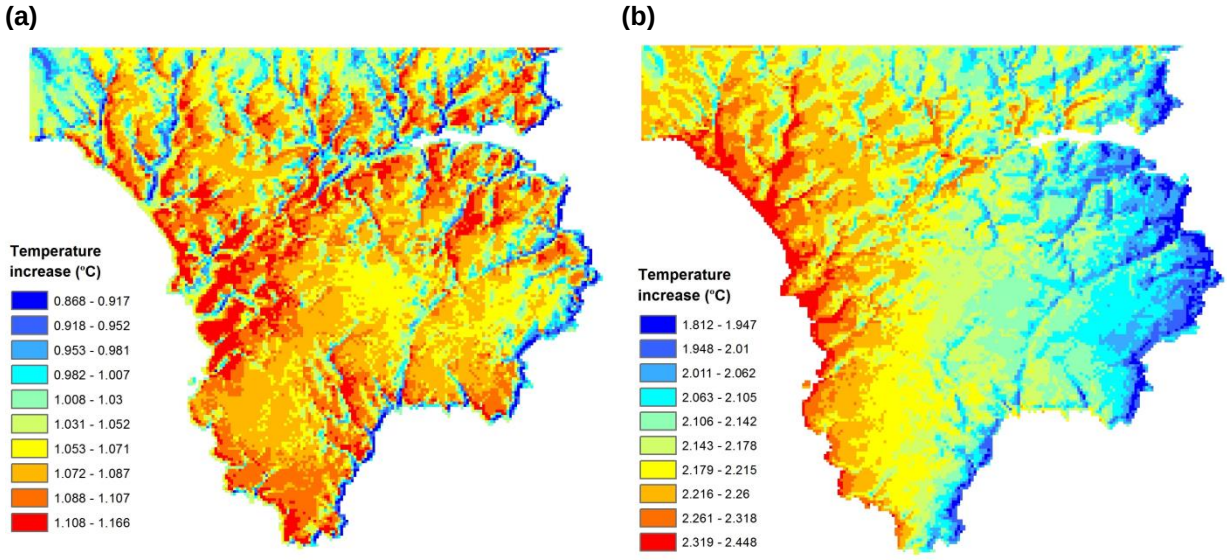

Fig. 1.4*. Spatial variation in temperature increase across the Lizard Peninsula derived from linear regression of hourly values in each 100m grid cell for the period 1979 to 2014 (a) and 2010 to 2014 (b), when land temperatures rose much faster than sea surface temperatures.*

Temperature increases were higher in the cold-season (22nd Dec-21st Mar) than in the warm- (18th Jun-15th Sep) and dry-season (14th Mar to 12th Jun), but were least marked in the wet-season (5th Oct-2nd Jan), implying that it is late-winter temperatures that have risen the most (Appendix 2g-j). Spatial patterns of change in bioclimatic variables (e.g. Appendix S2a-f) highlight that even moderate variations in temperature increase can lead to marked variation in biologically meaningful climate variables. The overall change in the number of hours of exposure to high temperatures (>20ºC) varied from a decrease of 15 hours to an increase of 256 hours, with the greatest increases occurring in areas with the greatest temperature increase, such as on southwest-facing slopes (Fig. 1.5a). The total increase in growing degree-days varied by more than a factor of 5, ranging from 51 ºC days on north-east facing

slopes at higher altitudes, to 267 ºC days on steep southwest-facing slopes (Fig. 1.5b). Changes in the length of the frost-free season also varied substantially, with marginal decreases of up to 11 days along sheltered river valleys subject to cold-air drainage, but substantial increases of up to 54 days along eastern coastal regions of our study area (Fig. 1.5c). Here, the strong east-west gradient is driven primarily by the overall likelihood of frost, which is markedly lower in western coastal areas.

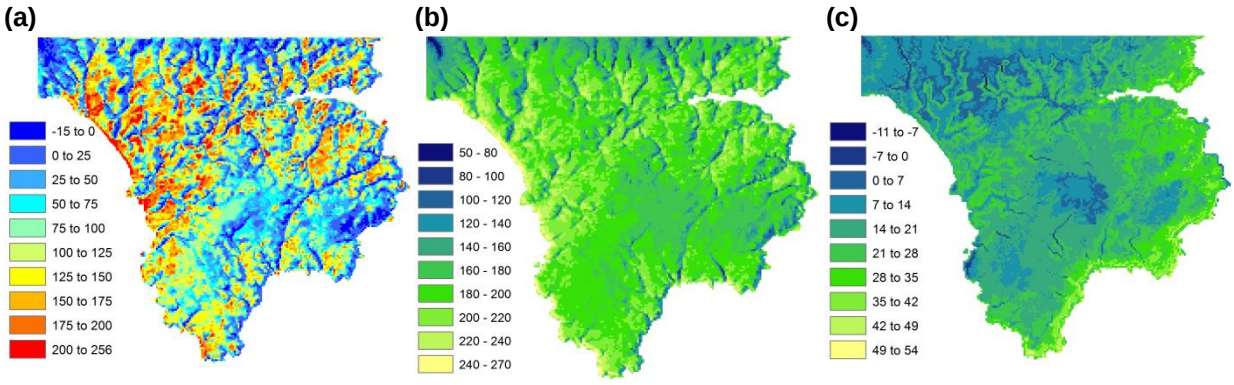

Fig. 1.5. *Spatial variation in trends in bioclimatic variables in each 100m grid cell derived from linear regression of yearly values for the period 1977 to 2014. The overall change in the number of hours of exposure to high temperatures (>20ºC) varied from a decrease of 15 hours to an increase of 256 hours (a). The total increase in growing degree-days (b) varied from 51 to 267 ºC days, whereas the overall change in the length of the frost free season (c) varied from a decrease of 11 days to an increase of 54 days.*

Closer inspection of the individual components of our model that most contribute to the spatial variation in warming suggests that the effects of solar radiation are most important (Fig. S9 in Appendix 1). This appears to have manifested itself in two ways. First, reductions in daytime cloud cover (Fig. 1.3c) have resulted in a general increase in direct radiation received at each cell, which in turn means that grid cells receiving high radiation have warmed by more than those receiving less radiation (Fig S9a in Appendix 1). Second, reductions in the westerly wind vector (Fig. 1.3g), and the concomitant increase in easterly winds, appears to have had the dual effects of decreasing the effects of radiation on these slopes (Fig S1.9c in Appendix 1) and increasing coastal effects towards the east of our study area, particularly during periods of slow rises in sea temperature (Fig 1.3b).

Discussion

Model performance

Our model provides reliable estimates of local temperatures, and demonstrates the potential advantage of modelling the physical processes that drive climatic variation, albeit that assumptions must be made about the functional relationships between temperature and the features that influence this. It also provides finer-grained and more accurate estimates than previous physical-based models (Gunton *et al*., 2015, Kearney *et al*., 2014). It is not surprising that our model provides more accurate estimates than attempts to model continent-wide local temperatures, as the geographical characteristics and weather patterns that influence local temperature anomalies are likely to vary by region. Attempts to model local ground temperatures based on local radiation budgets and weather station data situated within a few hundred metres of a study area, such that meso-climatic variation is implicitly accounted for, have resulted in models capable of estimating in excess of 90% of local variation in temperature (Bennie *et al*., 2008), emphasising that it is the influence of regional air flows on temperature rather than the effects of local radiation that are more difficult to model reliably. At fine scales, in the order of millimetres to metres, it is local radiation that dominates the

earth's energy budget, whereas at scales of metres to kilometres, the horizontal and vertical transfer of energy by moving air-masses becomes increasingly important (Geiger, 1965).

Nonetheless, over the extent of our study area, local variation in net solar radiation appears to be the dominant driver of variation in temperature, and it is thus worth highlighting that there are at least three limitations associated with our ability to capture the effects of this variation. First, because we have attempted to model long term changes in temperature, our estimates of incoming short-wave radiation are based on crude estimates of cloud cover at a single point location. Incoming radiation, as well as being affected by spatial variation in cloud clover, is also affected by cloud thickness and atmospheric conditions, notably by the concentration of aerosols and atmospheric gases (Kasten, 1996, Twomey, 1991). Spatial and temporal variation in these is unaccounted for by our model, and is likely to account for much of the unexplained variance in local temperatures. Second, our model makes no attempt to account for the effects of vegetation. Vegetation is known to have strong influence on local temperatures, and although these differences are greatest closest to the ground (Suggitt *et al*., 2011), canopy cover and leaf area density affect solar radiation budgets (Kuuluvainen & Pukkala, 1989). Our temperature loggers were all located in areas with minimal canopy cover and our model is intended to be of temperatures in land cover types in which temperatures a metre above the ground are not strongly affected by vegetative shading. Lastly, for the purposes of efficiently modelling hourly temperatures, we use a simple linear relationship between net radiation and temperature, thus making the assumption that soil heat flux is relatively small and temperatures rapidly achieve equilibrium with environmental conditions (see also Bennie *et al*., 2008). While it is likely that heat exchange may cause time-lags between radiation and temperature, perhaps a greater consideration is the scale-dependency of effects of topographic variation on the radiation budget. Estimates of slope and aspect for a 100 m grid cell essentially average the fine-scale variation in these measures. However, the aggregated effects on radiation of this variation may scale non-linearly with coarse-scale estimates of radiation, perhaps explaining why our model fails to capture perfectly the local temperature extremes. Future efforts to model local temperatures might benefit from exploring these non-linearities. Further improvements in modelling are also likely to be obtained by explicitly accounting for the effects of land-sea temperature gradients on coastal wind processes (e.g. Savijärvi, 2004), and by more sophisticated modelling of katabatic flows (e.g. Manins & Sawford, 1979). Our existing model provides poor representation of the effects of slope steepness on pooling and the cumulative time over which pooling occurs.

Overall, however, our study demonstrates the possibility of predicting temperatures at high spatial resolution and frequency using readily available data. We believe that the process of statistically calibrating variables that capture underlying physical processes ensures that a good combination of utility, analytical tractability and robustness, particularly to novel conditions, is achieved.

Spatial variation in climatic change

The results of this study provide evidence that there is at least some fine-scale variation in rates of warming, with rates of warming typically higher on southwest-facing slopes and in this respect, are similar to those of Ashcroft *et al.*, (2009) who also demonstrate fine scale variation in rates of warming, with higher warming on equatorward-facing slopes. While our results suggest that the variation in rates of warming is relatively moderate, being only ~20% higher on southwest-facing slopes, it is important to note that even moderate variation in temperature change manifests itself in substantial variation in the rate of change in biologically-meaningful climate variables. Overall increases in growing-degree days varied by more than a factor of five, and changes in exposure to high temperatures varied from a decrease to a marked increase. The greatest variation was, however, observed in the length of the frost free-season. Sheltered valleys subject to cold-air drainage have experienced a shortening in the frost-free season, likely due to the increase in clear-sky conditions, whereas coastal fringes in the east

of our study area have experienced an increase of over a month. Our results emphasise that in frost-rare environments even minor temperature changes can lead to a large change in the likelihood of frost and spatial variation in the prevalence of frost is amplified substantially.

These variations in bioclimatic variables imply that organisms occupying different parts of the landscape will experience variable rates of change. We emphasise that it is not the existence of cool microclimate *per se* that leads to the potential existence of microrefugia, but it is the extent to which changes in weather conditions lead to thermal decoupling of local trends in temperature change from those occurring regionally.

Across our study area and over the duration for which our model provides estimates of temperature, there appear to be two dominant trends in weather conditions that account for the variation in temperature increase. First, daytime cloud cover has generally declined, with a particularly substantial decline over the period between the early 1990s and 2010. As a consequence net solar radiation has increased, with the overriding effect that the temperature rise is amplified in areas receiving more radiation. In consequence, cooler microclimates are also those that have experienced the least change. Second, there has been a decline in westerly airflow, and west-facing slopes have thus become less exposed to wind, which has the effect of reducing the degree of thermal coupling of the surface to the atmosphere (Bennie *et al.*, 2008, Geiger, 1965). The overriding influence of this on temperature change is that the effects of increasing radiation are amplified on west-facing slopes. A secondary effect is, however, evident during periods in which sea-surface temperatures increased more slowly than land temperatures, such as between 2010 and 2014. In these circumstances, the attenuating effect of sea temperatures on coastal land temperatures appears to be counteracted on westerly seaboards, by the reduction in coastal influences caused by reductions in westerly winds. On eastern seaboards, however, the attenuating effects of the sea are magnified, resulting in a strong east-west gradient in temperature increase.

In common with other studies (e.g. Ashcroft *et al.*, 2009, Dobrowski, 2011, Hylander *et al.*, 2015), our results emphasise the importance of changes in weather patterns in driving local variation in temperature change, but also provide additional mechanistic insight into the factors responsible. Our findings are also supported by research on the long-term trends in the prevalence of different weather types in the North Atlantic, particularly those associated with weather patterns in spring and summer (Philipp *et al.*, 2007). Conditions associated with blocking highs over Great Britain, characterised by high pressure and clear skies have increased sharply, particularly in spring, likely accounting for the reduction in cloud cover and potentially also the reduction in westerly airflow. It is important to emphasise, however, that there is little evidence for uninterrupted long-term trends in the prevalence of synoptic weather conditions, and the majority undergo multi-decadal variation (Philipp *et al.*, 2007). In consequence, the localities least vulnerable to warming are prone to change, and microrefugia should be best viewed as temporary holdouts (see Hannah *et al.*, 2014 for further details of this concept). In the context of future climatic change, however, one likely effect is the slower rise in sea-surface temperatures relative to those on land (IPCC 2014). While in our study, the impacts of this are masked by trends in weather patterns, and the strong maritime influence across our entire study area, in most parts of the world coastal regions have undergone less temperature change. The effects of coastal buffering are evident in coarser-scale climatic variation across the UK (Jenkins, 2007), but are also likely to occur at finer scales. Overall, the influence of changes in weather conditions is unlikely to be unique to our study area and our findings thus provide insight into how trends in weather conditions may influence local variation in temperature change.

Ecological implications

Understanding spatial variation in rates of warming could act as a foundation for addressing the discrepancy between the scales at which organisms experience climatic changes and

those at which climatic effects are typically measured and modelled (Potter *et al.*, 2013) and may serve to identify locations where species are less vulnerable to climate change or where management could be targeted to offset the effects of climate change (Greenwood *et al*., 2016). For example, the wall brown butterfly (*Lasiommata megera*) has undergone widespread population extinctions due to warming temperatures in Northern Europe, but rates of decline are lower in areas experiencing less warming (Van Dyck *et al*., 2015).

The results of our study also help to elucidate the physical processes that define and create microrefugia. Our study suggests that the locations of microrefugia are likely to be influenced strongly by long-term trends in weather patterns, but in common with previous work (Ashcroft *et al*., 2009), the places experiencing the least warming under recent conditions are also those with coolest microclimates. The premise that ecological communities in such locations may be buffered against the effects of climatic change is also supported by the evidence that, within our study area, 30-year temperature-driven changes in plant communities are lower on north-east facing slopes (Maclean *et al*., 2015; Chapter 2).

Our study provides strong evidence that trends in synoptic weather patterns result in spatially variable rates of warming across a landscapes, leading to substantial spatial heterogeneity in biologically relevant climate variables. Most significant is the variation in the length of the frost-free season, which has slightly decreased at higher altitude inland, but has increased by over a month in south-east facing coastal regions. It is important to emphasise, however, that the long-term consistency in the locations least vulnerable to climatic changes are likely to be linked to long-term weather trends and may thus be ephemeral. Nonetheless, much of the ecology of long-term climatic change is likely to be occurring at finer scales than is currently appreciated. Methods that allow these changes to be quantified are much needed if these remaining uncertainties are to be resolved.

Chapter 2: Microclimates buffer the responses of plant communities to climate change.

Published version: Maclean IMD, Hopkins JJ, Bennie J, Lawson CR, Wilson RJ (2015). Microclimates buffer the responses of plant communities to climate change. *Global Ecology and Biogeography*, 24: 1340-1350. DOI: 10.1111/geb.12359

Abstract

Despite predictions of high extinction risk from climate change, range expansions have been documented more frequently than range retractions, prompting suggestions that species can endure climatic changes by persisting in cool or damp microclimates. We test whether such 'microrefugia' exist. We examine fine-scale changes in plant communities of coastal grassland on the Lizard Peninsula, UK, over a 30 year period in which spring temperatures increased by 1.4ºC. We examine whether changes in community composition and local colonisations and extinctions are related to microclimatic conditions. Our findings suggest that, while community reassembly was consistent with warming, changes were smaller on cooler, north-facing slopes. Closer inspection of patterns of species turnover revealed that species with low temperature requirements were able to persist on cooler slopes, while those with high moisture requirements suffered similar decreases in occupancy across all microclimates. Overall, our results suggest that cooler slopes may act as microrefugia, buffering the effects of increases in temperature on plant communities by delaying extinctions of species with low temperature requirements.

Introduction

Much biogeographic research is underpinned by the desire to predict how species distributions are altered by climate change (e.g. Pearson & Dawson, 2002; Hampe, 2004; Araújo *et al.*, 2005; Chen *et al.*, 2011; Maclean & Wilson, 2011). A widely-used approach for making such predictions is climate envelope modelling, in which the future range of a species is inferred from the climatic characteristics of localities in which it is currently known to occur (e.g. Berry *et al.*, 2002). However, a core assumption of this approach: that species will disappear from climatically unsuitable areas, is at odds with the phenomenon that range expansions have been documented more frequently than range retractions (Thomas *et al.*, 2006; Sunday *et al.*, 2012). Paradoxically, however, retractions are often inherently assumed. These models have predicted that many species are likely to have reduced future range sizes and thus will face higher extinction risk under climate change (e.g. Thomas *et al*., 2004), and the single most repeated suggestion for adapting conservation strategies to climate change is to facilitate movement towards climatically suitable areas (Heller & Zavaleta, 2009). However, to determine how effective these measures are likely to be for promoting species persistence under climate change, we require better understanding of the mechanisms governing range retractions.

A likely explanation for why range retractions have been documented less often than range expansions is the possibility that, instead of becoming entirely extirpated from a region, some proportion of trailing-edge populations survive (Hampe & Jump, 2011). This could be short-term survival whereby populations are committed to extinctions, but demographic and meta-population processes mean that population responses lag behind climatic trends (Kuussaari *et al.*, 2009; Dullinger *et al*. 2012). Alternatively, further delays in macro-scale range retractions may be caused by the continued survival of relic populations in suitable microclimate that are generated by fine-scale habitat and topographic structure, often termed microrefugia (Rull, 2009; Hampe & Jump, 2011; Ashcroft *et al.*, 2012). Even if range retractions are occurring in pace with climate change, they may be localised and not evident at coarser scales: many populations would need to go extinct before a coarse-scale grid cell is deemed unoccupied (Thomas *et al.*, 2006).

There is little consensus with regards to which trailing-edge populations can survive, and for how long. A fundamental reason for this is that the spatial scales at which shifts are measured and modelled are typically several orders of magnitude larger than the scales at which individuals actually experience and respond to climate (Potter *et al.*, 2013). While recent understanding of the topographic controls of local variation in climate and the development of fine-scale climate models has helped to quantify and locate potential microrefugia (Dobrowski, 2011; Ashcroft *et al*., 2012), empirical evidence for their existence in the context of recent climate change, and understanding of the mechanisms that could allow species to exploit suitable microclimate is limited. Both Randin *et al.* (2009) and Scherrer & Körner (2011) examine climate change-induced habitat losses in alpine plants and show that micro-scale models predict far greater persistence of suitable habitats in comparison to European-scale models. In direct contrast, Trivedi *et al.* (2009), working on high-altitude plants in Scotland, show that local-scale models predict the regional extinction of 70-80% of studied species, whereas European-scale models predict such loss for only one species. Both studies, however, make use of single snapshots of species distributions to test their models. In essence, the extent to which these individual responses to microclimate can be captured in aggregate by associations between population presence and macroclimate (Bennie *et al.*, 2014) will depend on two factors. Firstly, on variation in the availability of cool microclimates across a landscape. If the availability of cool microclimate is greater at the trailing edge of species' ranges then fine-scale models will typically reveal that species are less threatened than would be revealed by coarse-scale models. This pattern that can be readily captured by single-snapshot species distribution models and differences in the availability of cool microclimate in different landscapes readily explains the discrepancy between the findings of

previous studies. However, the relative rate at which populations vacate their current microhabitats and colonise new ones as ambient conditions change is also important. For example, if trailing-edge populations vacate microclimates at the same rate as leading-edge populations occupy microclimates, the effects of fine-scale heterogeneity in microclimate will "average out" and the species' distribution will shift in line with coarse-scale temperature averages. Conversely, if leading-edge microclimates are occupied more quickly than those at the trailing edge are vacated, populations at the trailing range margin may continue to persist in spite of rising temperatures, "buffering" the species against the negative effects of climate change. However, the importance of these fine-scale temporal dynamics have been difficult to quantify, because this requires species distribution data to be collected at both a sufficiently fine scale to map the distribution of individuals among microclimates, and at a sufficiently long time interval to encompass an appreciable level of global warming.

Here, we examine fine-scale changes in plant communities over a 30-year period in which conditions became warmer and drier to assess the mechanisms underlying climate-driven range shifts. Specifically, we test whether changes in local community composition (colonisations of and extinctions from 2×2m relevés) are related to topographic indices of microclimate and species' temperature and moisture requirements. We examine whether species with low moisture and high temperature requirements have become more common in microsites with warmer microclimates (south and south-west rather than north and north-east facing slopes) and determine whether cooler microclimates generated by topography may slow changes in community composition, providing a "buffer" against the effects of climate change.

Material and methods

Study site and species

The study was conducted on grasslands on the Lizard Peninsula (50º 2'N, 5º 10'W), a Special Area for Conservation (92/43/EEC) covering c. 3,250 ha on the most southern tip of the United Kingdom (UK) mainland. Relative to elsewhere in the UK, the climate in this area is comparatively mild, especially in winter. Over the period of our study (1979-2011), mean annual and spring temperatures have increased by approximately 1.4 ºC (Fig. 2.1a). Our study focused on plant species associated with unimproved *Cynosurus cristatus-Plantago lanceolata* grassland, most of which is subject to grazing by livestock. Three characteristics of our study system make it particularly well suited to studying the mechanisms governing climate-driven range shifts. Firstly, vegetation changes in most UK grasslands are strongly associated with nitrogen deposition (Stevens *et al*., 2004) but, probably due to the location of our site and prevailing wind direction, there was no evidence of an increase in species associated with higher levels of nitrogen (see also Powney *et al*., 2014). Secondly, while there have been localised changes in land-use, the entire study area has been under active grazing management that has changed little over the duration of our study. Thirdly, these grasslands host a large gradient of species that differ in their temperature and moisture requirements (Hill *et al*., 2004). Some, such as Long-headed Clover (*Trifolium incarnatum* susp. *molinerii*) and Twin-headed Clover (*T. boccenei*) have a predominantly Mediterranean Atlantic distribution and reach the northern extremity of their range on the Lizard Peninsula. Others, such as Spring Sandwort (*Minuartia verna*), have Boreal distributions and our study site constitutes the southern extremity of their range (Preston & Hill, 1997; Hopkins, 2006). There is also substantial variation in the moisture requirements of the species associated with this type of grassland (Ellenberg *et al*., 1991; Hill *et al*., 2004) and, in contrast to many systems, this correlates only very weakly with temperature. Consequently, the roles of temperature and moisture requirements in determining microclimate use can be distinguished from one another.

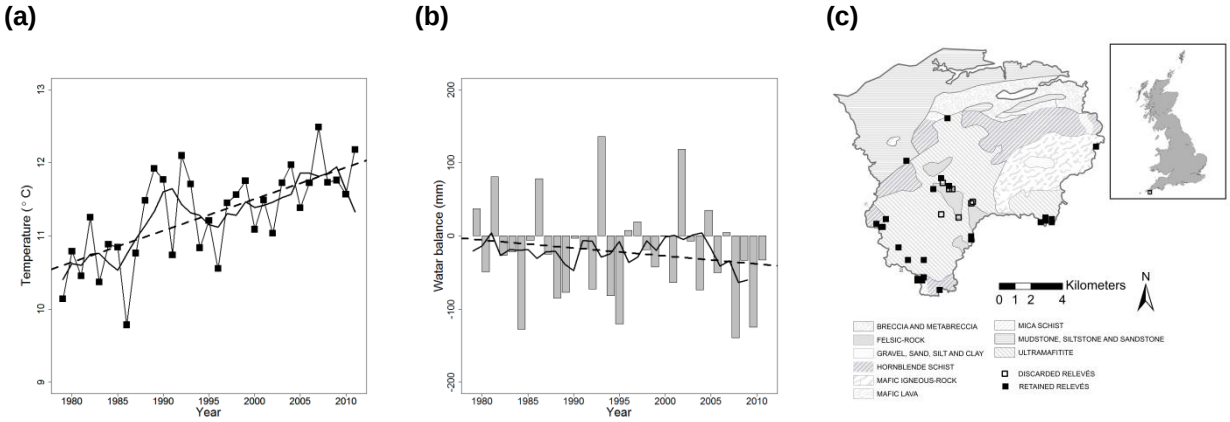

Fig. 2.1. *April-June temperature (**a**) and water-balance (**b**) trend for the Lizard Peninsula study site, with the location of sampled relevés shown (**c**). The temperature trend was calculated using weather station data from Culdrose (50.087ºN, 5.254ºW). The water-balance is the difference between rainfall (positive) and potential evapotranspiration (negative) and details of how this was calculated are provided in Appendix 3. Black squares depict mean (temperature) and summed (water-balance) seasonal values in each year. The dotted lines present linear trends and solid lines the five-year rolling mean. Bedrock geology was reproduced with the permission of the British Geological Survey ©NERC.*

Survey methods

We sampled community species composition in different microclimates (microhabitats with different slope and aspect) over two periods: 1979-1980 and 2011. Between mid-April and the end of June in 1979 and 1980, all higher plant species in 55 two metre x two metre relevés were recorded (Fig. 2.1b). A semi-subjective sampling strategy was adopted with the aim of

ensuring that several fairly widely spaced plots were placed at all localities in which vegetation was typical of that associated with the habitat type. This step was necessary both because this community type often occurs within small-scale mosaics and because the original survey was not carried out with the intention of sampling randomly. At each plot location, six figure (accurate to nearest 100m) grid references were recorded using 1:10.000 scale Ordnance Survey maps. The cover abundance of all taxa occurring within the sample plots was estimated visually and recorded using the ten point Domin scale described by Currall (1987). In addition, slope (measured using an Abney level), aspect (measured by compass and expressed as one of 16 points), sward height (from the soil surface to the mean maximum height of vegetation, ignoring individual extremes) and vegetation cover (everything except bare ground) were recorded. Further details of the survey protocols are given in Hopkins (1983).

In 2011 the survey was repeated by revisiting each of the study locations surveyed in 1979-80. However, sample plots were not georeferenced to high precision in 1979-80; consequently, a repeat survey of exactly the same plots as were surveyed in 1979-80 was not possible. The approximate locality (within 100m) of each relevé was thus revisited and a sample plot in *Cynosurus cristatus-Plantago lanceolata* grassland with similar geology, soil, sward height, vegetation cover, slope and aspect was selected for resurvey. While the uncertainty in historic plot locations may have inflated our estimates of species turnover, previous work has shown that estimates of changes in species composition are generally robust to location uncertainty (Kopecký & Macek, 2015). At nine localities, land use had changed considerably over the thirty year period and it was not possible to find a sample plot with appropriate characteristics. These plots were removed from subsequent analyses (Fig. 2.1b). Measurements were carried-out in the same way as in 1979-80, and IMDM (who carried out surveys in 2011) consulted with JJH (who carried out the surveys in 1979-80) prior to embarking on data collection. The only way in which the methods differed, was that plots in 2011 plot locations were georeferenced to high precision (sub 10 m) using a Global Positioning System (GPS). The dataset is thus 46 pairs of 2 x 2 m relevés located within 100m of each other but not in identical locations.

Microclimate

To provide a proxy of the microclimate, we calculated the proportion of potential direct irradiance intercepted by the surface in each relevé for a given solar zenith and azimuth (hereafter referred to as insolation) as follows:

$$Ri = \cos S \cos Z + \sin \beta \sin Z \cos(\Omega_s - \Omega)$$

where Ri is the proportion of potential direct irradiance intercepted by the slope, S is the angle of the slope, Z is the solar zenith, Ω_s is the solar azimuth and Ω is the slope aspect. The solar zenith and azimuth are functions of latitude, Julian day and were derived using methods detailed in Hofierka (2002) and Bennie *et al.* (2008). We used the mean value for every hourly period between 1st of May and 30th of June as our measure, as this period corresponds to the growing season. As the slopes and aspects were near-identical in each paired set of relevés, and geographic location independent of slope and aspect has little bearing on insolation at scales of a few hundred metres, our calculation of insolation is largely unaffected by location uncertainty. For subsequent analyses, we logit transformed insolation scores to ensure a continuous range of values.

While interactions between topography and the prevalent wind direction and cold-air drainage can have important strong effects on mesoclimatic variation (Ashcroft *et al.*, 2009; Bennie *et al.*, 2010; Chapter), topographically-driven variation in insolation is the dominant influence on near-surface temperatures and soil moisture content (Bennie *et al.*, 2008; Scherrer & Koerner, 2010; Maclean *et al.*, 2012; Chapter 1) and thus serves as the most useful proxy for

characterising microclimatic variation across our study area in the absence of fine-scale climate data. Using the approach described above, insolation scores are low for north-facing slopes with aspects in the range 0-100º and >290º and high for slopes with south-facing aspects in the range of 120-270º. The relationship between aspect and insolation depends on slope angle, but scores are typically higher on west-facing than east-facing slopes (Fig S3.1 in Appendix 3).

Community reassembly

To assess community reassembly, we measured the dissimilarity of plant assemblages between the two study periods in each relevé using the Sørensen's index, which measures dissimilarity in species presence, and the Morisita-Horn index, which also accounts for difference in abundance (Sørensen, 1948; Horn, 1966). As both indices are usually used to measure similarity, we expressed dissimilarity as 1- *S*, where *S* is the measure of similarity obtained using these indices. The Sørensen's index (D_S) was calculated as follows:

$$D_S = 1 - \frac{2A}{2A + B + C}$$

where *A* is the number of species shared in both periods and *B* and *C* are the number of species unique to both periods. The Morisita-Horn index (D_{MH}) was calculated as follows:

$$D_{MH} = 1 - \frac{2\sum_{i=1}^{S} a_i b_i}{\left(\sum_{i=1}^{S} \frac{a_i^2}{P_a^2} + \sum_{i=1}^{S} \frac{b_i^2}{P_b^2}\right) P_a P_b}$$

where P_a is the total proportion cover of individuals in the first period, P_b the total proportion cover of individuals in the second period, a_i the proportion cover of individuals of the i^{th} species in the first period, b_i the proportion cover of individuals in the second period and *S* the number of unique species. Both indices scale such that zero represents no reassembly (all species common to both periods) and one represents complete reassembly (no species common to both periods). We converted the Domin scores to proportion cover using the transformation recommended by Currall (1987):

$$C = \frac{D^{2.6}}{400}$$

Where *C* is proportion cover and *D* is the Domin score.

Linear-regressions, using each pair of relevés as a separate data point, were then used to examine whether the two measures of community dissimilarity were related to insolation.

Community characteristics

To determine links between climate change and community reassembly, we calculated community temperature and moisture indices. These indices were constructed as follows: first, we converted the Domin scores to proportion cover using the Currall (1987) method. Second, we derived the Ellenberg Indicator value for moisture (Ellenberg *et al*., 1991) for each species, again given in the data accompanying Hill *et al*. (2004) and hereafter referred to as the Ellenberg moisture index. Third, we obtained the mean July temperature of the 10-km squares in which each species occurs in Britain, Ireland and the Channel Islands as given in the data

accompanying Hill *et al.* (2004) and hereafter referred to as the species temperature index. We acknowledge that this temperature index may underestimate species' temperature requirements, but Ellenberg indicator values for temperature are unsatisfactory in an oceanic climate such as that of Britain and are therefore unavailable for UK plants. Lastly, the weighted (by proportion cover) mean species temperature and Ellenberg moisture index values across species of each relevé were calculated as follows:

$$CTI = \frac{\sum_{i=1}^{S} TI_i P_i}{\sum_{i=1}^{S} P_i} \text{ and } CMI = \frac{\sum_{i=1}^{S} EMV_i P_i}{\sum_{i=1}^{S} P_i}$$

Where *CTI* is the community temperature index, *CMI* is the community moisture index, TI_i and EMV_i are the species temperature and Ellenberg moisture index values for each species *i* present in the relevés, P_i is the proportional cover of that species and *S* is the number of species.

To examine whether changes in the community temperature and moisture indices between the two study periods were related to insolation we used a linear mixed model with community index values for each relevé modelled as a separate data point. Relevé was modelled as a random intercept and period and insolation and an interaction between these were treated as fixed effects. Analysis was performed using the nlme package (Pinheiro *et al*., 2004) for R (R Development Core Team, 2014).

Colonisations and extinctions

We examined differences in the temperature and moisture indices of species recorded in both periods or in one period only using analysis of variance. We also modelled colonisations and extinctions of each species from individual relevés using two generalised linear mixed models with binary response variables: (i) persistence or extinction of relevés in the second period (2011) of species recorded in the first period (1979-1980) and (ii) colonisation of relevés in the second period by species not recorded in the first period. Each species, in each relevé, was treated as a separate data point. Moisture, species temperature index values and insolation (logit transformed) associated with each pair of relevés were modelled as fixed factors along with interactions between insolation and the moisture and temperature indices. Species and relevé were modelled as random intercepts. To investigate the possible role of biotic interactions we also repeated the analyses with vegetation cover, sward height and species richness (in the earlier period for extinctions and in the later period for colonisations) included as additional explanatory terms. Parameter estimates were obtained for individual models and also by AIC-weighted model averaging of all plausible models ($\Delta AIC<6$) using the MuMIN package for R (Bartoń, 2014). Since the locations of the relevés could only be approximately matched between the two study periods, the true rates of colonisation of and extinction from relevés may be lower than estimated here (although see Kopecký & Macek, 2015).

Results

Community reassembly

The mean proportional dissimilarity in the community composition of relevés between the two study periods, as measured by Sørensen's index (1- D_S), which is only influenced by species presence, was 0.48 (mean ± 1 s.e. range: 0.46-0.50, *N* = 46). Dissimilarity using this measure was also positively associated with insolation (Δ*AIC* from null model = -7.49, *N* = 46; Fig. 2.2a). The mean proportional dissimilarity in the community composition of relevés between the two study periods, as indicated by Morisita-Horn Index, which is influenced by composition and abundance, was also 0.48 (mean ± 1 s.e. range: 0.44-0.53, *N* = 46). Dissimilarity measured using the Morisita-Horn Index was also positively associated with insolation (Δ*AIC* from null model = -10.71, *N* = 46; Fig. 2.2b).

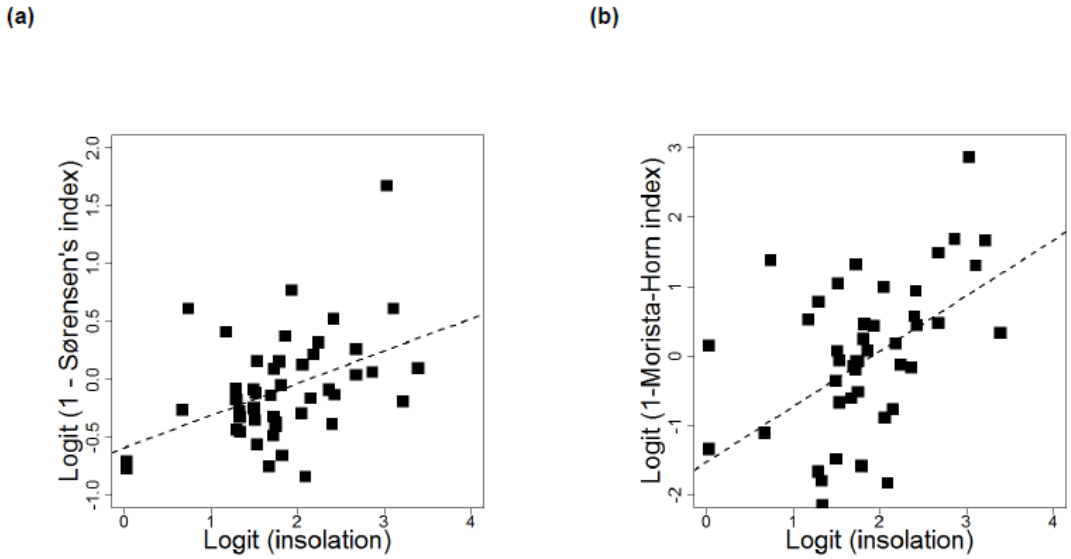

Fig. 2.2. *The effects of insolation on the dissimilarity in community composition of relevés sampled on the Lizard Peninsula between the 1979/80 and 2011 study periods, as indicated by Sørensen's index (**a**) and the Morisita-Horn index (**b**).*

Community characteristics

Between the two study periods, there was an increase in the community temperature index of sampled relevés (Δ*AIC* from model with just random effect of relevé = -55.4, *N* = 92). The most parsimonious model explaining the community temperature index was one in which period, insolation and an interaction between period and insolation were included (Δ*AIC* from model with just the random effect of relevé = -100.7, *N* = 92). This model suggested that the community temperature index was higher in areas with higher insolation and was also higher in 2011 than in 1979-80. In 2011, the relationship between the community temperature index and insolation was stronger than in 1979-80 (Fig. 2.3a). All other models were implausible (ΔAIC>6; Table 2.1).

Between the two study periods, there was a decrease in the community moisture index of sampled relevés (Δ*AIC* from model with just random effect of relevé = 35.8, *N* = 92). The most parsimonious model explaining the community moisture index was one in which period and insolation were included (Δ*AIC* from model with just the random effect of relevé = 87.5, *N* = 92), although a model that included these terms and an interaction between period and insolation was also plausible (Δ*AIC* = 2.3). The best model suggested that the community

moisture index was lower in areas with higher insolation and was also lower in 2011 than in 1979-80 (Fig. 2.3b). The results of the model dredge and coefficient estimate obtained by model averaging of plausible models (ΔAIC<6) are shown in Table 2.2.

(a) **(b)**

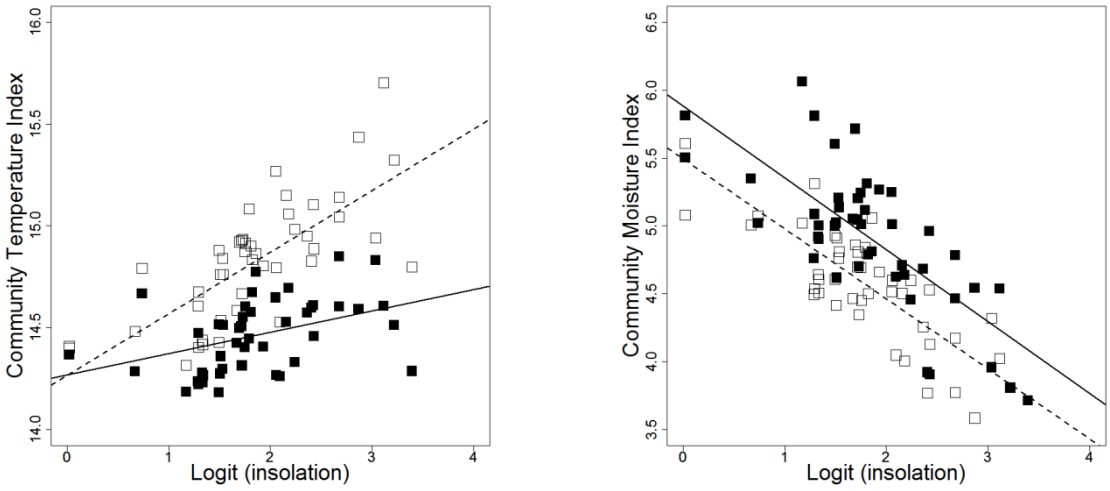

Fig. 2.3. *Community temperature (**a**) and moisture (**b**) indices of plant communities in relevés sampled on the Lizard Peninsula as a function of the period in which data were collected (solid squares = 1979/80, open squares = 2011) and logit insolation.*

***Table 2.1**. Results of linear mixed-effect analyses investigating the determinants of the plant community temperature index of sampled relevés. Parameter estimates, Akaike's Information Criterion (AIC), the change in AIC (ΔAIC) and Akaike weights for each model are shown. NA indicates that the term was not included in the model. Parameter estimates and 95 percent confidence intervals (95% CIs) derived from model averaging using Akaike weights are also shown.*

	Intercept	Period	Insolation	Period x insolation	AIC	ΔAIC	weight
Individual model estimates	14.27	-0.002	0.105	0.197	-52.2	0.0	1.00
	14.09	0.359	0.203	NA	-31.9	20.3	0.00
	14.46	0.359	NA	NA	-6.9	45.3	0.00
	14.27	NA	0.203	NA	26.8	78.9	0.00
	14.64	NA	NA	NA	48.5	100.7	0.00
95% CI upper bound	14.12	-0.146	0.029	0.124	Model averaged estimates		
Estimate	14.27	-0.002	0.105	0.197			
95% CI lower bound	14.42	0.143	0.181	0.270			

***Table 2.2**. Results of linear mixed-effect analyses investigating the determinants of the plant community moisture index of sampled relevés. Parameter estimates, Akaike's Information Criterion (AIC), the change in AIC (ΔAIC) and Akaike weights for each model are shown. NA indicates that the term was not included in the model. Parameter estimates and 95 percent confidence intervals (95% CIs) derived from model averaging using Akaike weights are also shown.*

	Intercept	Period	Insolation	Period x insolation	AIC	ΔAIC	weight
Individual model estimates	5.88	-0.384	-0.527	NA	45.9	0.00	0.755
	5.89	-0.409	-0.534	0.0138	48.2	2.3	0.245
	5.69	NA	-0.527	NA	81.6	35.7	0.000
	4.91	-0.384	NA	NA	97.7	51.7	0.000
	4.72	NA	NA	NA	133.4	87.5	0.000
95% CI upper bound	5.66	-0.557	-0.641	-0.130	Model averaged estimates		
Estimate	5.88	-0.390	-0.529	0.0138			
95% CI lower bound	6.11	-0.223	-0.416	0.157			

Colonisations and extinctions

We recorded a total of 183 species. Of these, 114 were present in at least one relevé in both periods, 32 in 1979-80 but not in 2011 and 37 in 2011 but not in 1979-80 (see Appendix 3). There were no significant differences in the temperature or moisture indices among species present in both periods or in only one period or the other.

The most parsimonious model explaining colonisation to relevés was the one in which the species temperature and Ellenberg moisture indices, insolation and an interaction between the species temperature index and insolation were included as explanatory terms (Δ*AIC* from model with just the random effect of species = 112.5, *N* = 1,354). There were a relatively large number of plausible models and fairly wide confidence intervals associated with coefficient estimates derived from model averaging (Table 2.3). Nonetheless, there is strong support that colonisations were more likely by species with a high temperature index and into areas with higher insolation, and that the increased colonisation likelihood of species with high

temperature requirements relative to those with low temperature requirements was more pronounced in areas with high insolation. There is fairly strong evidence that colonisations were less likely by species with high moisture requirements, although the 95% confidence intervals of the coefficient estimate for this term overlap with zero (Table 2.3). Models in which sward height, species richness and vegetation cover were additionally included as explanatory terms, suggested that colonisations were more likely to relevés with high species richness, higher vegetation cover and longer sward. The inclusion of sward height, species richness and vegetation cover into models had very little consequence for the effects of insolation and species temperature and Ellenberg moisture indices (Table S2.1).

Table 2.3*. Results of generalised linear mixed-effect analyses investigating the determinants of colonisations to sampled relevés. Parameter estimates, Akaike's Information Criterion (AIC), the change in AIC (ΔAIC) and Akaike weights for each model are shown. NA indicates that the term was not included in the model. Parameter estimates and 95 percent confidence intervals (95% CIs) derived from model averaging using Akaike weights are also shown.*

	Intercept	**Temperature index**	**Ellenberg Moisture index**	**Insolation**	**Insolation x Temperature index**	**Insolation x Ellenberg moisture index**	**AIC**	**ΔAIC**	**weight**
Individual model estimates	-60.0	4.08	-0.28	80.9	-6.41	NA	5691.1	0	0.517
	-35.7	3.37	-1.26	58.8	-5.38	1.42	5692.0	0.9	0.330
	23.0	-0.36	-1.93	-25.9	NA	2.38	5694.2	3.1	0.111
	15.0	-0.36	-0.28	-14.4	NA	NA	5696.2	5.1	0.041
	17.6	NA	-1.92	-26.2	NA	2.45	5703.6	12.4	0.001
	9.36	NA	-0.22	-14.3	NA	NA	5705.5	14.4	0.000
	4.93	-0.36	-0.28	NA	NA	NA	5717.6	26.5	0.000
	-56.0	4.32	NA	81.5	-6.45	NA	5719.5	28.4	0.000
	8.30	NA	NA	-14.4	NA	NA	5724.4	33.2	0.000
	10.51	-0.15	NA	-14.4	NA	NA	5724.5	33.3	0.000
	-0.64	NA	-0.22	NA	NA	NA	5726.9	35.8	0.000
	-1.744	NA	NA	NA	NA	NA	5745.7	54.5	0.000
	0.43	-0.15	NA	NA	NA	NA	5745.8	54.7	0.000
95% CI upper bound	2.0	6.72	0.50	140.3	-1.79	3.64	Model averaged estimates		
Estimate	-45.0	3.80	-0.66	72.3	-6.01	1.42			
95% CI lower bound	-92.1	0.89	-1.83	4.26	-10.23	-0.81			

The most parsimonious model explaining extinction from relevés was one in which the species temperature and Ellenberg moisture indices, insolation and an interaction between the species temperature and insolation were included as explanatory terms (Δ*AIC* from model with just the random effect of species = -27.4, *N* = 6,696). Again, there were a relatively large number of plausible models and fairly wide confidence intervals associated with coefficient estimates derived from model averaging (Table 2.4). Nonetheless, there was strong support that extinctions were more likely of species with low temperature indices and from areas with lower insolation, but the latter effect is overridden by the pattern that those species with low temperature indices were far less likely than species with high temperature indices to go extinct from areas with low insolation, as its directional effect is reversed when the interaction is not included. There is fairly strong evidence that extinctions were more likely by species with high moisture requirements, although the 95% confidence intervals of the coefficient estimate for this term overlap with zero (Table 2.4). Models in which sward height, species richness and vegetation cover were additionally included as explanatory terms, suggested that

extinctions were more likely from relevés with shorter sward. The inclusion of sward height, species richness and vegetation cover into models had very little consequence for the effects of insolation and species temperature and Ellenberg moisture indices (Table S3.1 in Appendix 3).

Table 2.4*. Results of generalised linear mixed-effect analyses investigating the determinants of extinctions from sampled relevés. Parameter estimates, Akaike's Information Criterion (AIC), the change in AIC (ΔAIC) and Akaike weights for each model are shown. NA indicates that the term was not included in the model. Parameter estimates and 95 percent confidence intervals (95% CIs) derived from model averaging using Akaike weights are also shown.*

	Intercept	**Temperature index**	**Ellenberg Moisture index**	**Insolation**	**Insolation x Temperature index**	**Insolation x Ellenberg moisture index**	**AIC**	**ΔAIC**	**weight**
Individual model estimates	240.5	-17.1	0.28	-344.3	24.5	NA	1666.2	0	0.589
	209.0	-15.4	1.44	-299.5	21.9	-1.67	1668.1	1.9	0.231
	241.7	-17.1	NA	-340.4	24.2	NA	1669.4	3.2	0.120
	-10.45	NA	0.26	14.1	NA	NA	1672.9	6.6	0.022
	-23.0	NA	2.97	32.0	NA	-3.87	1673.3	7.1	0.017
	-11.52	0.07	0.27	14.1	NA	NA	1674.8	8.6	0.008
	-24.1	0.07	2.99	31.9	NA	-3.87	1675.2	9.0	0.007
	-9.0	NA	NA	13.9	NA	NA	1676.0	9.8	0.004
	-7.7	-0.10	NA	14.0	NA	NA	1677.8	11.6	0.002
	-0.6	NA	0.26	NA	NA	NA	1684.4	18.1	0.001
	-2.2	0.10	0.28	NA	NA	NA	1686.2	20.0	0.000
	0.7	NA	NA	NA	NA	NA	1687.6	21.4	0.000
	1.7	-0.07	NA	NA	NA	NA	1689.6	23.3	0.000
95% CI upper bound	124.6	-23.7	-1.89	-483.6	13.7	-7.75	Model averaged estimates		
Estimate	231.6	-16.6	0.60	-331.7	23.7	-1.67			
95% CI lower bound	338.6	-9.5	3.10	-179.7	33.8	4.41			

Discussion

Two complementary analyses suggest that local community reassembly is at least partly driven by climate change. Firstly, the increase in community temperature indices and decrease in community moisture indices suggest that plant communities are now more dominated by species whose ranges are associated with higher temperatures and lower moisture levels. While the observed changes in the community temperature indices were lower than the magnitude of temperature warming, plant community responses to climate change typically lag behind climate change, particularly in lowland ecosystems (Bertrand *et al*., 2011). Secondly, colonisations and extinctions by individual species were related to their macro-climatic requirements. Those with a high species temperature and low Ellenberg moisture indices were more likely to have colonised new relevés than those with low temperature and high moisture requirements. Similarly, species with low temperature and high Ellenberg moisture indices were more likely to go extinct from relevés. Thus, the community composition has shifted towards species with higher temperature and lower moisture requirements.

Although community composition has shifted towards species with lower moisture requirements, and there is some evidence that species with high moisture requirements are more likely to have gone locally extinct, our analysis of the climatic characteristics of plant communities suggests that the overall change in moisture requirements of species assemblages is fairly uniform across the landscape. It is thus possible that, although the distribution of at least some species may become increasingly limited by water availability, the presence of damp microclimates would not help to buffer this effect. One might therefore expect the distributions of water-limited species to shift in line with coarse-scale changes in water availability, and there is little evidence that fine-scale data on water availability would be needed to understand current or future climatic constraints on plant distributions (see e.g. Potter *et al*., 2013). It is worth noting, however, that there is often considerable fine-scale spatial variation in water availability (Maclean *et al.*, 2012), making it difficult to detect moisture-driven range-retractions if distributions are mapped on a coarse-resolution grid as many local extinctions would need to occur before a grid cell is deemed empty. The fine-scale variation in components of climate, be it temperature or water availability, may be one of the reasons why consistent latitudinal range retractions are hard to detect (Thomas *et al.*, 2006).

In contrast, the thermophilisation of the grassland plant community was much greater in areas with higher insolation, and local extinctions by cold-adapted species were far less likely from areas with low insolation. It is thus more likely to be the cooler temperatures of north-facing slopes, rather than their higher soil moisture availability, that are responsible for the patterns of change in community composition, which reveal that less species turnover has occurred in localities with lower insolation. Our results provide compelling evidence that microclimates buffer the effects of climate change on ecological communities, insofar as species threatened by increasing temperatures may be able to persist for some time in cooler microclimates.

The reasons why plant community responses to climate change are buffered by the presence of cool microclimates are less straightforward to elucidate, not least because our study does not quantify temporal changes in fine-scale temperature at the fine resolution at which plants were sampled. However, a possible explanation is that cooler slopes are less prone to long-term temperature change as is evident at coarser scales (Maclean *et al.* 2016; Chapter 2). Previous work by Ashcroft *et al.* (2009) has also shown that cooler microclimates often experience less warming (see also chapter 1). Conducted in south-west Australia, this study showed that changes in annual maximums, and spring and summer temperatures between 1972 and 2007, were markedly lower on poleward-facing slopes, likely due to changes in weather patterns. It is possible that changing weather patterns within our study area have also resulted in less warming on poleward slopes. An alternative, albeit less plausible, explanation is that the communities associated with cooler microclimates are inherently less sensitive to warming and have consequently responded to a lesser degree.

Nonetheless, our findings differ somewhat from a previous study investigating whether microclimate moderates plant responses to macroclimate warming (De Frenne *et al.*, 2013). While the study by De Frenne *et al.* demonstrates that the thermophilisation of understory plant communities was attenuated by microclimate, this change was driven by concurrent gains of warm-adapted species and loss of cold-adapted species. Responses to warming were only moderated in instances where the microclimate itself had become cooler, as a result of greater canopy caused by a lengthening growing season. Our results showing a shift in species composition towards a community with higher temperature and lower moisture requirements also contrast with the only previous study of the influence of insolation on long-term changes in a British grassland plant community (Bennie *et al*., 2006), in which the major change was a shift towards a community dominated by more competitive species typical of mesotrophic grasslands. In the study of Bennie *et al.*, however, this change in community composition may have been due to the effects of both habitat fragmentation and nutrient enrichment, whereas in our study there was no evidence of nutrient enrichment, and changes appear to be predominantly driven by temperature.

Although species with high moisture requirements were more likely to have gone locally extinct, our analysis of the climatic characteristics of plant communities suggests that the overall change in moisture requirements of species assemblages is fairly uniform across the landscape.

In a UK grassland, we show that areas with high insolation are dominated by plants with warmer macro-climatic associations and that the plant community has responded to climate change, but not uniformly across the landscape. We demonstrate that individual species are able to exploit fine-scale climate heterogeneity as a buffer against the effects of climate change, and consequently communities as a whole are more stable in cooler microclimates. Our study provides new evidence of the importance of topographic heterogeneity in mediating range retractions. More generally, strategic conservation planning in the face of climate change, which to date is mostly informed by analyses using coarse-scale data, could benefit from giving greater credence to the importance of fine-scale climate heterogeneity.

Chapter 3. Microclimate, microrefugia and plant species persistence in a changing climate

Abstract

Over the last 15 years bioclimate models have been widely used to predict ecological responses to climate change. Results from these models suggest catastrophic consequences for life on earth, but thus far, relatively few species have gone extinct. A likely explanation of this discrepancy is that species may be able survive in regions of unsuitable climate in pockets of suitable microclimate, termed 'microrefugia'. Conventional models fail to identify microrefugia, and hence over-estimate extinction risk, simply because the data used to construct and drive the models are not sufficiently fine-grained. Here, we test whether fine-scale variation in rates of warming affects local patterns of extinction and persistence for a suite of plant species vulnerable to climate change. We show that, across all species, persistence is higher at locations experiencing the slowest rates of warming, although the effects are weak. Overall, our results suggest that north- and east-facing slopes, which have experienced less warming, may serve as microrefugia, buffering the effects of increases in temperature on plant communities by delaying extinctions of species with low temperature requirements. However, there are a number of limitations associated with the methods. More refined knowledge of the circumstances in which coarse-scale models fail to predict how species respond to climate change, and greater empirical validation using fine-scale data, is required before the nature of microrefugia can be fully understood.

Introduction

There is a great need to determine the level of threat posed by climate change to biodiversity, and the most effective means to adapt conservation to this threat. Nevertheless, there is much uncertainty in predicted changes to species distributions based on bioclimate models (Thuiller 2004), hitherto the most widely used tool for assessing extinction threat (Maclean & Wilson 2011). Over the last 15 years bioclimate models have been widely used to predict ecological responses to climate change. Results from these models suggest catastrophic consequences for life on earth, predicting for example, that by 2050, between 15 and 37% of species will be committed to extinction (Thomas *et al.* 2004). Thus far, however, climate change has been implicated as a major cause of the extinction of just nine species (IUCN 2015). Most such models rely on coarse-resolution spatial associations between species distributions and climate variables measured over tens to hundreds of kilometres, whereas the conditions experienced by many organisms vary over scales from millimetres to tens of metres (Potter *et al.* 2013). Empirical studies show that fine-resolution spatial differences in temperature can be as large as inter-continental differences at coarser resolutions, and niche models using fine-resolution climate data lead to large discrepancies with coarse-scale models (Trivedi *et al* 2008; Randin *et al.* 2009).

It has been proposed that decoupling of local from regional climatic conditions may buffer species against climate change by influencing fine-resolution patterns in climatic conditions. This hypothesis is supported by evidence from contemporary patterns of genetic variability, which show that species survived previous periods of warming in microrefugia, where populations were buffered by unusually stable or otherwise atypical conditions relative to regional climates (Rull 2010). The potential role of microrefugia in supporting species through periods of adverse climate contrasts with expectations from bioclimate models that regions with favourable climates will soon lie beyond the natural limits of colonisation from current species distributions, and hence that the redesign of protected area networks or species translocations may be needed (Araújo *et al.* 2011; Thomas 2011). The relevance and urgency of such conservation measures depends to a great extent on whether and for how long species are able to survive *in situ* in parts of their ranges that are threatened by climate change. Nevertheless, there is much disagreement with regards to how microclimate modifies the effects of regional climate on species persistence. Some authors have shown that micro-scale models predict far greater species persistence in comparison to coarse-scale models (Randin *et al.* 2009), whereas others show entirely the reverse pattern (Trivedi *et al.* 2008), and a convincing body of theory and evidence is yet to be presented to understand microclimate effects on persistence in a changing climate.

In chapter one, we showed that rates of warming, even within a relatively small region, can be remarkably spatially variable. As a consequence species may be able to persist for longer at localities experiencing less warming. To date, however, there has been no rigorous test of this hypothesis. Here, by relating fine-scale patterns in extinction and persistence in plant communities to changes in temperature over a 38 year period, we assess the evidence for microrefugia. Specifically we test whether climatically-driven localised extinctions are occurring and whether patterns of these are related to the magnitude of climatic change. Our study system comprises a suite of species predicted by macro-scale modelling to be highly threatened by climate change, but which have none the less persisted in one of the warmest parts of the United Kingdom.

Methods

Study site and species

The study was conducted on plants associated with grassland, heathland and woodland on the Lizard Peninsula (50º 2'N, 5º 10'W), a Special Area for Conservation (92/43/EEC) covering c. 3,250 ha on the most southern tip of the United Kingdom (UK). One characteristic of our study system that makes it particularly well suited to studying the mechanisms governing climate-driven range shifts is that vegetation changes throughout much of the UK are strongly associated with nitrogen deposition (Stevens *et al*. 2004) but, probably due to the location of the Lizard and prevailing wind direction, there is no evidence of an increase in species associated with higher levels of nitrogen (see also Powney *et al*. 2014).

Our study focuses on plant species predicted by macroclimatic modelling to be threatened by climate change and on those for which historic data geolocated to high precision are available. We first compiled an extensive database of c. 2 million higher plant records for the Lizard Peninsula from a variety of sources including the Environmental Recording in Cornwall Automated (ERICA) database, those held by the Environmental Records Centre for Cornwall and the Isles of Scilly (ERCCIS) and those collected for research purposes during 1970s and 1980s (Malloch 1972; Marrs and Proctor 1980; Hopkins 1983). From these records, we selected all those that were recorded during the period 1970 to 1989 with a geoprecision of 100m or greater. From these data, we compiled a final list of species predicted by macroclimatic warming to contract their range under future climate scenarious (Pearce-Higgins *et al.* 2015). The resulting dataset is a list of 17 species, recorded at a total of 348 locations across the Lizard Peninsula (Table 3.1). The locations from which climate-threatened plant species were historically recorded are shown in Figure 3.1.

Table 3.1. *List of climate sensitive species for which historic data geolocated to high precision were available. The total number of records, excluding those removed from data analyses because of land use change is also shown.*

Common name	**Latin binomial**	**Number of records**
Annual Pearlwort	*Sagina apetala*	10
Bog Myrtle	*Myrica gale*	1
Dropwort	*Filipendula vulgaris*	70
Great Burnet	*Sanguisorba officinalis*	16
Heath Pearlwort	*Sagina subulata*	19
Many-seeded Goosefoot	*Chenopodium polyspermum*	2
Marsh Cinquefoil	*Potentilla palustris*	2
Marsh Yellow-cress	*Rorippa palustris*	2
Opposite-leaved Golden Saxifrage	*Chrysosplenium alternifolium*	18
Round-leaved Sundew	*Drosera rotundifolia*	5
Scurvy Grass	*Cochlearia sp.*	22
Spring Sandwort	*Minuartia verna*	21
Swine-cress	*Lepidium coronopus*	14
Three-nerved Sandwort	*Moehringia trinervia*	3
Treacle Mustard	*Erysimum cheiranthoides*	1
Wall Pennywort	*Umbilicus rupestris*	78
Winter-cress	*Barbarea vulgaris*	1
Total		**285**

Survey methods

Between May and August 2014, each of the 100 grid cells in which climate-threatened plants were historically recorded was revisited at times appropriate to the flowering phenology of the

species in question. If accessible, the entire 100 m grid cell was thoroughly searched to verify the persistence or extinction of the species in question. Data from inaccessible locations or those that had undergone agricultural improvement or other evident changes in land-use were removed from analyses. 63 records from 14 locations were thus omitted.

Statistical analyses

The persistence or extinction of species was modelled as a function of the overall degree of climatic change occurring at each location using a generalized linear mixed-effects model with a binomial error distribution and species included as a random intercept. Analyses were performed using the lme 4 package for R statistical software (Bates *et al.* 2007).

Fig 3.1. *Locations of historically recorded plant records that were resurveyed in 2014. Solid squares represent persistence and open squares represent extinctions. Not all data are shown, as in some instances there are numerous records for different species from the same square.*

Results

48% of all historically recorded plant records were extinct by 2014. The probability of persistence was weakly related to the overall magnitude of temperature increase associated with each location. While the effect was non-significant ($P > 0.05$), the inclusion of temperature increase resulted in a marginal improvement in model parsimony in comparison to the null model with just the random effect of species included ($\Delta AIC = 2.12$). Estimated (mean and 95% confidence intervals) probability of extinction as a function of temperature increase is shown in Figure 3.2.

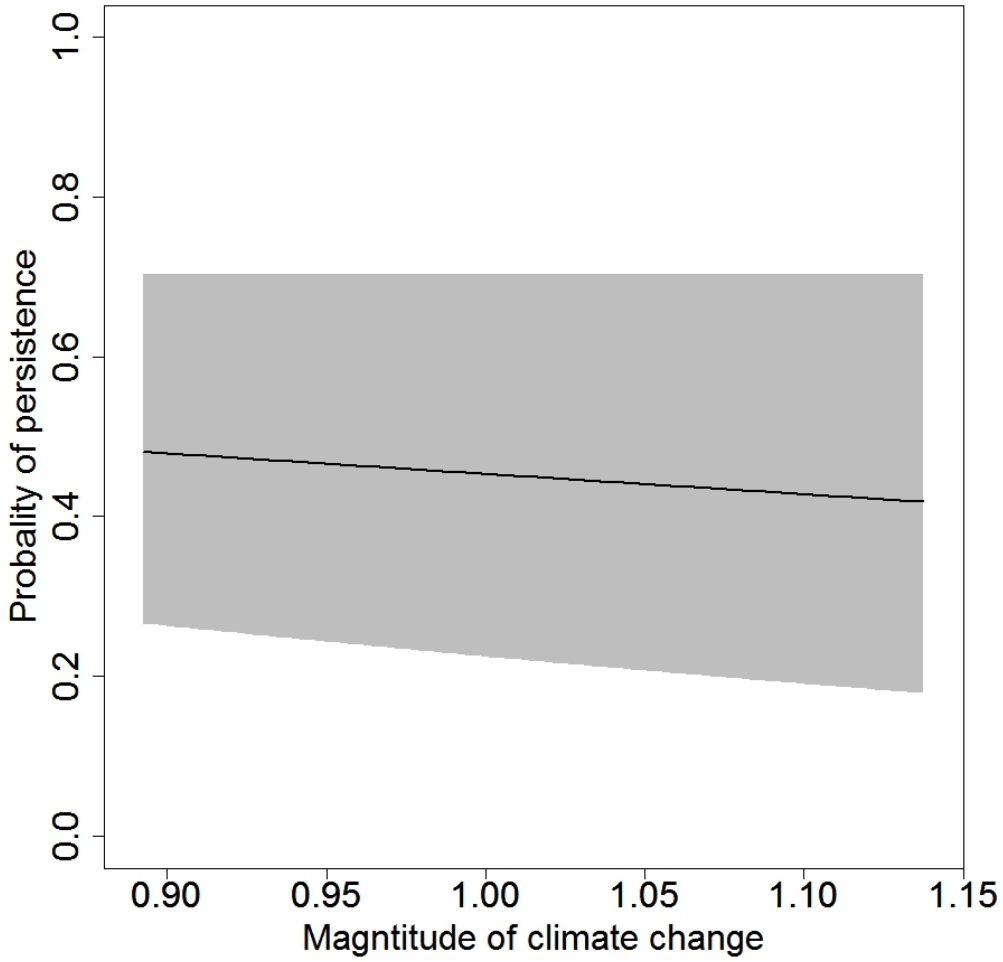

***Fig. 3.2**. Modelled probability of persistence of plants recorded between 1970-89 and 2014 as a function of temperature increase. The solid black represents the mean estimate and shaded grey area the 95% confidence intervals.*

Discussion

The key objective of this study was to determine whether climate-vulnerable species are more likely to persist at localities that experienced slower rates of warming. Our study provides at least some evidence that this is the case: species were on average more likely to persist at localities with slower rates, albeit that the results are non-significant. However, there are several limitations associated with our approach that warrant further discussion, many of which strengthen the case for the existence of microrefugia.

First, while we made use of a comprehensive dataset of historic plant distribution records, it should be noted the availability of data for individual species is rather scarce. Consequently, we carried out combined analyses in which each species is treated as a "random intercept". While this allows each species to exhibit individualistic responses to climate change to a degree, the response in somewhat constrained and assumed to have the same directional effect. In practise, species may exhibit highly individualistic responses to climate change (Huntley 1991), with some species showing a marked greater tendency to persist at specific localities than others. It would have been preferable to construct individual models for each species, but in practice insufficient historical plant records georeferenced to high precision were available to permit such analyses. While the Lizard Peninsula has among the most comprehensive datasets of historical plant records in the world, the general paucity of records georeferenced to high precision hampers our ability to infer fine-scale ecological responses to climate change. Similarly, numerous factors unrelated to climate change drive localised patterns of extinction and, particularly at fine scales, plant species distributions in many systems are thought to be subject a degree of natural turnover (Maarel & Sykes 1993). These manifest themselves by introducing greater variance into patterns of extinction and persistence, increasing the size of the dataset that must be obtained before consistent but weak patterns can be detected.

Second, the areas subject to greatest long-term stability in climate may also be subject to lower short-term variability. North and east facing slopes, identified in chapter one as exhibiting the slowest rates of climate change, are also those that experience the lowest diurnal temperature range (Bennie et al. 2008). Consequently, plant species that preferentially inhabit these microclimates may be more sensitive to temperature change. While many of the species included in this study occupy a range of slopes and aspects, localised variability in phenotype expression in relation to microclimate remains unknown. In other systems, species have shown greater capability and increased variety of habitat use at expanding range margins, implying that evolutionary processes, specifically localised variation in the prevalence of different phenotypes, can have an important bearing on ecological responses to climate change (Thomas et al. 2001). However, the extent to which individuals within populations exhibit localised variation in their sensitivity to climate change in response to microclimate remains largely unstudied. Allied to this, measured at fine scales near the ground, temperatures are typically far more temporally variable than suggested by coarse-scale models. A potential explanation for the role of microclimate in enhancing species persistence may thus not be that specific parts of the landscape are more climatically stable, but simply that coarse-scale models underestimate the thermal tolerance of species and hence their sensitivity to climate change.

All the above issues highlight how the detection and determination of the characteristics of microrefugia are inherently dependent on the details of the methodology used. In this study, we focus primarily on rates of warming and show that there is at least some evidence that plant species are more likely to persist in areas experiencing the least warming. Many researchers have proposed that the existence of microclimate will enhance the resilience of species to climate change (e.g. Laurie 2009; Rull 2009; 2010; Ashcroft 2010; Keppel et al. 2012). However more refined knowledge of the circumstances in which coarse-scale models

fail to predict how species respond to climate change and greater empirical validation using fine-scale data is required before the nature of microrefugia can be fully understood.

Concluding remarks

In chapter one, we present a model that is applied to provide fine-grained (100m), multi-decadal estimates of temperature change based on the underlying physical processes that influence microclimate. We apply the model to the Lizard Peninsula and show that accurate hourly estimates of temperature can be obtained. We show that rates of warming vary across a landscape primarily due to long-term trends in weather conditions, with the slowest rates of warming evident on north-east-facing slopes. This variation contributes to substantial spatial heterogeneity in trends in bioclimatic variables: for example, the change in the length of the frost-free season varied from +11 to -54 days and the increase annual growing degree-days from 51 to 267 ºC days. Our results emphasise the importance of multi-decadal trends in weather conditions in determining spatial variation in rates of warming, suggesting that locations experiencing least warming are unlikely to remain consistent under future climate change.

In chapter 2, we examine fine-scale (<5m) changes in plant communities of coastal grassland on the Lizard Peninsula over a 30 year period in which spring temperatures increased by 1.4ºC. We determine whether changes in community composition and local colonisations and extinctions are related to microclimatic conditions. We show that, while community reassembly was consistent with warming, changes were smaller on cooler, north-facing slopes. While we did not explicitly model changes in microclimatic conditions at the resolution at which plants were sampled, the results of chapter one, in which climatic conditions were modelled at 100 m resolution, suggest that cooler, north-facing slopes are also prone to less warming. Closer inspection of patterns of species turnover shows that species with low temperature requirements were able to persist on cooler slopes, while those with high moisture requirements suffered similar decreases in occupancy across all microclimates. Overall, our results suggest that north-facing slopes may act as microrefugia, buffering the effects of increases in temperature on plant communities by delaying extinctions of species with low temperature requirements.

In chapter 3, we explicitly test whether fine-scale (100m) variation in rates of warming affects local patterns of extinction and persistence for a suite of plant species vulnerable to climate change. We show that, across all species, persistence is higher at locations experiencing the slowest rates of warming, although the effects are not very strong, implying that many other factors have also affected the persistence of plant species within the study area. Overall, our results suggest that north- and east-facing slopes, which have experienced less warming, may serve as microrefugia, buffering the effects of increases in temperature on plant communities by delaying extinctions of species with low temperature requirements. However, there are a number of limitations associated with the methods. More refined knowledge of the circumstances in which coarse-scale models fail to predict how species respond to climate change, and greater empirical validation using fine-scale data, is required before the nature of microrefugia can be fully understood.

Nevertheless, taken together, the evidence presented in this report provides compelling evidence that microclimate plays a significant role in moderating ecological responses to macroclimatic warming and provides at least some insight into the likely locations in which species may be most likely to survive climate change. The expectation that range shifts for many species will not to keep pace with climate change is prevalent in the scientific literature, leading to widespread calls for the redesign of protected area networks (e.g. Hannah *et al.* 2002; Araújo *et al.* 2011) and assisted colonisations (Thomas 2011). Finite conservation resources and competing land-uses in many instances render such approaches impractical, emphasising the need for robust measures for carrying-out conservation *in situ* (see Greenwood *et al.* 2016 for a review of possible methods). Conservation at locations with high microrefugium potential, could provide a practical and cost-effective means of reducing extinction threat because this can be targeted on specific suitable locations, including many

existing protected sites. Overall, our findings provide a compelling scientific case for making the identification and protection of microrefugia a cornerstone of climate change adaptation for biodiversity conservation.

Acknowledgements

We thank Nick Macgregor for commissioning this study and for providing comments on the report. Humphrey Crick, Simon Duffield and Mike Morecroft also provided very helpful comments. We are grateful to Fraser Bell, Sally Luker, Tony Blunden and Derek Green for help with fieldwork, Ros Shaw for statistical advice and Ray Lawman for logistic support. Colin Beale's help in selecting species particularly vulnerable to climate change is also greatly appreciated. The study was jointly funded by Natural England, the Natural Environment Research Council and the University of Exeter.

References

Allen, R.G., Pereira, L.S., Raes, D. & Smith, M. (1998) *Crop evapotranspiration-Guidelines for computing crop water requirements-FAO Irrigation and drainage paper 56*. FAO, Rome, **300**

Araújo, M.B., Alagador, D., Cabeza, M., Nogués-Bravo, D., & Thuiller, W. (2011) Climate change threatens European conservation areas. *Ecology Letters* **14**, 484-492.

Araújo, M.B., Pearson, R.G., Thuiller, W. & Erhard, M. (2005) Validation of species–climate impact models under climate change. *Global Change Biology*, **11**, 1504-1513.

Ashcroft, M.B. (2010) Identifying refugia from climate change. *Journal of Biogeography*, **37**, 1407-1413.

Ashcroft, M.B., Chisholm, L.A. & French, K.O. (2009) Climate change at the landscape scale: predicting fine-grained spatial heterogeneity in warming and potential refugia for vegetation. *Global Change Biology*, **15**, 656-667.

Ashcroft, M.B., Gollan, J.R., Warton, D. & Ramp, D. (2012) A novel approach to quantify and locate potential microrefugia using topoclimate, climate stability, and isolation from the matrix. *Global Change Biology*, **18**, 1866-1879.

Barr, S. & Orgill, M.M. (1989) Influence of external meteorology on nocturnal valley drainage winds. *Journal of Applied Meteorology*, **28**, 497-517.

Bartoń, K. (2014) *MuMIn: multi-model inference*. R package version 1.9.13. Available: http://CRAN.R-project.org/package=MuMIn. Accessed: 11 Nov 2014.

Bates, D., Sarkar, D., Bates, M.D., & Matrix, L. (2007). *The lme4 package*. *R package version*, *2*(1).

Bennie, J., Hill, M.O., Baxter, R. & Huntley, B. (2006) Influence of slope and aspect on long-term vegetation change in British chalk grasslands. *Journal of Ecology*, **94**, 355-368.

Bennie, J., Huntley, B., Wiltshire, A., Hill, M.O. & Baxter, R. (2008) Slope, aspect and climate: spatially explicit and implicit models of topographic microclimate in chalk grassland. *Ecological Modelling*, **216**, 47-59.

Bennie, J., Wilson, R.J., Maclean, I.M.D. & Suggitt, A.J. (2014) Seeing the woods for the trees - when is microclimate important in species distribution models? *Global Change Biology*, **20**, 2699-2700.

Bennie J., Wiltshire, A.J., Joyce, A.N., Clark, D., Lloyd, A.R., Adamson, J., Parr, T., Baxter, R. & Huntley, B. (2010) Characterising inter-annual variation in the spatial pattern of thermal microclimate in a UK upland using a combined empirical–physical model. *Agricultural and Forest Meteorology*, **150**, 12-19.

Berry, P.M., Dawson, T.P., Harrison, P.A. & Pearson, R.G. (2002) Modelling potential impacts of climate change on the bioclimatic envelope of species in Britain and Ireland. *Global Ecology and Biogeography*, **11**, 453-462.

Bertrand, R., Lenoir, J., Piedallu, C., Riofrío-Dillon, G., de Ruffray, P., Vidal, C., Pierrat, J.-C. & Gégout, J.-C. (2011) Changes in plant community composition lag behind climate warming in lowland forests. *Nature*, **479**, 517-520.

Bluesky, L. (2014) Colour InfraRed (CIR) data for England and Wales. NERC Earth Observation Data Centre.

Chen, I.C., Hill, J.K., Ohlemuller, R., Roy, D.B. & Thomas, C.D. (2011) Rapid range shifts of species associated with high levels of climate warming. *Science*, **333**, 1024-1026.

Clark, J.S., Fastie, C., Hurtt, G., Jackson, S.T., Johnson, C., King, G.A., Lewis, M., Lynch, J., Pacala, S. & Prentice, C. (1998) Reid's Paradox of Rapid Plant Migration Dispersal theory and interpretation of paleoecological records. *BioScience*, **48**, 13-24.

Currall, J.E.P. (1987) A transformation of the Domin scale. *Vegetatio*, **72**, 81-87.

De Frenne, P., Rodríguez-Sánchez, F., Coomes, D.A., Baeten, L., Verstraeten, G., Vellend, M., Bernhardt-Römermann, M., Brown, C.D., Brunet, J., Cornelis, J., Decocq, G.M., Dierschke, H., Eriksson, O., Gilliam, F.S., Hédl, R.,Heinken, T.,Hermy, M., Hommel, P., Jenkins, M.A., Kelly, D.L., Kirby, K.J., Mitchell, F.J.G., Naaf, T., Newman, M., Peterken, G., Petřík, P., Schultz, J., Sonnier, G., Calster, H.M., Waller, D.M., Walther, G.-R., White, P.S., Woods, K.D., Wulf, M., Graae, B.J. & Verheyen, K. (2013) Microclimate moderates

plant responses to macroclimate warming. *Proceedings of the National Academy of Sciences*, **110**, 18561-18565.
Dobrowski, S.Z. (2011) A climatic basis for microrefugia: the influence of terrain on climate. *Global Change Biology*, **17**, 1022-1035.
Dullinger, S., Gattringer, A., Thuiller, W., Moser, D., Zimmermann, N. E., Guisan, A., Willner, W., Plutzar, C., Leitner, M., Mang, T., Caccianiga, M., Dirnböck, T., Ertl, S., Fischer, A., Lenoir, J., Svenning, J.-S., Psomas, A., Schmatz,D.R., Silc, U., Vittoz P. & Hülber, K. (2012) Extinction debt of high-mountain plants under twenty-first-century climate change. *Nature Climate Change*, **2**, 619-622.
Ellenberg, H., Weber, H.E., Düll, R., Wirth, V., Werner, W. & Paulissen D (1991) Zeigerwerte von Pflanzen in Mitteleuropa. *Scripta Geobotanica*, **18**, 1-248.
Elith, J. & Leathwick, J.R (2009) Species distribution models: ecological explanation and prediction across space and time. *Annual Review of Ecology, Evolution and Systematics*, 40, 677-697.
Evans, M.R. (2012) Modelling ecological systems in a changing world. *Philosophical Transactions of the Royal Society B: Biological Sciences*, **367**, 181-190.
Forsythe, G.E., Malcolm, M.A. & Moler, C.B. (1977) *Computer Methods for Mathematical Computations*. Wiley, New York.
Franklin, J., Davis, F.W., Ikegami, M., Syphard, A.D., Flint, L.E., Flint, A.L. & Hannah, L. (2013) Modeling plant species distributions under future climates: how fine scale do climate projections need to be? *Global Change Biology*, **19**, 473-483.
Fritsch, A. & Ickstadt, K. (2009) Improved criteria for clustering based on the posterior similarity matrix. *Bayesian analysis*, **4**, 367-391.
Geiger, R. (1965) *the climate near the ground. Translated by Scripta Technica, Inc*. Harvard University Press.
Gillingham, P., Huntley, B., Kunin, W. & Thomas, C. (2012) The effect of spatial resolution on projected responses to climate warming. *Diversity and Distributions*, **18**, 990-1000.
Greenwood, O., Mossman, H.L., Suggitt, A.J., Curtis, R.J. & Maclean, I.M.D (2016) Using *in situ* management to conserve biodiversity under climate change. *Journal of Applied Ecology*, **53**, 885-894.
Gunton, R.M., Polce, C. & Kunin, W.E. (2015) Predicting ground temperatures across European landscapes. *Methods in Ecology and Evolution*,
Gustavsson, T., Karlsson, M., Bogren, J. & Lindqvist, S. (1998) Development of temperature patterns during clear nights. *Journal of applied meteorology*, **37**, 559-571.
Hampe, A. (2004) Bioclimate envelope models: what they detect and what they hide. *Global Ecology and Biogeography*, **13**, 469-471.
Hampe, A. & Jump, A.S. (2011) Climate relicts: past, present, future. *Annual Review of Ecology, Evolution, and Systematic*s, **42**, 313-333.
Hannah, L., Flint, L., Syphard, A.D., Moritz, M.A., Buckley, L.B. & McCullough, I.M. (2014) Fine-grain modeling of species' response to climate change: holdouts, stepping-stones, and microrefugia. *Trends in ecology & evolution*, **29**, 390-397.
Hannah, L., Midgley, G.F. & Millar, D (2002) Climate change-integrated conservation strategies. *Global Ecology and Biogeography*, **11**, 485-495 (2002).
Haugen, R. & Brown, J. (1980) Coastal-inland distributions of summer air temperature and precipitation in northern Alaska. *Arctic and Alpine Research*, 403-412.
Heller, N.E. & Zaveleta, E.S. (2009) Biodiversity management in the face of climate change: a review of 22 years of recommendations. *Biological Conservation*, **142**, 14-32.
Hijmans, R.J., Cameron, S.E., Parra, J.L., Jones, P.G. & Jarvis, A. (2005) Very high resolution interpolated climate surfaces for global land areas. *International Journal of Climatology*, **25**, 1965-1978.
Hijmans, R.J. & Graham, C.H. (2006) The ability of climate envelope models to predict the effect of climate change on species distributions. *Global Change Biology*, **12**, 2272-2281.

Hill, M.O., Preston, C.D. & Roy, D.B. (2004) *Attributes of British and Irish plants: status, size, life history, geography and habitats*. Biological Records Centre, NERC Centre for Ecology and Hydrology, Wallingford.

Hofierka, J. & Suri, M. (2002) The solar radiation model for Open source GIS: implementation and applications. *Proceedings of the Open source GIS-GRASS users conference* (ed by, pp. 1-19.

Hopkins, J.J. (1983) *Studies of the historical ecology, vegetation and flora of the Lizard District, Cornwall, with particular reference to heathland*. PhD Thesis. University of Bristol.

Hopkins, J.J. (2006*) An introduction to the flora of the Lizard Peninsula, Cornwall. In: Botanical Links in the Atlantic Arc* (ed. by Leach, S.J., Page, C.N., Peytoureau, Y. & Sandford, M.N.), Proceedings of an Anglo-Hiberno French meeting arranged by the Botanical Society of the British Isles, Camborne.

Horn, H.S. (1966) Measurement of overlap in comparative ecological studies. *The American Naturalist*, **100**, 419-424.

Huntley, B. (1991) How plants respond to climate change: migration rates, individualism and the consequences for plant communities. *Annals of Botany*, 67, 15-22.

Hylander, K., Ehrlén, J., Luoto, M. & Meineri, E. (2015) Microrefugia: Not for everyone. *Ambio*, **44**, 60-68.

IPCC (2014) *Climate Change 2013: The Physical Science Basis* (eds Stocker T, Qin D, Plattner G-K et al.), Cambridge University Press, Cambridge.

IUCN (2015) *The IUCN Red List of threatened species.* Gland, Switzerland

Jenkins, G.J. (2007) *The climate of the United Kingdom and recent trends*. Exeter: Met Office Hadley Centre.

Kasten, F. (1996) The Linke turbidity factor based on improved values of the integral Rayleigh optical thickness. *Solar energy*, **56**, 239-244.

Kasten, F. & Young, A.T. (1989) Revised optical air mass tables and approximation formula. *Applied optics*, **28**, 4735-4738.

Kearney, M.R., Shamakhy, A., Tingley, R., Karoly, D.J., Hoffmann, A.A., Briggs, P.R. & Porter, W.P. (2014) Microclimate modelling at macro scales: a test of a general microclimate model integrated with gridded continental-scale soil and weather data. *Methods in Ecology and Evolution*, **5**, 273-286.

Keppel, G., Van Niel, K.P., Wardell-Johnson, G.W., Yates, C.J., Byrne, M., Mucina, L., Schut, A.G.T., Hopper S.D& Franklin, S.E. (2012) Refugia: identifying and understanding safe havens for biodiversity under climate change. *Global Ecology and Biogeography*, **21**, 393-404.

Kopecký, M. & Macek, M. (2015) Vegetation resurvey is robust to plot location uncertainty. *Diversity & Distributions*, **21**, 322-330.

Kuuluvainen, T. & Pukkala, T. (1989) Simulation of within-tree and between-tree shading of direct radiation in a forest canopy: effect of crown shape and sun elevation. *Ecological modelling*, **49**, 89-100.

Kuussaari, M., Bommarco, R., Heikkinen, R. K., Helm, A., Krauss, J., Lindborg, R., Öckinger, E., Pärtel, M., Pino, J., Rodá, F., Stefanescu, C., Teder, T., Zobel, M. & Steffan-Dewenter, I. (2009) Extinction debt: a challenge for biodiversity conservation. *Trends in Ecology & Evolution*, **24**, 564-571.

Lassueur, T., Joost, S. & Randin, C.F. (2006) Very high resolution digital elevation models: Do they improve models of plant species distribution? *Ecological Modelling*, **198**, 139-153.

Loarie, S.R., Duffy, P.B., Hamilton, H., Asner, G.P., Field, C.B. & Ackerly, D.D. (2009) The velocity of climate change. *Nature*, 462, 1052-1055.

Maarel, E. & Sykes, M.T (1993) Small-scale plant species turnover in a limestone grassland: the carousel model and some comments on the niche concept. *Journal of Vegetation Science*, **4**, 179-188.

Maclean, I.M.D, Bennie, J.J., Scott, A.J. & Wilson, R.J. (2012) A high-resolution model of soil and surface water conditions. *Ecological Modelling*, **237**, 109-119.

Maclean, I.M.D, Hopkins, J.J., Bennie, J., Lawson Callum R & Wilson, R.J. (2015) Microclimates buffer the responses of plant community to climate change. *Global Ecology and Biogeography*, 14: 1340-1350.

Maclean I.M.D, Suggitt A.J., Wilson R.J., Duffy J.P., Bennie J.J. (2016) Fine-scale climate change: modelling spatial variation in biologically meaningful rates of warming. *Global Change Biology*, in press. DOI: 10.1111/gcb.13343

Maclean, I.M.D. & Wilson, R.J. (2011) Recent ecological responses to climate change support predictions of high extinction risk. *Proceedings of the National Academy of Sciences*, **108**, 12337-12342.

Malloch, A.J.C. (1972) Salt-spray deposition on the maritime cliffs of the Lizard Peninsula. *Journal of Ecology*, **60**, 103-112.

Manins, P. & Sawford, B. (1979) A model of katabatic winds. *Journal of the Atmospheric Sciences*, **36**, 619-630.

Marrs, R.H., Proctor, J. (1980) Vegetation and soil studies of the enclosed heathlands of the Lizard Peninsula, Cornwall. *Vegetatio*, **41**, 121-128.

Marshall, J., Kushnir, Y., Battisti, D., Chang, P., Czaja, A., Dickson, R., Hurrell, J., McCARTNEY, M., Saravanan, R. & Visbeck, M. (2001) North Atlantic climate variability: phenomena, impacts and mechanisms. *International Journal of Climatology*, **21**, 1863-1898.

McGregor, G. & Bamzelis, D. (1995) Synoptic typing and its application to the investigation of weather air pollution relationships, Birmingham, United Kingdom. *Theoretical and Applied Climatology*, **51**, 223-236.

Pearce-Higgins, J.W., Ausden, M.A., Beale, C.M., Oliver, T.H. & Crick, H.Q.P. (2015). Research on the assessment of risks & opportunities for species in England as a result of climate change. *Natural England Commissioned Reports*, Number 175.

Pearson, R.G. & Dawson, T.P. (2003) Predicting the impacts of climate change on the distribution of species: are bioclimate envelope models useful? *Global Ecology and Biogeography*, **12**, 361-371.

Perry, M. & Hollis, D. (2005) The generation of monthly gridded datasets for a range of climatic variables over the UK. *International Journal of Climatology*, **25**, 1041-1054.

Pepin, N., Daly, C. & Lundquist, J. (2011) The influence of surface versus free-air decoupling on temperature trend patterns in the western United States. *Journal of Geophysical Research: Atmospheres (1984–2012)*, **116**

Philipp, A., Della-Marta, P.-M., Jacobeit, J., Fereday, D.R., Jones, P.D., Moberg, A. & Wanner, H. (2007) Long-term variability of daily North Atlantic-European pressure patterns since 1850 classified by simulated annealing clustering. *Journal of Climate*, **20**, 4065-4095.

Phillips, B.L., Brown, G.P., Travis, J.M. & Shine, R. (2008) Reid's paradox revisited: the evolution of dispersal kernels during range expansion. *The American Naturalist*, **172**, S34-S48.

Pike, G., Pepin, N. & Schaefer, M. (2013) High latitude local scale temperature complexity: the example of Kevo Valley, Finnish Lapland. *International Journal of Climatology*, **33**, 2050-2067.

Pinheoro, J., Bates, B., Debroy, S. & Sarkar, D. (2014) *nlme: Linear and nonlinear mixed effects models. R package V 3.1-109*. Available: http://cran.r-project.org/package=nlme. Accessed: 11 Nov 2014.

Posselt, R., Müller, R., Stöckli, R. & Trentmann, J. (2011) CM SAF surface radiation MVIRI Data Set 1.0—Monthly means/daily means/hourly means. *Satellite application facility on climate monitoring*.

Potter, K.A., Arthur Woods, H. & Pincebourde, S. (2013) Microclimatic challenges in global change biology. *Global change biology*, **19**, 2932-2939.

Powney, G.D., Preston, C.D., Purvis, A., Van Landuyt, W. & Roy, D.B. (2014) Can trait-based analyses of changes in species distribution be transferred to new geographic areas? *Global Ecology and Biogeography*, **23**, 1009-1018.

Preston, C.D. & Hill, M.O. (1997) The geographical relationships of British and Irish vascular plants. *Botanical Journal of the Linnean Society*, **124**, 1-120.
R Development Core Team (2014) *R: A Language and Environment for Statistical Computing*. R Foundation for Statistical Computing, Vienna.
Randin, C.F., Engler, R., Normand, S., Zappa, M., Zimmermann, N.E., Pearman, P.B., Vittoz, P., Thuiller, W. & Guisan, A. (2009) Climate change and plant distribution: local models predict high-elevation persistence. *Global Change Biology*, **15**, 1557-1569.
Rayner, N., Parker, D.E., Horton, E., Folland, C., Alexander, L., Rowell, D., Kent, E. & Kaplan, A. (2003) Global analyses of sea surface temperature, sea ice, and night marine air temperature since the late nineteenth century. *Journal of Geophysical Research: Atmospheres (1984–2012)*, **108**
Reid, C. (1899) *The origin of the British flora*. Dulau & Company, London.
Rice, K. (2004) Sprint research runs into a credibility gap. *Nature*, **432**, 147-147.
Rull, V. (2009) Microrefugia. *Journal of Biogeography*, **36**, 481-484.
Rull, V (2010) On microrefugia and cryptic refugia. *Journal of Biogeography* **37**, 1623-1625.
Ryan, B.C. (1977) A mathematical model for diagnosis and prediction of surface winds in mountainous terrain. *Journal of Applied Meteorology*, **16**, 571-584.
Savijärvi, H. (2004) Model predictions of coastal winds in a small scale. *Tellus A*, **56**, 287-295.
Scherrer, D. & Koerner, C. (2010) Infra-red thermometry of alpine landscapes challenges climatic warming projections. *Global Change Biology*, **16**, 2602-2613.
Scherrer, D. & Körner, C. (2011) Topographically controlled thermal-habitat differentiation buffers alpine plant diversity against climate warming. *Journal of Biogeography*, **38**, 406-416.
Sebastiá, M.-T. (2004) Role of topography and soils in grassland structuring at the landscape and community scales. *Basic and Applied Ecology*, **5**, 331-346.
Sørensen, T. (1948) A method of establishing groups of equal amplitude in plant sociology based on similarity of species and its application to analyses of the vegetation on Danish commons. *Biologiske Skrifter*, **5**, 1-34.
Stacey, F.D. & Davis, P.M. (1977) *Physics of the Earth*. Wiley New York.
Stevens, C.J., Dise, N.B., Mountford, J.O. & Gowing, D.J. (2004) Impact of nitrogen deposition on the species richness of grasslands. *Science*, **303**, 1876-1879.
Stewart, J.R. & Lister, A.M. (2001) Cryptic northern refugia and the origins of the modern biota. *Trends in Ecology & Evolution*, **16**, 608-613.
Suggitt, A.J., Wilson, R.J., August, T.A., Beale, C.M., Bennie, J.J., Dordolo, A., Fox, R., Hopkins, J.J., Isaac, N.J.B., Jorieux, P., Macgregor, N.A., Marcetteau, J., Massimino, D., Morecroft, M.D., Pearce-Higgins, J.W., Walker, K. & Maclean, I.M.D. (2014) Climate change refugia for the flora and fauna of England. Natural England, Peterborough.
Suggitt, A.J., Gillingham, P.K., Hill, J.K., Huntley, B., Kunin, W.E., Roy, D.B. & Thomas, C.D. (2011) Habitat microclimates drive fine-scale variation in extreme temperatures. *Oikos*, **120**, 1-8.
Sunday, J.M., Bates, A.E., Dulvy, N.K. (2012) Thermal tolerance and the global redistribution of animals. *Nature Climate Change*, **2**, 686-690.
Thomas, C.D. (2011) Translocation of species, climate change, and the end of trying to recreate past ecological communities. *Trends in Ecology and Evolution* **26**, 216-221.
Thomas, C.D., Bodsworth, E.J., Wilson, R.J., Simmons, A.D., Davies, Z.G., Musche, M. & Conradt, L. (2001) Ecological and evolutionary processes at expanding range margins. *Nature*, **411**, 577-581.
Thomas, C.D., Cameron, A., Green, R.E., Bakkenes, M., Beaumont, L.J., Collingham, Y.C., Erasmus, B.F.N., de Siqueira, M.F., Grainger, A., Hannah, L., Hughes, L., Huntley, B., van Jaarsveld, A.S., Midgley, G.F., Miles, L., Ortega-Huerta, M.A., Peterson, A.T., Phillips, O.L. & Williams, S.E. (2004) Extinction risk from climate change. *Nature*, **427**, 145-148.
Thomas, C.D., Franco, A. & Hill, J.K. (2006) Range retractions and extinction in the face of climate warming. *Trends in Ecology and Evolution*, **21**, 415-416.

Thuiller W (2004) Patterns and uncertainties of species' range shifts under climate change. *Global Change Biology*, **10**, 2020-7.

Trigo, I.F. (2006) Climatology and interannual variability of storm-tracks in the Euro-Atlantic sector: a comparison between ERA-40 and NCEP/NCAR reanalyses. *Climate Dynamics*, **26**, 127-143.

Trivedi, M.R., Berry, P.M., Morecroft, M.D. & Dawson, T.P. (2008) Spatial scale affects bioclimate model projections of climate change impacts on mountain plants. *Global Change Biology*, **14**, 1089-1103.

Twomey, S. (1991) Aerosols, clouds and radiation. *Atmospheric Environment. Part A. General Topics*, **25**, 2435-2442.

Tzedakis, P., Emerson, B. & Hewitt, G. (2013) Cryptic or mystic? Glacial tree refugia in northern Europe. *Trends in Ecology & Evolution*, **28**, 696-704.

Van Dyck, H., Bonte, D., Puls, R., Gotthard, K., Maes, D. (2015) The lost generation hypothesis: could climate change drive ectotherms into a developmental trap? *Oikos*, 124, 54-61.

Willis, K.J., Bhagwat, S.A. (2009) Biodiversity and climate change. *Science*, **326**, 806.

Worth, J.R., Williamson, G.J., Sakaguchi, S., Nevill, P.G. & Jordan, G.J. (2014) Environmental niche modelling fails to predict Last Glacial Maximum refugia: niche shifts, microrefugia or incorrect palaeoclimate estimates? *Global Ecology and Biogeography*, **23**, 1186-1197.

Appendix 1: Detailed assessment of model performance

(See chapter 1)

Radiation from cloud cover

Our cloud-cover derived model provided good approximations of direct (Mean error = 34.9 Wm^{-2}; RMS error = 71.8 Wm^{-2}), diffuse (mean error = 21.1 Wm^{-2}; RMS error = 39.5 Wm^{-2}) and total solar irradiance (Mean error = 38.6 Wm^{-2}; RMS error = 74.6 W^{m-2}). Though the model provides good estimate of intra-day hourly estimates of diffuse radiation, some of the intra-seasonal daily variation was underestimated (Fig. S1.1). Overall, log-log correlations of hourly observed and predicted values suggested that our model predicted 77% of the variance in direct irradiance and 92% of the variance in diffuse irradiance.

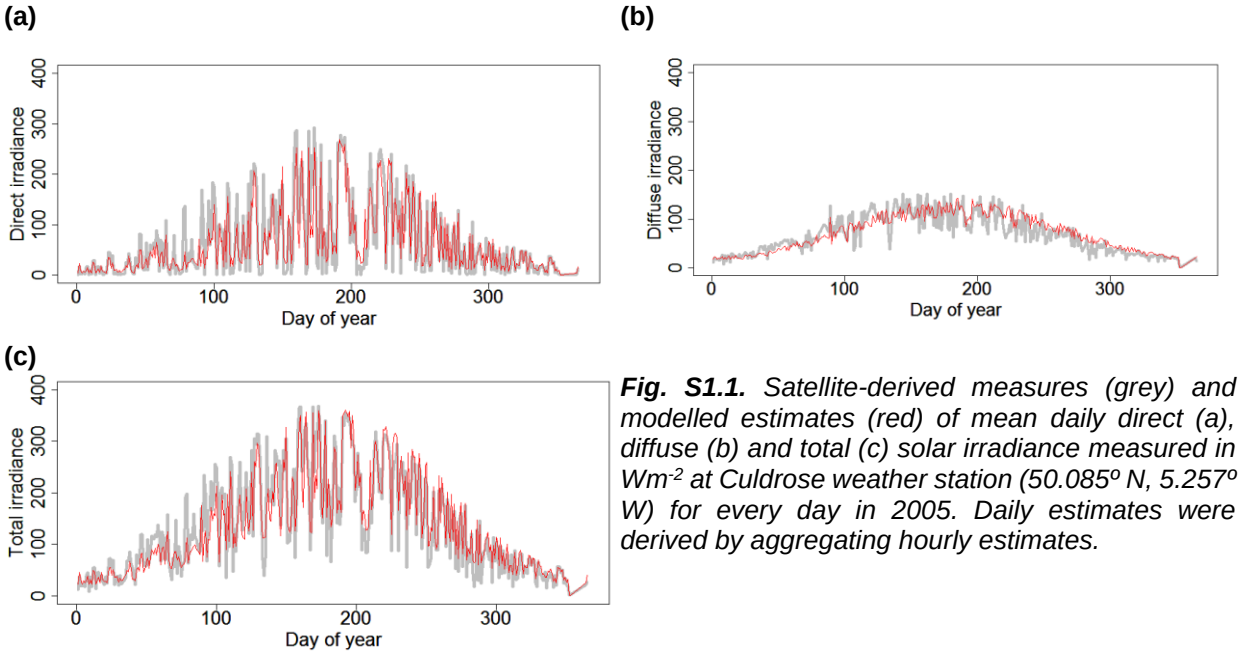

Fig. S1.1. *Satellite-derived measures (grey) and modelled estimates (red) of mean daily direct (a), diffuse (b) and total (c) solar irradiance measured in Wm^{-2} at Culdrose weather station (50.085º N, 5.257º W) for every day in 2005. Daily estimates were derived by aggregating hourly estimates.*

Synoptic weather types

Our cluster analysis of weather variables identified seven synoptic weather types, one of which represents conditions where no clear pattern could be discerned (Table S1.1). Box and whisker plots indicating the median and range in meteorological variables associated with each weather type are shown in Fig. S1.2. Met Office synoptic charts for dates conforming to each synoptic weather type are shown in Fig. S1.3. The certainty with which each of the main synoptic weather types could be identified was broadly similar across weather types, with a mean of 0.596. Weather type 7, that associated with no clear pattern, could be identified with less certainty (mean = 0.377).

Table S1.1. *Summary of conditions associated with synoptic weather types derived from cluster analyses of meteorological data from Culdrose weather station (50.085º N, 5.257º W).*

Type	Summary conditions
1	Weakly anticyclonic conditions; easterly winds, high pressure, moderate relative humidity.
2	Weakly cyclonic conditions; high cloud cover, low visibility, very high relative humidity, low diurnal temperature range.
3	Northerly winds, cold temperatures, very low dewpoint, fairly low diurnal temperature range, low pressure and low relative humidity.
4	Low cloud cover, high pressure, high diurnal temperature range, good visibility, low relative humidity.
5	Cyclonic conditions; good visibility, north-westerly winds, high pressure, moderate cloud cover, low relative humidity.
6	Strongly cyclonic conditions; strong south-westerly winds, high cloud cover, high relative humidity, high temperatures, low pressure, low diurnal temperature range.
7	No clear weather pattern dominated.

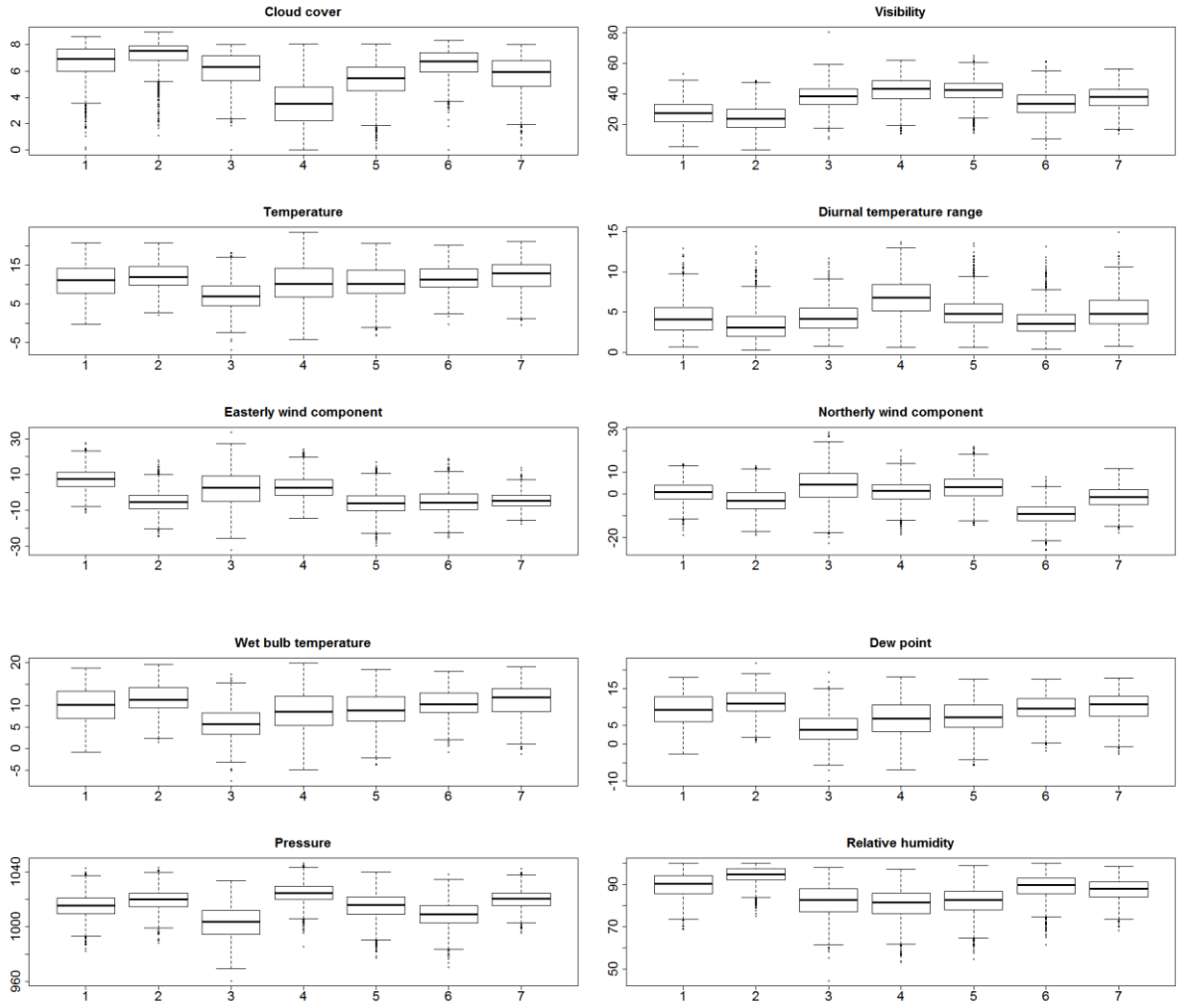

Fig. S1.2. *Box and whisker plots indicating the median and range in meteorological variables associated with synoptic weather types derived from cluster analyses of meteorological data from Culdrose weather station (50.085º N, 5.257º W). Solid line indicates the median values associated with each weather type. The boxes extend from the lower to upper quartiles, and the whiskers extend to 1.5 times the interquartile range, and extreme values outside this range are depicted by small dots.*

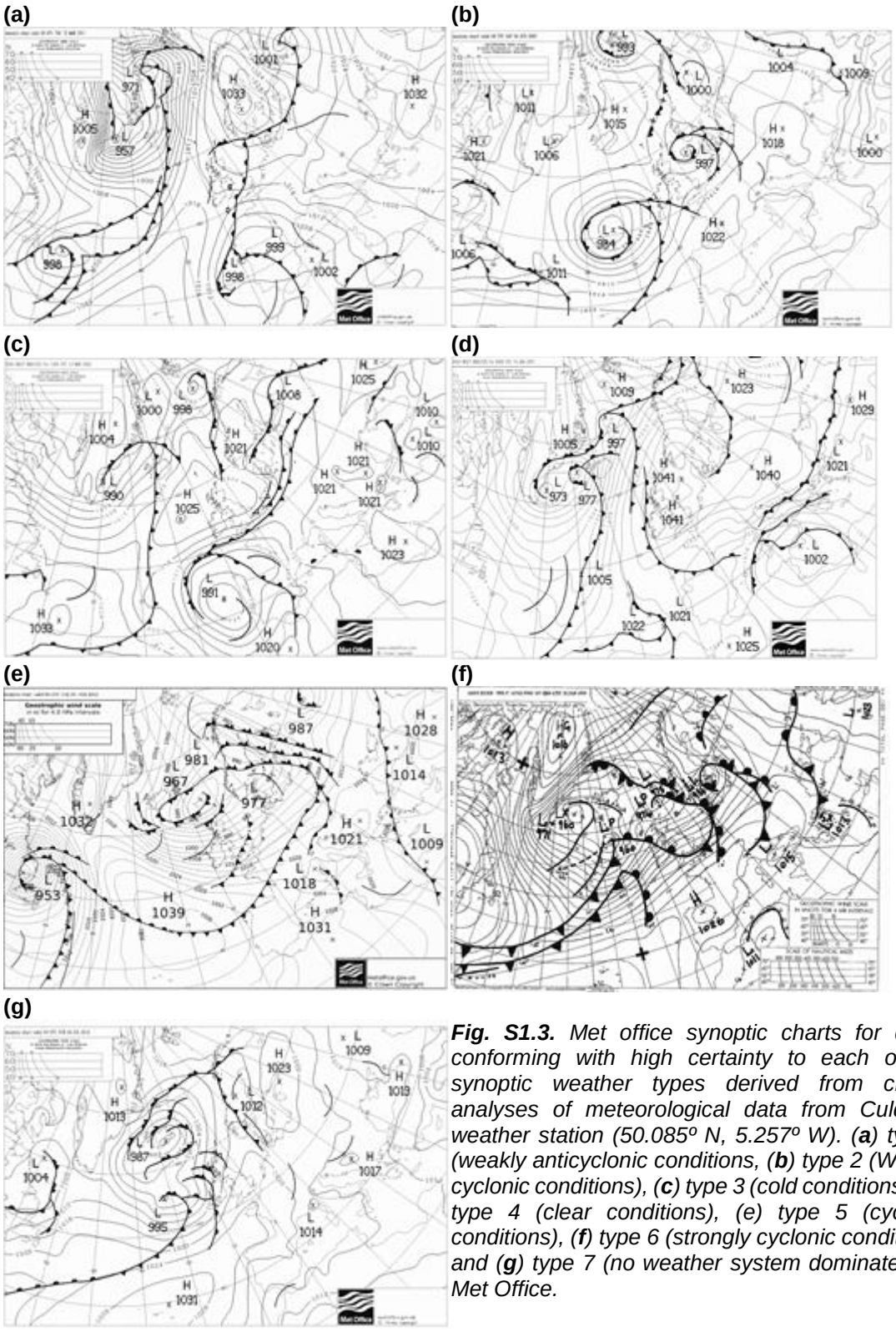

Fig. S1.3. *Met office synoptic charts for dates conforming with high certainty to each of the synoptic weather types derived from cluster analyses of meteorological data from Culdrose weather station (50.085º N, 5.257º W). (**a**) type 1 (weakly anticyclonic conditions, (**b**) type 2 (Weakly cyclonic conditions), (**c**) type 3 (cold conditions), (**d**) type 4 (clear conditions), (e) type 5 (cyclonic conditions), (**f**) type 6 (strongly cyclonic conditions) and (**g**) type 7 (no weather system dominates). © Met Office.*

Overall model performance

The most parsimonious models tended to be those in which all terms were included (Table S1.2), but sample size influenced the number of terms retained. However, all terms were retained with sample sizes in excess of 500 and all terms except those associated with cold air drainage were retained when sample sizes were in excess of 100. Hourly modelled versus measured temperatures for all sites are shown in Fig. S1.4. Frequency histograms of the ΔAIC values associated with sequentially adding terms for each model run are shown in Fig S1.5 and the variation in parameter estimates associated with the 9999 model runs in Fig. S1.6.

***Table S1.2**. Percentage of 999 model runs in which each term was included in the most parsimonious model.*

Parameter	Median
R_{net}	100.0%
u_1	100.0%
u_1R_{net}	99.6%
u_i	60.7%
L	100.0%
T_S	100.0%
u_iL	51.3%
u_1T_S	59.2%
E	100.0%
C	100.0%
W	100.0%
I_c	90.2%
F	100.0%
I_cF	58.7%

R_{net} is net radiation, u_1 is wind speed one metre above the ground, u_i is the inverse of wind speed given by $1/(u_1^{0.5}+1)$, L is the inverse distance-weighted measure upwind land-to-sea ratio at Culdrose minus that at the site, T_s is sea-surface temperature minus that at Culdrose, E is evapotranspiration at Culdrose minus that at the site, C is condensation at Culdrose minus that at the site, W is the change in lapse rate due to water condensation, F is accumulated flow and I_c is a categorical variable set at one when temperature inversions exist, and 0 when temperature inversion conditions do not exist.

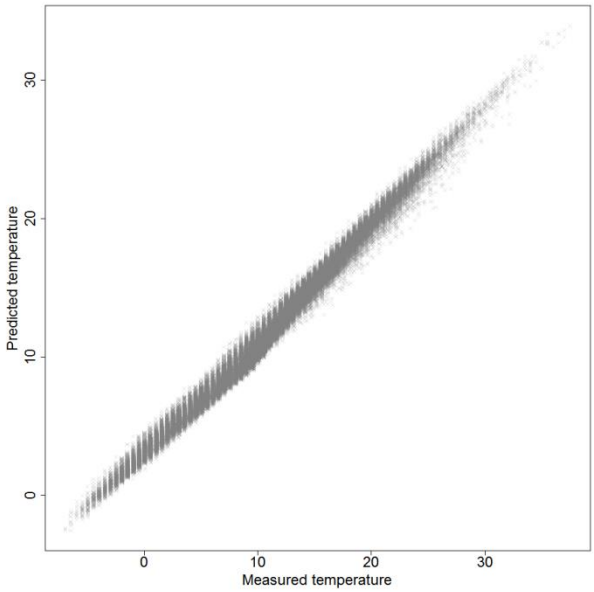

***Fig. S1.4.** Hourly modelled vs. measured temperatures across the Lizard Peninsula in Cornwall derived from data pooled across 30 loggers deployed between March and November 2014.*

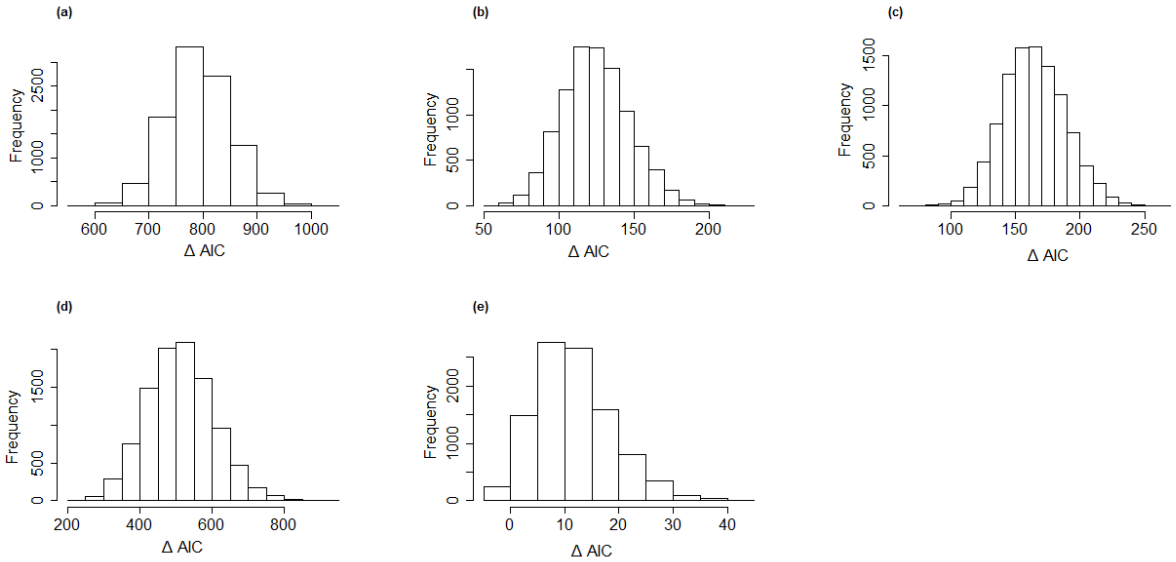

Fig. S1.5. *Frequency histograms of ΔAIC values associated with each of the 9999 model simulations. (a) Represents the difference between models with solar radiation terms included in comparison to null models. (b) Represents the difference between models with solar radiation and coastal influence terms included in comparison to models with just solar radiation terms. (c) Represents the difference between models with solar radiation, coastal influence and altitudinal terms included in comparison to models with just solar radiation and coastal influence terms. (d) Represents the difference between models with solar radiation, coastal influence, altitudinal and latent heat exchange terms included in comparison to models with just solar radiation, coastal influence and altitudinal. (e) Represents full models in comparison to models without cold air drainage terms included.*

To assess the extent to which correlations among variables were responsible for variation in parameter estimates, we performed Pearson's product-moment correlation tests between each of the terms in our model. None of the terms were correlated with one another, with the exception of u_i (a proxy for inverse of wind speed), which was inevitably inversely correlated with actual wind speed (Table S3). To assess the effects of including interactions between terms on the variation in parameter estimates, we repeated our model-fitting procedure with interaction terms excluded from the model. While greater parsimony was obtained when interaction terms were included (Table S2), the inclusion of interaction terms was responsible for much of the variation in parameter estimates (*c.f.* Fig. S6 and S7).

Table S3. *Pearson's product-moment correlation (r^2) among model terms. For delimitations of terms, see Table S1.2.*

	R_{net}	u_1	u_i	L	T_S	E	C	W	I_c	F
R_{net}	1.000	0.003	0.006	0.002	0.187	0.097	0.003	0.016	0.001	0.011
u_1		1.000	0.854	0.003	0.029	0.006	0.003	0.005	0.002	0.018
u_i			1.000	0.003	0.032	0.012	0.004	0.011	0.002	0.028
L				1.000	0.013	0.000	0.002	0.008	0.005	0.000
T_S					1.000	0.034	0.001	0.001	0.000	0.007
E						1.000	0.001	0.010	0.001	0.000
C							1.000	0.111	0.000	0.005
W								1.000	0.000	0.013
I_c									1.000	0.000
F										1.000

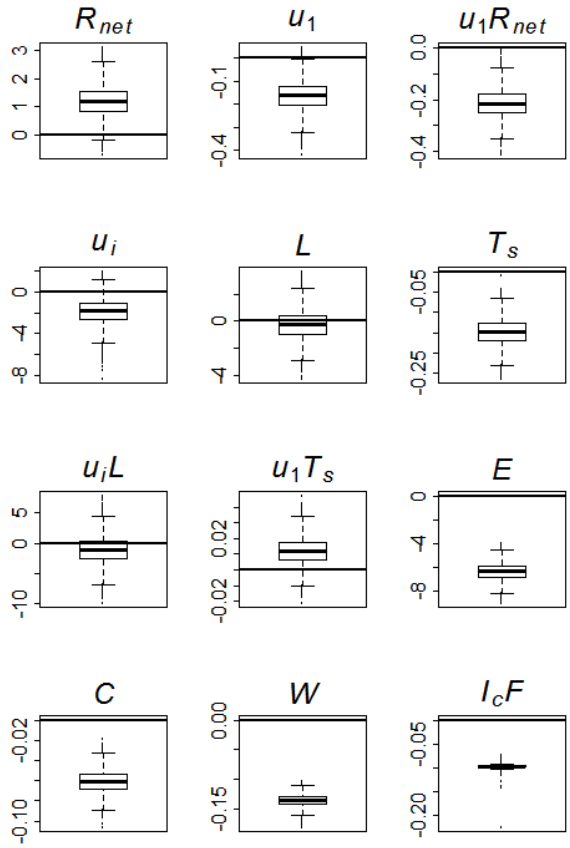

Fig. S1.6. *Box and whisker plots indicating the median and range in parameter estimates derived from the 9999 model runs. For definitions of terms, see Table S1.2. A solid line indicates the median values associated with each weather type. The boxes extend from the lower to upper quartiles, and the whiskers extend to 1.5 times the interquartile range, and extreme values outside this range are depicted by small dots.*

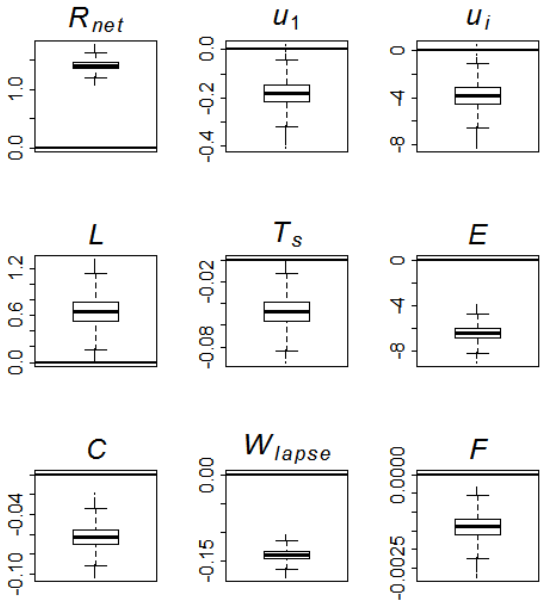

Fig. S1.7. *Box and whisker plots indicating the median and range in parameter estimates derived from the 9999 model runs when models were fitted without interaction terms. For definitions of terms, see Table S1.2. A solid line indicates the median values associated with each weather type. The boxes extend from the lower to upper quartiles, and the whiskers extend to 1.5 times the interquartile range, and extreme values outside this range are depicted by small dots. Considerably variability among parameter estimates is evident than for model with interaction terms included.*

Assessment of spatial performance

To assess the ability of our model to capture spatial variation in biologically important climate variables, we calculated, for each site, (i) mean temperature (ºC), (ii) exposure to high (>20ºC) temperatures (no. hours), (iii) frost exposure (no. hours), (iv) the length of the frost-free season (days), (v) growing-degree days (ºC day), (vi) diurnal temperature ranges (ºC), (vii) temperature isothermality, (viii) temperature seasonality, (ix) maximum annual temperatures (ºC), (x) minimum annual temperatures (ºC), (xi) annual variations in temperature and (xii-xv) mean temperatures in the warmest, coldest, driest and wettest quarter of each year (ºC). Details of how each variable was calculated are provided in the main text. In each instance we compared the difference bioclimate variables derived from temperatures measured at each site in 2010-11 (for which a full year of data are available) and those derived using (a) modelled temperatures and (b) temperatures recorded at our reference Meteorological station. Boxplots showing the differences across sites are shown in Fig. S8 and a summary of the Mean absolute and RMS error across sites for each variable are shown in Table S4. For all variables,

the model provides much better estimates of local bioclimate variables than would be obtained using data from a standard Meteorological station.

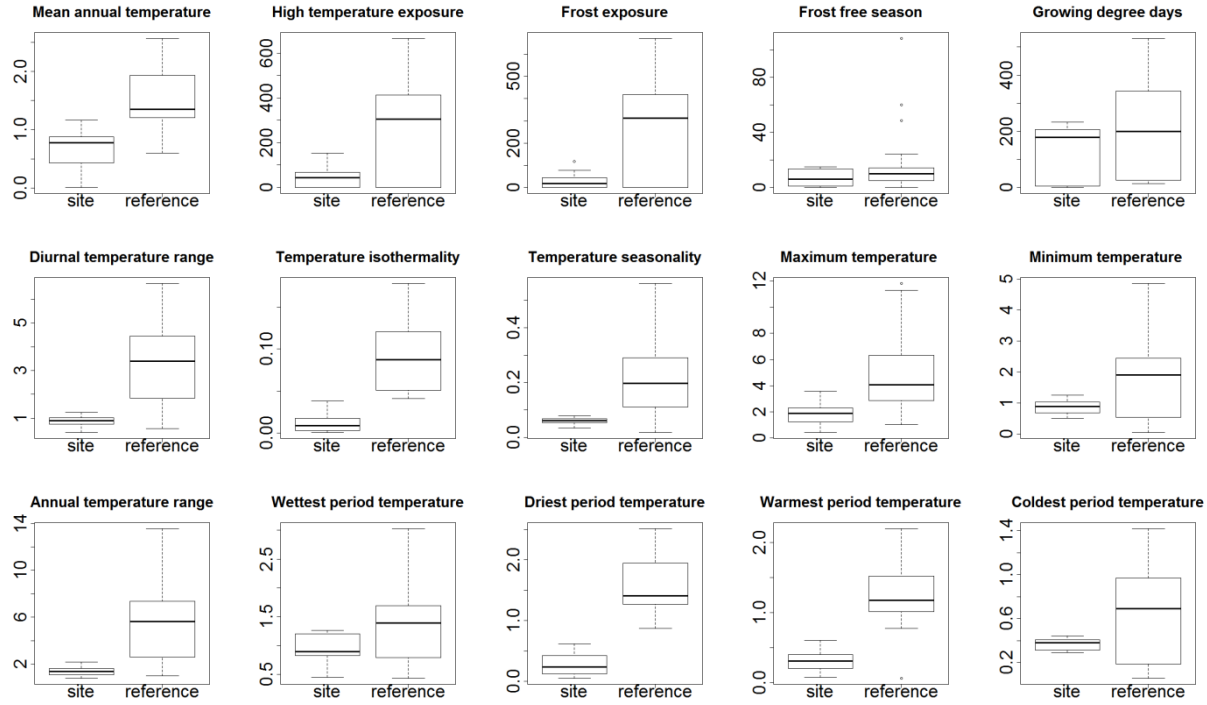

Fig. S8. Residual difference in the values of 15 bioclimate variables calculated using temperatures measured at each site compared with those obtained through model predictions (site) and temperatures measured at each site compared with those recorded at our reference Meteorological station at RNAS Culdrose (reference).

To gain insight into the factors affecting warming, we reran the model calculating the separate contribution of each of the five groups of factors to estimates of hourly temperatures. This was achieved by fitting the model using only coefficients associated with to each group of terms, holding all other terms constant at their mean value. The separate model estimates hourly values were then used to derive long-term trends in warming using linear regression for each grid cell. Closer inspection of the resulting patterns suggests that the effects of solar radiation are most important and influencing long-term temperature trends (Fig. S9). To gain further insight into the factors affecting warming, we also calculated the trend in the prevalence of each synoptic weather type. The synoptic weather type associated with easterly winds, weather type 1, also indicative of weakly anticyclonic conditions, high pressure and high relative humidity, decreased by 2.2% from 10.1% to 8.0% (n=38, 95% CIs = -4.3 to -1.3%) and was the only type for which a trend was evident (Fig S10).

Table S1.4. *Mean and RMS errors in the values of 15 bioclimate variables calculated using data measured at each site compared with those obtained through model predictions (site) and data measured at each site compared to temperatures recorded at our reference Meteorological station at RNAS Culdrose (reference).*

Variable	Mean error		RMS error	
	Site	Reference	Site	Reference
Mean annual temperature (ºC)	0.68	1.5	0.74	1.6
Exposure to high (>20ºC) temperatures (no. hours)	40	253	56	327
Frost exposure (no. hours)	26	256	38	331
Length of the frost-free season (days)	120	222	153	279
Growing-degree days (ºC day)	7.3	21	9.3	36
Diurnal temperature range (ºC)	0.87	3.3	0.90	3.7
Temperature isothermality	0.013	0.091	0.017	0.099
Temperature seasonality	0.059	0.22	0.060	0.27
Maximum temperature (ºC)	1.9	4.9	2.0	5.7
Minimum temperature (ºC)	0.88	1.8	0.90	2.2
Annual temperature range (ºC)	1.3	5.5	1.4	6.6
Mean temperature of wettest period (ºC)	0.96	1.4	0.99	1.5
Mean temperature of driest period (ºC)	0.28	1.6	0.32	1.6
Mean temperature of warmest period (ºC)	0.32	1.3	0.35	1.4
Mean temperature of coldest period (ºC)	0.37	0.67	0.37	0.8

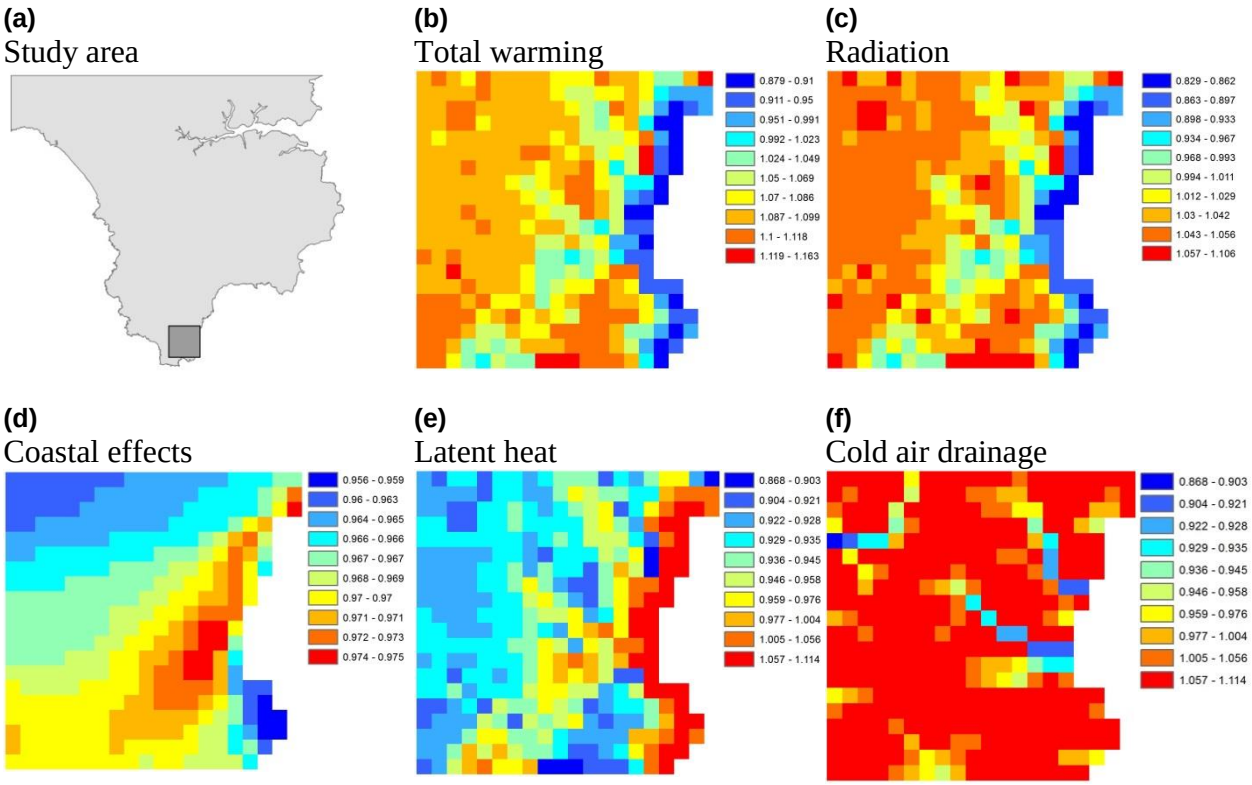

Fig. S1.9. *For a selected portion of our study area (a), the effects of individual components of our model on overall temperature increase (b) are shown. The effects of net solar radiation (c) appear to dominate, although coastal effects (d) are also important. The contributions of latent heat exchange (e) are inversely related to the overall pattern, as evapotranspirative cooling is strongly associated with increased net radiation. Cold air drainage (f) has only a minor effect, mostly in valley bottoms. Net radiation is the primary contributor to overall temperature increase.*

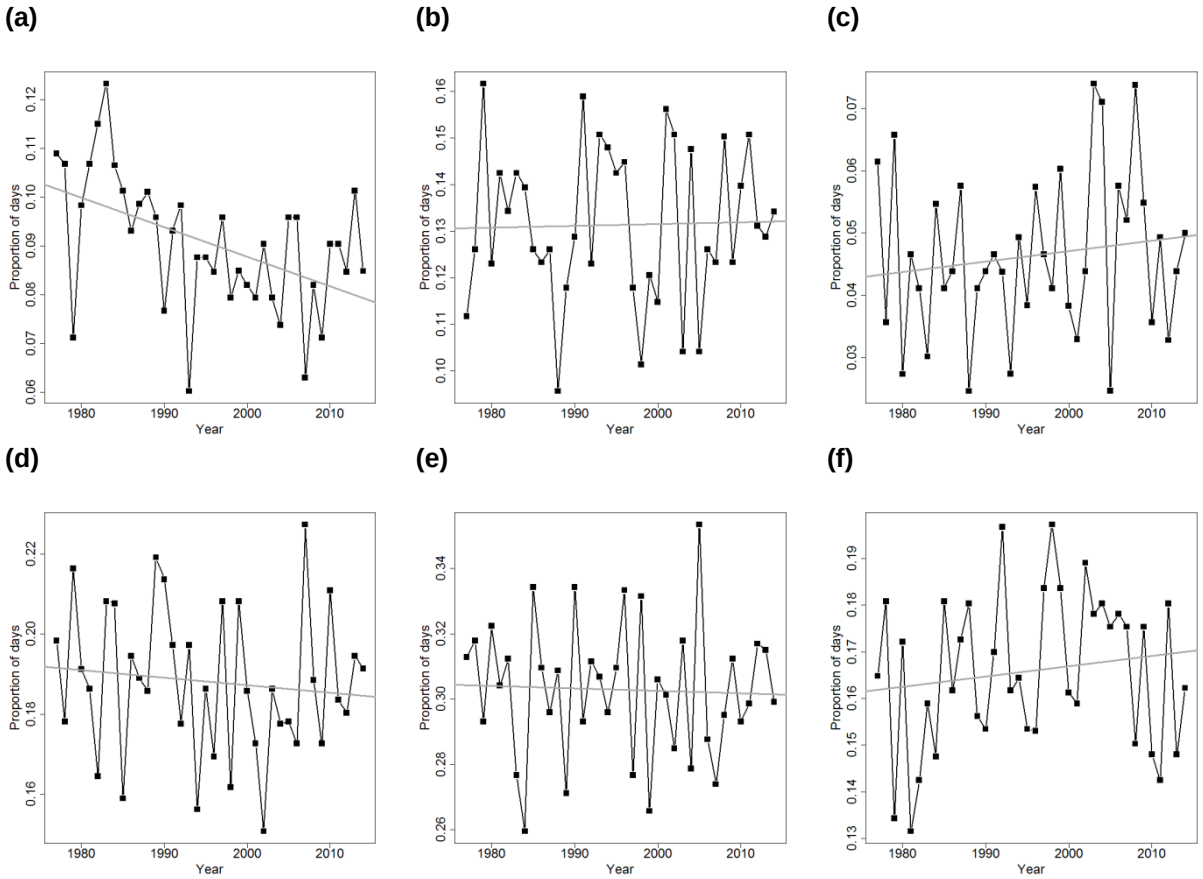

Fig. S1.10. *Yearly values (black lines) and linear trends (grey lines) in the prevalence of synoptic weather types derived from cluster analyses of meteorological data from Culdrose weather station (50.085º N, 5.257º W) as determined by the proportion of days in which each weather type prevailed. Descriptions of each type are given in Table S1.1.*

Assessment of temporal performance

Comparisons between modelled hourly predictions of temperature and recorded temperatures at two sites with divergent local climatic conditions are shown in Figure 2 in the main text. Comparisons between modelled and recorded daily minimum, mean and maximum temperatures for the same two sites ate shown in Fig. S1.11. To assess how well our model performs in predicting short-term temporal trends at each site, we calculate the RMS and mean absolute error in hourly temperatures and daily minimum, maximum and mean temperatures at each site (Fig S1.12). As for seasonally aggregated bioclimate variables, these are derived from comparisons between measured temperatures at each site and (a) model predictions and (b) using data obtained from our reference meteorological station at RNAS Culdrose.

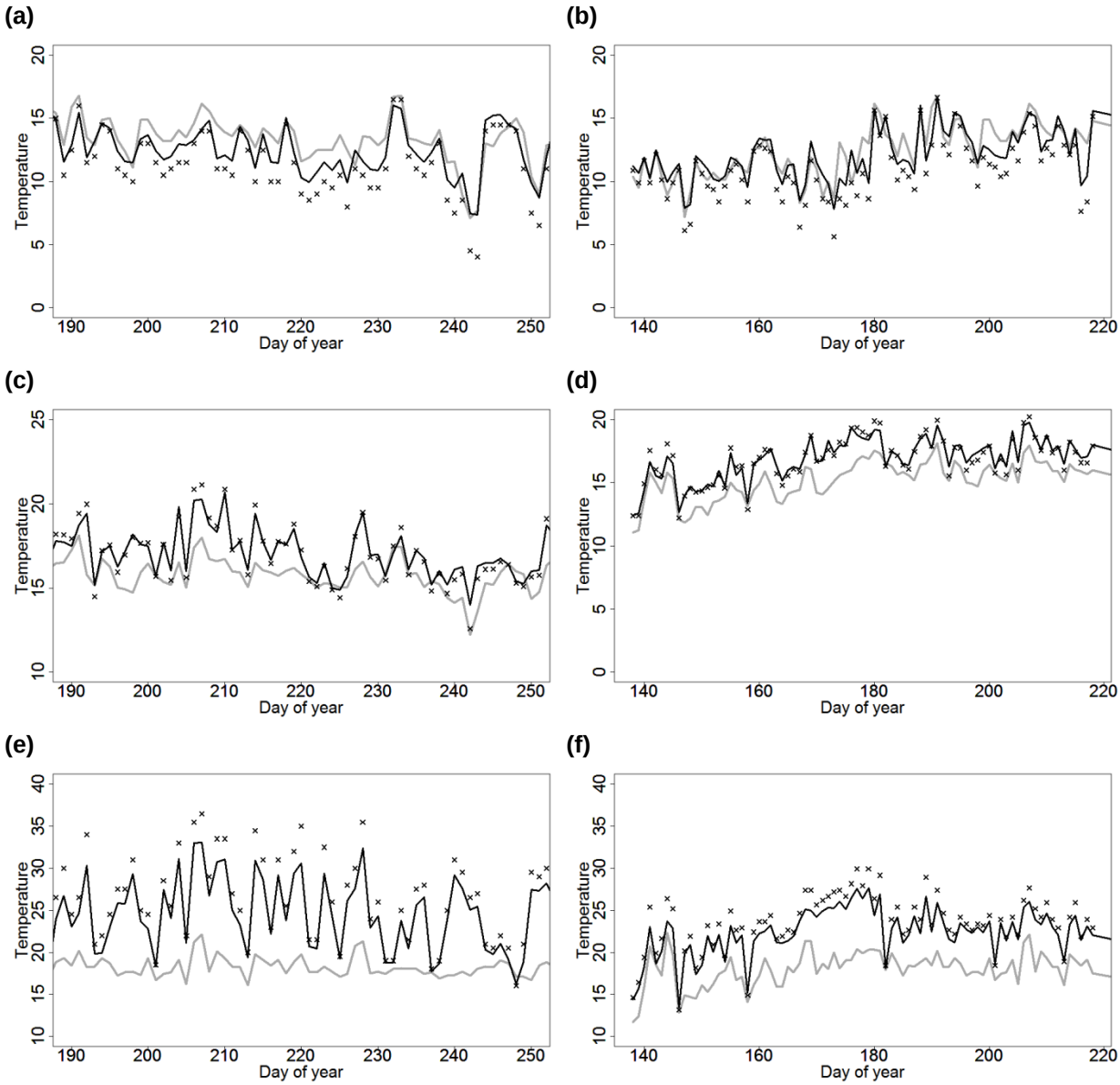

Fig. S1.11. *Daily minimum (a,b), mean (c,d) and maximum (e,f) temperatures recorded during summer 2014 using iButton temperature loggers (black crosses) and modelled using a 100 m spatial resolution mesoclimate model (black lines) compared to temperatures observed at a regional weather station (grey lines) five km from the sample site (RNAS Culdrose). Data for two sites with divergent mesoclimatic conditions are shown, (a,c,e) Poltesco (49.9981ºN, 5.1727ºW), a steep south-facing slope, and (b,d,f) Kennack Sands (50.0070ºN, 5.1594ºW), a relatively flat and open coastal area*.

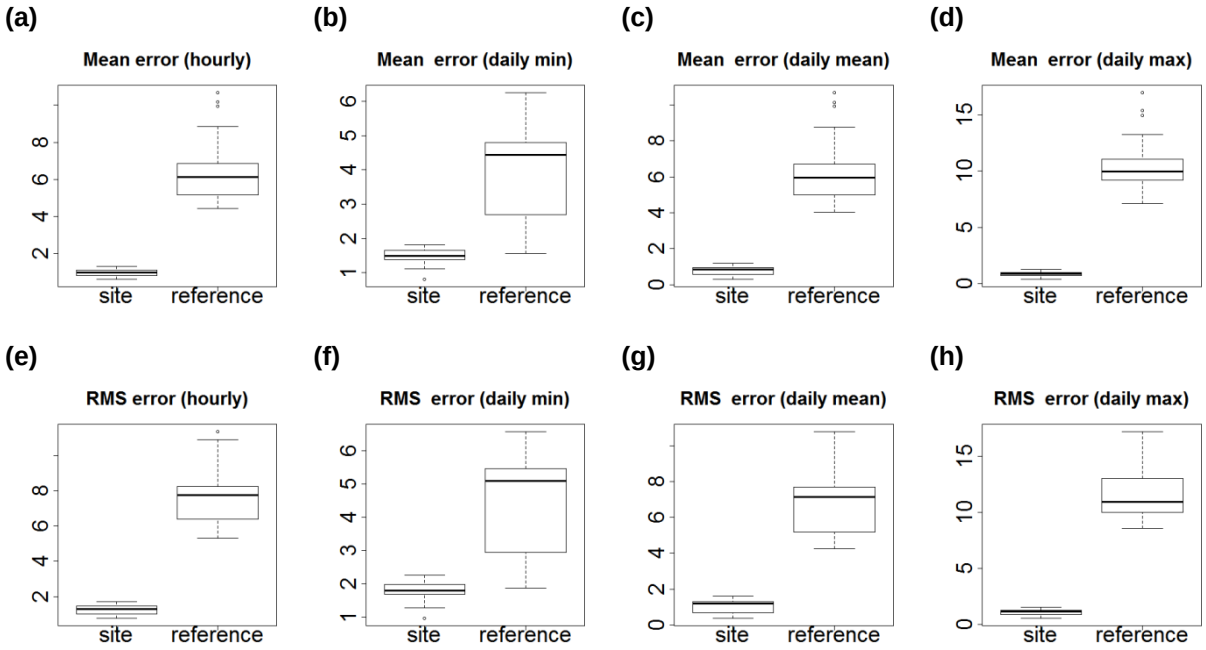

Fig. S1.12. *Mean (a-d) and RMS (e-h) error in hourly (a,e) and daily minimum (b,f), mean (c,g) and maximum (d,h) temperatures derived using temperatures measured at each site compared with those obtained through model predictions (site) and with those recorded at our reference Meteorological station at RNAS Culdrose (reference).*

Appendix 2. Spatial variation in trends in bioclimate variables

(see chapter 1)

Values in each 100m grid cell were derived from linear regression of modelled yearly values for the period 1977 to 2014. Data for the overall change in the mean diurnal temperature range (a), isothermality (b), temperature seasonality (c), maximum temperature (d), minimum temperature (e), temperature annual range (f) and the mean temperatures of the wettest, driest, warmest and coldest quarters (g-j) are shown.

(a) Mean Diurnal Range

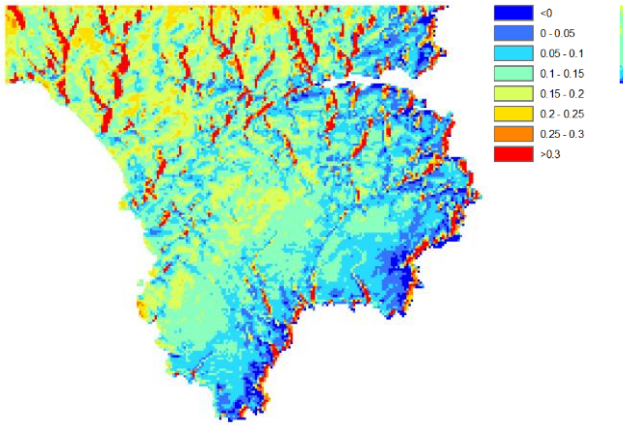

(b) Isothermality

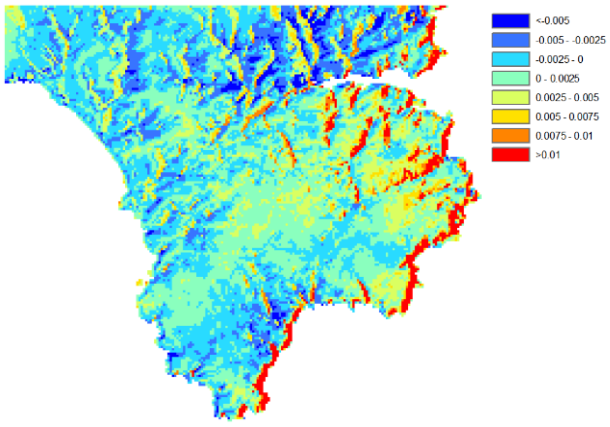

(c) Temperature seasonality

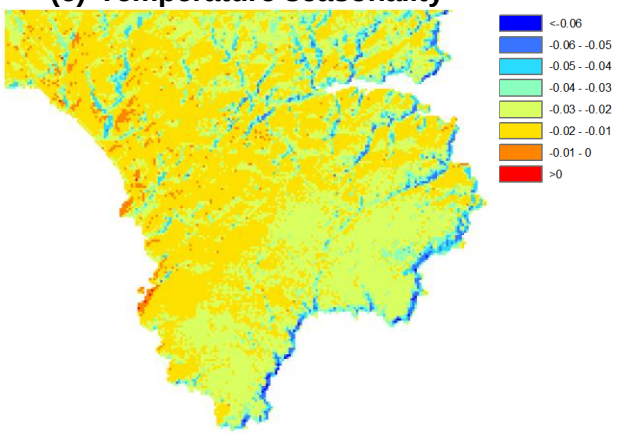

(d) Maximum temperature

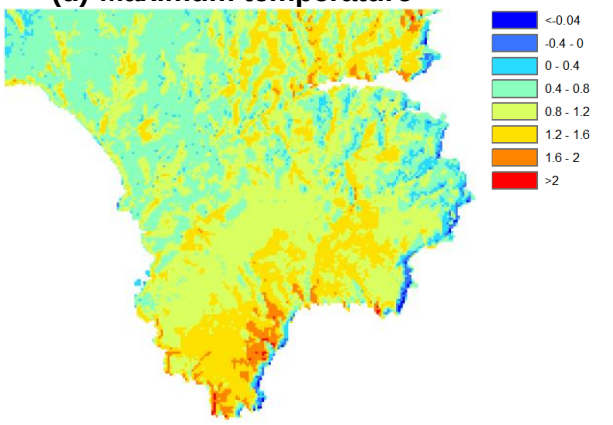

(e) Minimum temperature

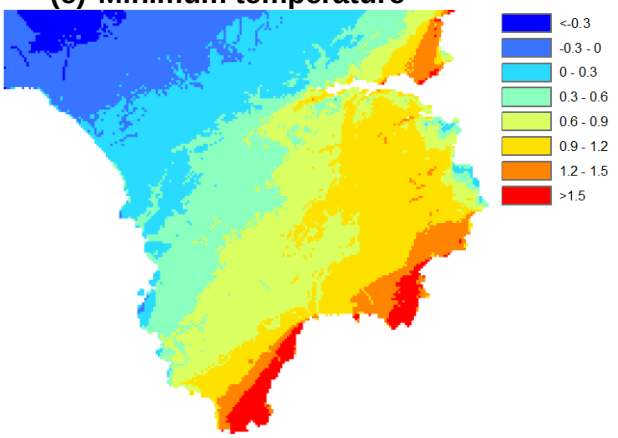

(f) Temperature annual range

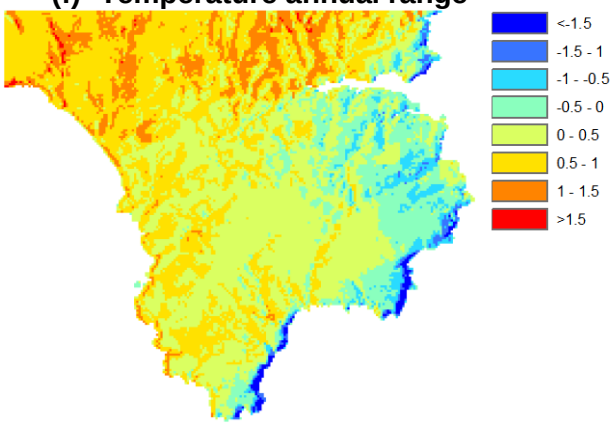

(g) Mean temperature of wettest quarter

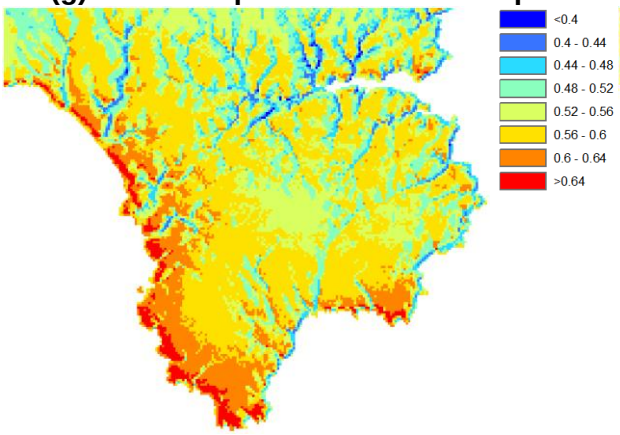

(h) Mean temperature of driest quarter

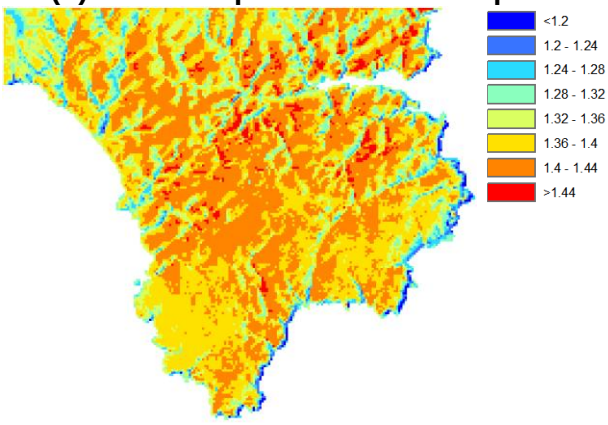

(i) Mean temperature of warmest quarter

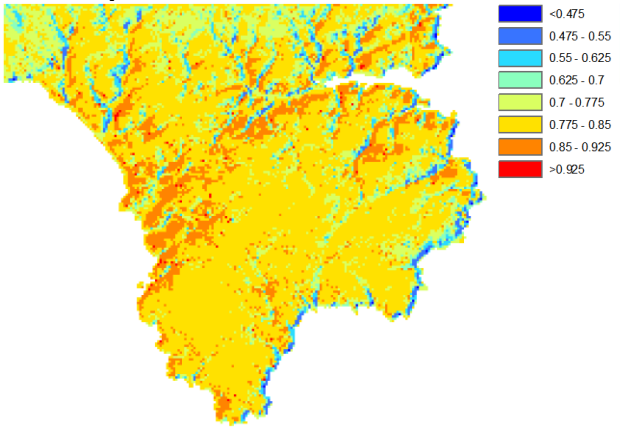

(j) Mean temperature of coldest quarter

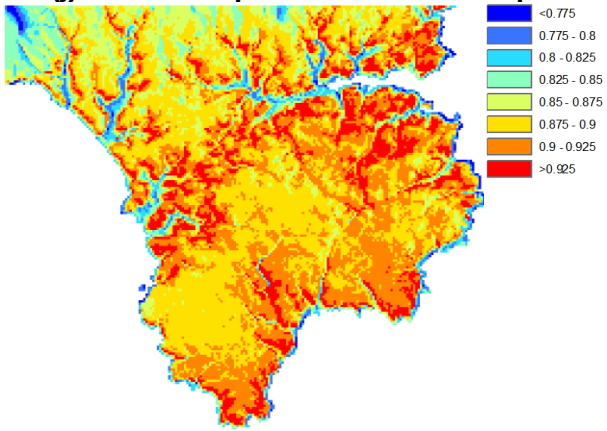

Appendix 3. Supplementary figures and tables associated with chapter 2

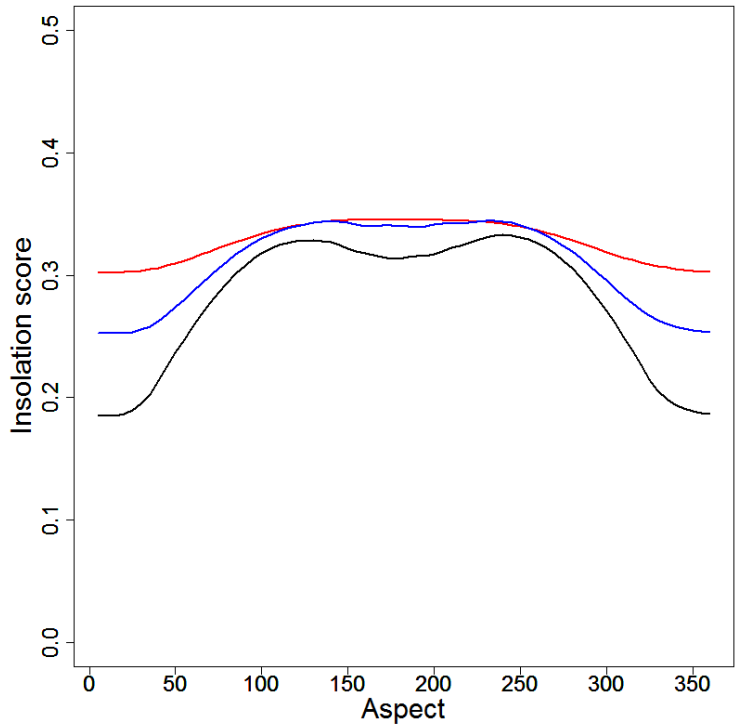

Fig. S3.1*. The proportion of potential direct irradiance intercepted by a surface (insolation) is a function of slope angle. Here scores across the full range of aspects are shown for slope angles of 15º (red), 30º (blue) and 45º (black).*

Table S3.1. *Results of generalised linear mixed-effects analyses investigating the possible role of biotic interactions as determinants of colonisations to and extinctions from sampled relevés. Parameter estimates (mean and 95% confidence intervals) for the effects of species richness and sward height in addition to the effects of insolation, temperature and Ellenberg moisture indices, and interactions between insolation and the temperature are assessed. Results for the most parsimonious model are shown. Vegetation cover was included as an explanatory term, but was not retained in the best model.*

	Colonisations			**Extinctions**		
	Estimate	**Lower 95% CI**	**Upper 95% CI**	**Estimate**	**Lower 95% CI**	**Upper 95% CI**
Intercept	10.37	4.23	16.51	-20.04	-26.18	-13.90
Temperature index	0.854	0.804	0.904	-1.635	-1.685	-1.585
Moisture index	-3.796	-3.858	-3.734	0.419	0.357	0.481
Insolation	-28.19	-28.61	-27.77	5.395	4.973	5.817
Species richness	0.075	-0.447	0.597	0.075	-0.447	0.597
Sward height	--	--	--	-5.933	-6.679	-5.187
Insolation x temperature index	5.933	5.187	6.679	--	--	--

Method for calculating water-balance.

The water-balance is the difference between rainfall (positive) and evapotranspiration (negative). As no continuous rainfall records is available for a single rainfall gauge within our study area, we obtained 5 km x 5km gridded monthly rainfall data for the UK from the Met Office (Perry & Hollis 2005) for the period 1971 to 2011 and extracted the data for the grid cell surrounding Culdrose Weather station (50.087ºN, 5.254ºW). Cumulative April to June rainfall was then calculated for each year. Potential evapotranspiration was calculated using the Penman-Monteith equation as detailed in (Allen *et al.* 2008). Using this method, evapotransporation can be derived from hourly weather data (temperature, relative humidity, pressure and wind speed) and an estimate of net shortwave radiation. Hourly weather data for Culdrose weather station were obtained from the British Atmospheric Data Centre.

Net shortwave radiation was estimated from cloud cover, (measured in octals) and calibrated using hourly satellite derived estimates for 2005, from the Satellite Application Facility on Climate Monitoring (Posselt *et al*. 2011), a step that was necessary because the satellite-derived estimates do not span the duration of our study. First, because solar irradiance is affected by solar azimuth and zenith, we computing the proportion of potential direct irradiance intercepted by a flat surface located at Culdrose (hereafter referred to as the solar coefficient) for every hour using the methods outlined in Hofierka & Suri (2002). Second, because solar energy is attenuated more by clouds when the sun is low above the horizon, we calculated the airmass coefficient for every hour in 2005. The airmass coefficient is the direct optical path length of a solar beam through the Earth's atmosphere, expressed as a ratio relative to the path length vertically upwards. To account for the earth's curvature, we used the method by Kaston & Young (1989) in which the air mass coefficient can be derived from the solar zenith. Next, to estimate the effects of cloud cover on full beam solar irradiance, we divided each satellite-derived estimate of direct and diffuse solar irradiance by the solar coefficient. As direct irradiance is affected both by cloud cover and the airmass coefficient, we fitted a linear model with the full beam estimates of direct irradiance as a dependent variable, and optical thickness, cloud cover and an interaction between cloud cover and the airmass coefficient as predictor variables. To reduce heteroscedasticity, we performed square-root transforms on cloud cover and full-beam irradiance and a logarithmic transform on optical thickness. As diffuse irradiance is highest with intermediate levels of cloud cover, we fitted a linear model with just cloud cover and the square of cloud cover as predictor variables. Again to reduce heteroscedascity, we square-root transformed scaled solar irradiance. Coefficient estimates of these models were then used to derive hourly estimates of full beam solar irradiance and diffuse radiation for the entire duration of our study.

Appendix 4. Species list (in descending order of number of relevés occupied)

(See chapter 2)

Species common to both periods

Ribwort Plantain (*Plantago lanceolata*)
Common Bent (*Agrostis capillaris*)
Cock's foot (*Dactylis glomerata*)
Lady's Bedstraw (*Galium verum*)
Lesser Trefoil (*Trifolium dubium*)
Crested Hair-grass (*Koeleria macrantha*)
Knotted Clover (*Trifolium striatum*)
Crested Dog's-tail (*Cynosurus cristatus*)
Silver Hairgrass (*Aira caryophyllea*)
Common Mouse-ear (*Cerastium fontanum*)
Daisy (*Bellis perennis*)
Sheep's Fescue (*Festuca ovina*)
Sweet Vernal Grass (*Anthoxanthum odoratum*)
Spring Squill (*Scilla verna*)
Bird's-foot Trefoil (*Lotus corniculatus*)
Smooth Meadow-grass (*Poa pratensis* sens.lat.)
Bulbour Buttercup (*Ranunculus bulbosus*)
Buck’s-horn Plantain (*Plantago coronopus*)
Sea mouse-ear (*Cerastium diffusum*)
Cat's ear (*Hypochaeris radicata*)
Lesser Hawkbit (*Leontodon saxatilis*)
Changing Forget-me-not (*Myosotis discolor*)
Perennial Rye-grass (*Lolium perenne*)
Yarrow (*Achillea millefolium*)
Wild Thyme (*Thymus polytrichus*)
Autumn Squill (*Scilla autumnalis*)
Subterranean Clover (*Trifolium subterraneum*)
Yorkshire Fog (*Holcus lanatus*)
English Stonecrop (*Sedum anglicum*)
Blink spp (*Montia fontana*)
Wild Carrot (*Daucus carota*)
White Clover (*Trifolium repens*)
Brome Fescue (*Vulpia bromoides*)
Common Sorrel (*Rumex acetosa*)
Field Woodrush (*Luzula campestris*)
Toad Rush (*Juncus bufonius*)
Thrift (*Armeria maritima*)
Sea Plantain (*Plantago maritima*)
Red Clover (*Trifolium pratense*)
Rough Clover (*Trifolium scabrum*)
Birdeye pearlwort (*Sagina procumbens*)
Dropwort (*Filipendula vulgaris*)
Hairy Bird's-foot Trefoil (*Lotus subbiflorus*)
Annual Meadowgrass (*Poa annua*)
Yellow Hairgrass (*Aira praecox*)
Common Kidneyvetch (*Anthyllis vulneraria*)
Scarlet Pimpernel (*Anagallis arvensis*)
Brown Bent (*Agrostis vinealis*)
Betony (*Stachys officinalis*)
Annual Pearlwort (*Sagina apetala*)
Common Gorse (*Ulex europaeus*)
Spring Sedge (*Carex caryophyllea*)
Sticky Mouse-ear (*Cerastium glomeratum*)
Rough Bluegrass (*Poa trivialis*)

Burnet Saxifrage (*Pimpinella saxifraga*)
Erect Chickweed (*Moenchia erecta*)
Sheep's-bit Scabious (*Jasione montana*)
Land Quillwort (*Isoetes histrix*)
Ling (*Calluna vulgaris*)
Chamomile (*Chamaemelum nobile*)
Spear Thistle (*Cirsium vulgare*)
Meadow Buttercup (*Ranunculus acris*)
Common Dog-violet (*Viola riviniana*)
Common Dandelion (*Taraxacum* agg.)
Creeping Buttercup (*Ranunculus repens*)
Blackberry (*Rubus fruticosus* agg.)
Twin-headed Clover (*Trifolium bocconei*)
Common Centaury (*Centaurium erythraea*)
Burnet Rose (*Rosa pimpinellifolia*)
Common Sowthistle (*Sonchus oleraceus*)
Sloe (*Prunus spinosa*)
Creeping Bent-grass (*Agrostis stolonifera*)
Common Milkwort (*Polygala vulgaris*)
Common Restharrow (*Ononis repens*)
Soft Brome (*Bromus hordeaceus*)
Hairy Bittercress (*Cardamine hirsuta*)
Bell Heather (*Erica cinerea*)
Ragwort (*Senecio jacobaea*)
Cut-leave Cranesbill (*Geranium dissectum*)
Glaoucous Sedge (*Carex flacca*)
Fringed Rupturewort (*Herniaria ciliolata*)
Common Vetch (*Vicia sativa*)
Common Self-heal (*Prunella vulgaris*)
Foxglove (*Digitalis purpurea*)
Hare'sfoot Clover (*Trifolium arvense*)
Dwarf Rush (*Juncus capitatus*)
Dove'sfoot Crane'sbill (*Geranium molle*)
Dyer's Greenweed (*Genista tinctoria*)
Oxeye Daisy (*Leucanthemum vulgare*)
Wild Chive (*Allium schoenoprasum*)
Creeping Thistle (*Cirsium arvense*)
Common Hogweed (*Heracleum sphondylium*)
Western Clover (*Trifolium occidentale*)
Red Fescue (*Festuca rubra*)
Spring Sandowrt (*Minuartia verna*)
Pale Flax (*Linum bienne*)
Sheep's Sorrel (*Rumex acetosella*)
Mouse-ear Hawkweed (*Pilosella officinarum*)
False Brome (*Brachypodium sylvaticum*)
Bracken (*Pteridium aquilinum*)
Bush Vetch (*Vicia sepium*)
Common Tormentil (*Potentilla erecta*)
Cornish Heath (*Erica vagans*)
Long-headed Clover (*Trifolium incarnatum* subsp. *molinerii*)
Common Heath Grass (*Danthonia decumbens*)
Saw-wort (*Serratula tinctoria*)
Autumn Hawkbit (*Leontodon autumnalis*)
False Oat-grass (*Arrhenatherum elatius*)
Red Campion (*Silene dioica*)
Curled Dock (*Rumex crispus*)
Common Hawthorn (*Crataegus monogyna*)
Smooth Hawk'sbit (*Crepis capillaris*)
Upright Bedstraw (*Galium mollugo*)
Upright Clover (*Trifolium strictum*)

Species recorded in 1979/80 but not in 2011

Corn Speedwell (*Veronica arvensis*)
Slender Trefoil (*Trifolium micranthum*)
Bird's-foot (*Ornithopus perpusillus*)
Bird's-foot Clover (*Trifolium ornithopodioides*)
Slender parsley piert (*Aphanes arvensis* agg.)
Trailing St John's-wort (*Hypericum humifusum*)
Lesser Knapweed (*Centaurea nigra*)
Spring Draba (*Erophila verna*)
Devil's-bit Scabious (*Succisa pratensis*)
Lesser Celendine (*Ranunculus ficaria*)
Common Knotgrass (*Polygonum aviculare*)
Eyebright spp. (*Euphrasia* spp.)
Danish Scurvy-grass (*Cochlearia danica*)
Smith's Pepperwort (*Lepidium heterophyllum*)
Slender St John's-wort (*Hypericum pulchrum*)
Barren Strawberry *(Potentilla sterilis*)
Black Medic (*Medicago lupulina*)
Stiff Sand-grass (*Catapodium marinum*)
Heath Pearlwort (*Sagina subulata*)
Germander Speedwell (*Veronica chamaedrys*)
Green-winged Orchid (*Orchis morio*)
Heath Milkwort (*Polygala serpyllifolia*)
Common Agromony (*Agrimonia eupatoria*)
Wild Privet (*Ligustrum vulgare*)
Marsh Thistle (*Cirsium palustre*)
Greater Birds-foot Trefoil (*Lotus pedunculatus*)
Early Forget-me-not (*Myosotis ramosissima*)
Heath Wood-rush (*Luzula multiflora*)
Clustered Clover (*Trifolium glomeratum*)
Sea Stork's-bill (*Erodium maritimum*)
Common Bistort (*Persicaria bistorta*)
Carnation Sedge (*Carex panicea*)

Species recorded in 2011 but not in 1979/80

Sea Campion (*Silene uniflora*)
Hard-grass (*Parapholis strigosa*)
Field Bindweed (*Convolvulus arvensis*)
Lesser Burdock (*Arctium minus*)
Rough Hawk'sbeard (*Crepis biennis*)
Hairy Rock-cress (*Arabis hirsuta*)
Common Comfrey (*Symphytum officinale*)
Bluebell (*Hyacinthoides non-scripta*)
Early Dog-violet (*Viola reichenbachiana*)
Western Gorse (*Ulex gallii*)
Ivy (*Hedera helix*)
Small-flowered Crane's-bill (*Geranium pusillum*)
Prickly Sow-thistle (*Sonchus asper*)
Lousewort (*Pedicularis sylvatica*)
Bloody Crane's-bill (*Geranium sanguineum*)
Green Bristle-Grass (*Setaria viridis*)
Cotton Thistle (*Onopordum acanthium*)
Cow Parsley (*Anthriscus sylvestris*)
Greater Plantain (*Plantago major*)
Milk Thistle (*Silybum marianum*)
Honeysuckle (*Lonicera periclymenum*)
Heath Spotted-Orchid (*Dactylorhiza maculata*)
Meadow Thistle (*Cirsium dissectum*)

Tufted Vetch (*Vicia cracca*)
Yellow Sedge (*Carex viridula*)
Thyme-leaved Sandwort (*Arenaria serpyllifolia*)
Smaller Cat's-tail (*Phleum bertolonii*)
Common Nettle (*Urtica dioica*)
Flea Sedge (*Carex pulicaris*)
Great Burnet (*Sanguisorba officinalis*)
Fool's Parsley (*Aethusa cynapium*)
Wall Pennywort (*Umbilicus rupestris*)
Common Couch (*Elytrigia repens*)
Slender Thistle (*Carduus tenuiflorus*)
Creeping Cinquefoil (*Potentilla reptans*)
Field Scabious (*Knautia arvensis*)
Yellow Rattle (*Rhinanthus minor*)